BADJI MOKHTAR ANNABA-UNIVERSITY
Faculty of the Technology
Department of Mechanical Engineering

Domain: Science and Technology
Branch: Mechanical Engineering
Major: Mechanical Manufacturing and Production

Optimization of FDM printer Parameters using Desirability function and their influence on the mechanical properties of PLA printed specimens

A Dissertation Submitted to the Department of Mechanical Engineering in Partial Fulfillment of the Requirements for the Master Degree in Mechanical Manufacturing and Production

Submitted by   **Supervised by**

Khammar Nouara Nour El Houda   **Pr. Rabia Khelif**

Board of Examiners

Pr. Chaoui Kamel	Professor	Badji Mokhtar-Annaba University
Pr. Rabia Khelif	Professor	Badji Mokhtar-Annaba University
Dr. Nehal Abdelaziz	MCA	Badji Mokhtar-Annaba University

Academic Year: 2021/2022

Summary

It is well known that the manufacturing process has a direct influence on the mechanical properties of elaborated material such as strength resistance, fatigue life, corrosion resistance, stiffness among others.

In this study, the influence of 3d printing parameters: infill density, nozzle temperature, printer speed, layer height has been investigated in order to analyze their impacts on young modulus and yield strength of PLA material. The mechanical properties have been obtained from tensile test according to ASTM D-638. A central composite design was used to perform the experimentation. Furthermore, a model of prediction for young modulus and yield strength was established based on experimental data using regression model and MANFIS model. Using the obtained regression function model, a multi-objective optimization has been applied through the desirability function method.

Keywords:

Additive Manufacturing, 3D Printing, Fused Filament Fabrication, Mechanical Behavior, Young Modulus, Yield Stress, Central Composite Design, Desirability Function, MANFIS.

Résumé:

Il est bien connu que le processus de fabrication a une influence directe sur les propriétés mécaniques du matériau élaboré telles que la résistance, la durée de vie en fatigue, la résistance à la corrosion, la rigidité, entre autres.

Dans cette étude, l'influence des paramètres d'impression 3D : densité de remplissage, température de la buse, vitesse de l'imprimante, hauteur de la couche a été étudiée afin d'analyser leur impact sur le module de Young et la limite d'élasticité du matériau PLA. Les propriétés mécaniques ont été obtenues à partir d'essais de traction selon la norme ASTM D-638. Un plan composite central a été utilisé pour réaliser l'expérimentation. En outre, un modèle de prédiction du module de Young et de la limite d'élasticité a été établi sur la base des données expérimentales en utilisant un modèle de régression et un modèle MANFIS. En utilisant le modèle de régression obtenu, une optimisation multi-objective a été appliquée par la méthode de la fonction de désirabilité.

Mots-clés :

Fabrication additive, impression 3D, fabrication par filament fondu, comportement mécanique, module d'Young, limite d'élasticité, conception composite centrale, fonction de désirabilité, MANFIS.

ملخص

كما تم فحص كثافة التعبئة، ودرجة حرارة الفوهات، وسرعة الطابعة، :في هذه الدراسة تأثير معاملات الطباعة الثلاثية الأبعاد البوليلاكتيك حمض وارتفاع الطبقة من أجل تحليل تأثيراتها على الموديلات الشابة وزيادة قوة المادة

وقد أستخدم تصميم مركب 638,أ س ت م د .وقد تم الحصول على الخصائص الميكانيكية من إختبار الشد وفقا للطراز مركزي لإجراء التجربة.

استنادا إلى بيانات تجريبية باستخدام نموذج الانحدار ونموذج وقوام إجهاد وعلاوة على ذلك، وضع نموذج للتنبؤ بمعامل يونغ نظام مانفيس.

وباستخدام نموذج دالة التراجع الذي تم الحصول عليه، تم تطبيق تحسين متعدد الأهداف من خلال أسلوب دالة الرغبة

الكلمات الأساسية

تصميم الناتج، إجهاد شاب، معامل ميكانيكي، سلوك منصهرة، خيوط تصنيع الأبعاد، ثلاثية طباعة مضاف، تصنيع مانفيس مرغوبة، وظيفة مركزي، مركب.

Acknowledgement

Dedications

First and foremost, I want to thank Allah for providing me with strength and patience to carry on with this task.

I'd also like to thank myself I worked hard and honestly, I deserve this

Islem, you were always there, wherever and whenever possible. Each rant, each time I sobbed and yelled and vowed to quit. Thank you for being there for me.

Ibtissem, Amira, Imene, Hichem, Houssem, Djo, Alo, and Vicky. I could never thank you guys enough, I am blessed to have y'all in my life, thank you for believing in me more than I believed in myself,

I pray that Allah grants all of your hearts desires.

Finally, and most importantly, my Parents deserves nothing but the best.

Thank you for your unwavering, and loving support. You've always been there for me, and this was no exception. Mom, thank you for all of your affection and for constantly reminding me of the end goal; and dad thanks for raising me to the women I am today.

I wouldn't be here without you two; I hope you're proud of me.

Table of Contents

List of Figures

List of Tables

Abbreviations

AM   Additive Manufacturing

3D   Three Dimensional

FFF   Fused Filament Fabrication

FDM   Fused Deposition Modeling

PLA   Polylactic Acid

CNC   Computer Numerical Control

CAD   Computer-Aided Design

ISO   International Standards Organization

SLA   Stereolithography

DLP   Digital Light Processing

SLS   Selective laser sintering

DOD   Drop On Demand

DMLS   Direct Metal Laser Sintering

SLM   Selective Laser Melting

EBM   Electron Beam Melting

ASTM   American Society of Testing Materials International

DOE   Design Of Experiment

ANOVA   Analysis of Variance

NN   Neural Network

MANFIS   Multi Output Adaptive Neuro-Fuzzy Inference System

CCD   Central Composite Design

Chapter 0

State of Art

State of Art:

This part defines the FFF technology through the specification of variable production factors that contribute to the process, the mechanical qualities that are the focus of this dissertation, and the great bulk of the evaluated bibliography.

I. FFF's relevant configurable settings:

The most well-known and recognized FFF method is 3D printing using thermoplastic and elastomeric materials extrusion. To build functional parts, it is necessary to understand how different parameters affect the mentioned properties, which are quite varied and can affect the final characteristics of the samples in various ways, such as part quality, mechanical behavior, geometrical details, surface texture, and cost. As a result, it is critical to understand which of these factors are crucial in order to carefully determine their values.

The subsections that follow outline the most important parameters studied in this dissertation.

1. Orientation:

The manufacturing direction, also known as build orientation, is one of the most critical elements that can affect load transmission between filaments and interfaces. The usefulness of this parameter in terms of the laying direction of extruded filaments may vary depending on the mechanical test and subsequent load application. Tensile testing, in which the traction force attempts to break the filaments in the 0X orientation or split the layers in the 0Y direction, is one mechanical test that can detect this efficacy. The finished surface and print time can also be affected by orientation.

Several studies have lately been done to investigate the impact of this characteristic on the strength of produced components. According to [10], Results demonstrated that shear modulus and shear strength for 45° flat orientation was about 1.55 GPa and 36 MPa, whereas for upright specimens they were about 0.95 GPa and 18MPa showing weaker strength than the 45° flat orientation.

This study [11] results showed that the build orientation and layer thickness were the two most crucial aspects determining dimensional accuracy, which was conditioned by the length of the movement of the extruder, and the accumulation of layers.

2. Layer height:

The height of the extruded filaments, also known as layer height, determines the height along the vertical axis measured before extruding a new layer on top of the preceding one, the

connection between the extruded wires could be affected by the height of the layers, and this could influence the mechanical properties of the printed parts.

The influence of liquefier temperature, print speed, layer height, and platform temperature on the temperature development and mechanical behavior of PA6 reinforced with chopped carbon fibers generated by FFF is discussed in this study [12]. The preliminary findings indicated that there are variances in crystallinity percentages, and failure stress/strain may be used to evaluate the mechanical qualities of FFF-made goods. Furthermore, evaluating the temperature profile of the deposited filaments indicated that process factors have a significant impact on the cooling process of deposited filaments, which influences the bonding of nearby filaments. The slower cooling rate was caused by the higher temperatures.

The current paper investigates the effect of geometrical parameters (Nozzle Diameter, Layer Thickness, and Printing Speed) of the FFF 3D printing process on printed part strength using PLA, with the results revealing a significant influence of geometric process parameters on the sample mesostructured, and thus on sample strength [13]. Over the entire range of layer height values evaluated, layer height had the largest effect on intra-layer cohesiveness, with part strength decreasing as layer height increased for all nozzles studied. The reduction in strength while shifting layer height from minimum to maximum was approximately 3.5 times for the samples under consideration.

3. Nozzle diameter:

In important efforts, the diameter of the nozzle defines the diameter of the extruded wire, and its efficacy on mechanical qualities and surface roughness is explored. The layer height may be changed as a critical printing parameter to minimize the size of voids; the lower the layer height, the smaller the void size. The trade-off is that by lowering the layer height, printing time rises. When the layer height is smaller than the nozzle diameter, the raster's cross-section deforms to a rectangular shape with round corners. The impact of this setting on printing velocity can also vary.

Shahriar Bakrani Balani [14] sought to optimize the printing conditions of the FFF process based on trustworthy qualities such as printing parameters and polymer physical properties, with findings indicating a fluctuation in shear rate depending on nozzle diameter and intake velocity. At high intake velocities and smaller diameters, the shear rate reached its maximum near the interior wall.

The suggested study [15] lays out the primary faults generated by a variety of printing factors that may affect layer slicing, hence impacting the defect rate. For the first point, all extruded material must be confined behind the nozzle; otherwise, faults on the print surface may arise. As a result of choosing to maintain the width constant and equal to the nozzle diameter, additional defect reduction is achievable through the implementation of the suggested optimization approach, which would allow for the collection of the right value of printing settings.

4. Infill density:

This parameter specifies the distance between the lines of the interior filling and, as a result, the solidity percentage of the piece's interior. The proportions of this parameter can have a considerable impact on the mechanical characteristics of the components depending on the internal fullness of the parts, and the quantity of this percentage is crucial in increasing/decreasing overall material consumption and prices.

The purpose of this experimental study [16] is to investigate the effect of infill density on the tensile mechanical parameters "tensile strength and elastic modulus" of PLA. tPLA material demonstrated the highest tensile strength for all infill densities when only specimens with infill structure were examined (20 %, 60 % and 80%). When the elastic modulus is measured, cPLA has the greatest value for infill density of 80%, cPLA and tPLA materials have the same value for infill density of 60%, and cPLA and tPLA materials have the same value for infill density of 20%.

While [17], the paper examines the performance of FFF-built components, revealing the relationship between printing orientation and structural performance. Furthermore, the mechanical behavior of the exterior contour and the interior structure (in-fills or lattice). When it was demonstrated that the mechanical behavior of aligned-type and crossed-type samples is transversely isotropic the isotropic plane changes depending on the printing design. The crossed-type samples are transversely isotropic, with XZ being the isotropic plane and stiffness being lower in the Y direction. Transverse isotropy is also found in mixed-type and aligned-type samples. However, YZ is the isotropic plane, thus the stiffness in the X direction is lower.

5. Infill pattern:

The infill pattern allows you to fill the inside of the samples with various geometrical forms such as (rectilinear, honeycomb, Hilbert curve, triangular, etc.). The impact of the various infill patterns on the raster angle and load direction might be significant, hence it has been carefully considered in the current study.

This work [18] investigates the effects of infill patterns on the mechanical response of PLA-printed parts. The mechanical responses of parts printed with different infill patterns ''Rectilinear, Honeycomb, Triangle, and Grid patterns" were tested on impact resistance and tensile strength. Considering mechanical response from both tensile and impact tests along with printed mass, the Honeycomb pattern was considered the toughest.

The effect of infill type and density on tensile characteristics, 3D printing time, and volume of 3D printed material was examined and published in this paper [19]. A total of 13 distinct forms of infill were examined, and for each type, 9 specimens with varied infill density were tested, ranging from 10% to 90%. The ultimate tensile strength and yield strength also rose for each type

of infill pattern. The "Concentric" infill pattern likewise provided the best ultimate tensile strength and yield strength, according to the results.

6. Printing velocity:

The printing velocity specifies the linear speed at which the extruder head moves across the build platform's XY plane. While varying printing speeds can affect the width or diameter of the extruded wire, it's worth considering how it affects the mechanical qualities of the printed pieces.

In [20], the goal of the study was to see how different printing parameters (five different printing regimes, varying layer height, number of outline perimeters, infill density, and sample humidity) affected the mechanical properties of printed PLA and PLA-X samples, "five samples each" and mechanical testing on a standard tensile testing machine. The elastic modulus values of PLA and PLA-X materials did not differ significantly.

The mechanical characteristics of 3D printed PLA lattice structures were investigated using digital image correlation (DIC) in [21]. The experimental results reveal that when the printing temperature increases, the tensile strength and elastic modulus rise first, then drop. While the yield strength, plastic platform stress, and densification strain of lattice structures are all decreasing, the yield strength, plastic platform stress, and densification strain are all increasing. The tensile strength and elastic modulus soar as the printing speed increases.

II. Mechanical properties and materials:

One of the most important concerns for engineers to consider when designing a building is selecting the material based on an appropriate set of mechanical characteristics. These characteristics might be measured using approved measurement standards that specify material behavior owing to load resistance.

One of the well-known phenomena requiring integrated geometric and material nonlinear analysis of solids is large strain plasticity, which has been reported in numerous materials. Materials begin to fail due to plastic deformation (non-linear stress vs. strain) or brittle fracture as stress increases. One method for quantifying failure behavior is to calculate yield strength, ultimate strength, and impact strength. Each of them can be characterized in terms of the loading mode: tension, compression, flexure, shear, or torsion [22].

Furthermore, polymers are crucial for AM since they have the largest market penetration and user accessibility. Polymeric materials have grown in popularity in engineering applications. As a consequence of continual fiber/matrix improvement and the development of revolutionary

fabrication processes, advanced polymeric composites provide opportunities for large leaps in design, production, energy saving, product usefulness, and variety.

Many of these materials have been hardened to increase impact and fracture resistance, however, it is unclear if AM fully exploits these advantages. These materials are mostly used for developing ideas and producing low-performance parts, although there is an increasing demand for novel high-performance polymer materials and composites [1-9].

The following table summarize the research that has been done to investigate the effect of 3D printing on mechanical properties:

Table 1. Table summarizing the different research

Study	Research objectives/topic	Materials, machines, standards	Variable parameters	Mechanical properties
Tymrak, 2014 [1]	Mechanical properties in realistic conditions for different opensource printers	ABS, PLA, and Open-source printers (Lulzbot Prusa, Prusa Mendel, Custom Most RepRap, Mendel RepRap), ASTM D638, Slic3r®, Cura®, Skeinforge®	Variations of layer thickness and raster orientations	Tensile strength, elastic modulus
Ebel, 2014 [2]	Mechanical properties comparison ABS vs. PLA	ABS, PLA, Felix 1.0e, CB-printer or uPrint Plus, DIN EN ISO 527	Infill pattern, infill percentage	Tensile strength
Wittbrodt, 2015 [3]	Colour effect on mechanical Properties	PLA, Lultzbot TAZ, ASTM D638	5 colors (white, black, blue, Gray, natural)	Tensile strength
Lanzotti, 2015 [4]	Material properties of MakerBot 3D printer	PLA, Rep Rap Prusa I, ASTM D638	Layer thickness (2 levels), print orientation (2 levels), infill percentage (3 levels)	Tensile strength, elastic modulus
Torres, 2015 [5]	Influences of process parameters on torsion	PLA, MakerBot Replicator 2, ASTM E143	Layer thickness, infill density, postprocessing heat-treatment time at 100 °C (3 levels each)	Shear stress
Li, 2016 [6]	Process parameters effect on bonding degree and mechanical properties	PLA, MakerBot Z18, ASTM D638	Individual assessment of layer thickness (7 values), deposition velocity (8 values), infill rate (6 values)	Tensile strength

Torres, 2016 [7]	Mechanical properties optimization	PLA, Replicator 2, ASTM D638, ASTM E143, ASTM D648	Temperature, infill direction, infill percentage, layer thickness (2 levels for each)	Tensile strength
Liu, 2017 [8]	Process parameter effect on mechanical properties	PLA, MakerBot Replicator 2, GB/T 1040.2–2006, GB/T 9341–2008, GB/T 1043.1–2008	Deposition orientation, layer thickness, deposition style, raster variation, raster gap (3 levels each)	Tensile strength, flexural strength, impact strength
Chacon, 2017 [9]	Mechanical properties of PLA structures and optimal parameters selection	PLA, Wit Box desktop 3D printer, Cura®, ASTM D638, ASTM D790	3 building orientations, 4 layers thicknesses, feed rate (3 levels)	Tensile strength, flexural strength
H. Gonabadi,2020 [10]	the effect of processing parameters on the mechanical characteristics of PLA produced by a 3D FFF printer	PLA, (Creality Ender-3, Shenzhen, China) Cura 4.0, Tinius Olsen Universal testing machine, ASTM D638, ASTM D5379	build orientation, infill density and infill pattern (4 levels each)	Tensile strength and young's modulus, tension
Eustaquio García Plaza,2019 [11]	Analysis of PLA Geometric Properties Processed by FFF Additive Manufacturing: Effects of Process Parameters and Plate-Extruder Precision Motion	PLA, BQ Witbox, Cura, Talys urf CLI-1000, ISO 178	build orientation, layer thickness, feed rate (3 levels each)	Dimensional accuracy, flatness error, and surface texture
Khaled Benfriha, 2021 [12]	Effect of process parameters on thermal and mechanical properties of polymer-based composites using fused filament fabrication	CF-PA6, Flash Forge Adventurer 3, ZEISS (OLYMPUS BH2), HITACHI 4800 SEM–high resolutions, MA Q800, ISO 527-2, INSTRON 4301	liquefier temperature and platform temperature (4levels) print speed, layer height (3levels)	Temperature evolution, tensile strength, crystallinity
Vladimir E. Kuznetsova, 2018 [13]	Strength of PLA Components Fabricated with Fused Deposition Technology Using a Desktop 3D Printer as a Function of Geometrical Parameters of the Process	PLA, Ultimaker 2, Tescan Vega 3 LMH microscope, universal electromechanical testing machine	Nozzle Diameter, Layer Thickness, Printing Speed	Print Strength

Bakrani Balani, 2018 [14]	Influence of printing parameters on the stability of deposited beads in fused filament fabrication of poly(lactic) acid	PLA, HAAKE Rheomex OS, HAAKE PolyLab OS, HAAKE Melt pump OS, DSC Q200, ARES-LN2	Nozzle diameter, feed rate, and layer height	Shear rate and temperature. Velocity, viscosity
Patrich Ferretti 2021 [15]	Relationship between FDM 3D Printing Parameters Study: Parameter Optimization for Lower Defects	PLA, E3D v6 and E3D volcano nozzles, Slic3r, Cura	Shell Number, Layer Height, Nozzle diameter	tensile strength, compressive strength
Adi Pandžić, 2021 [16]	Experimental Investigation on Influence of Infill Density on Tensile Mechanical Properties of Different FDM 3D Printed Materials	PLA, ABS-Cura, Ultimaker S3 desktop 3D printer, Shimadzu AGS-X, Trapezium-X ISO 527-2	infill density	tensile strength and elastic modulus
Narges Dialami ,2020 [17]	Numerical and experimental analysis of the structural performance of AM components built by fused filament fabrication	PLA, Prusa i3 MK2S, Ultimaker Cura, ASTMD638, ISO 527-2 1A.	printing orientation, infill density	tensile strength and elastic modulus, Poisson's ratio
Vinicius Cabreira, 2020 [18]	Effect of infill pattern in Fused Filament Fabrication (FFF) 3D Printing on materials performance	PLA, Prusa i3, Slic3r v1.3.0, CEAST Impact Izod, Instron Emic 23 D, Marte, AY220 ASTM 256 and ASTM D638	infill patterns	resistance and tensile strength
Adi Pandzic 2019 [19]	Effect of Infill Type and Density on Tensile Properties of PLA Material for FDM Process	PLA, 3D Republika, Ultimaker 2+ FDM 3D, Shimadzu AGS-X machine, ISO 527-2, ISO 627-2	Infill type, infill density	tensile strength yield strength.

Aleksa Milovanović, 2020 [20]	Comparative analysis of printing parameters effect on mechanical properties of natural PLA and advanced PLA-X material	PLA and PLA-X, ISO 527-2, Shimadzu AGS-X, Trapezium-X'	layer height, infill density, printing orientation and sample humidity	tensile strength yield strength.
Can Tang 2020 [21]	Effect of process parameters on mechanical properties of 3D printed PLA lattice structures	Z-603s 3D printer, S-3400N tungsten filament scanning electron micro- scope, VIC-2D system	Printing temperature (°C) Printing speed Layer thickness	tensile strength yield strength elastic modulus.
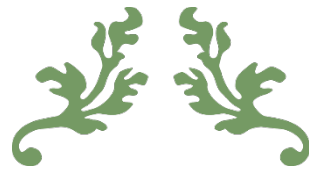
Chapter I

Industry 4.0 and Additive Manufacturing

A. Introduction on industry 4.0:

I. History

Future has always brought new technologies to simplify the humans' living requirements, initially it began with the first industrial revolution 1.0 at the end of the 18th century, were steam-powered machinery was introduced, resulting the reduction of human efforts.

By the discovering of electricity in the time frame of "1870,1914" the second industrial revolution 2.0 appeared, where it offered "increase of speed, mass production, while maintaining low designs and manufacturing flexibility ".

In 1969, the third industrial revelation 3.0 emerged, which brought about electronics and automation. This new technology enhanced the quality speed and flexibility by introducing digital technologies, robots monitored by computers affecting designing and manufacturing.

Ultimately, the fourth industrial revolution 4.0 was brought onward around the 2010 era, aiming to fulfil the futuristic needs of the industry; the latter is highly dependent on disruptive technologies such as:

- ❖ Additive manufacturing;
- ❖ Smart machines;
- ❖ Autonomous robots;
- ❖ Smart materials;
- ❖ Internet of tings;
- ❖ Virtual Reality / augmented reality;
- ❖ Cloud computing;
- ❖ Artificial intelligence.

All in the sole purpose of combining manufacturing machines with IT creating smart factories.

Industry 4.0 advantage is the fact it is connected and uses digital technologies, which is not available in the conventional machining, meanwhile additive manufacturing seems to be an adequate choice to integrate digital technologies such as cloud computing, big data, artificial intelligence.

Additive manufacturing is a vital part of providing extensive contribution to industry 4.0, it reduces material wastage to create a board impact on the environment, and it is now a reliable as a disruptive technology to complete the required task in industry 4.0 it is the integration of design software in 3d printing machines, to complete the manufacturing of the product, AM is an innovative manufacturing process by which inventory is stored in digital form and complete manufacturing tasks when required, so it is a flexible approach.

Additive manufacturing has the ability to reach its full potential in tomorrow's smart factories when designing items for production, the technique of manufacture is frequently the most essential issue for an engineer. A design can be created via a variety of production processes, each

with their own set of advantages and disadvantages. Any mechanical part is designed to accomplish a specific task relies on their mechanical property, and the mechanical properties is lean on the manufacturing processes method used to elaborate the mechanical part.

II. Classification of manufacturing techniques:

II.1. Formative (injection molding, casting, stamping and forging):

To produce the plastic deformation of a material into a desired shape, forming procedures employ stresses such as compression, tension, shear, or any combination of these. This is a common production technique for polymers and metals. It requires a substantial initial investment in tooling (molds) but it subsequently produces parts fast and at a relatively low unit price.

II.2. Subtractive (CNC, turning, drilling):

Subtractive manufacturing is a method of producing an object by eliminating superfluous materials from a stock in order to get the required shape. Best suited for pieces with generally basic shapes, manufactured in low-to-medium numbers, and typically composed of functional materials.

II.3. Additive (3D printing):

Additive manufacturing (AM) or additive layer manufacturing (ALM) is the industrial production name for 3D printing, which is a computer-controlled process that creates three-dimensional objects by depositing materials, usually in layers, and is best suited for low volume, complex designs that formative or subtractive methods cannot produce, or when a unique one-off rapid prototype is required.

III. Cost comparison:
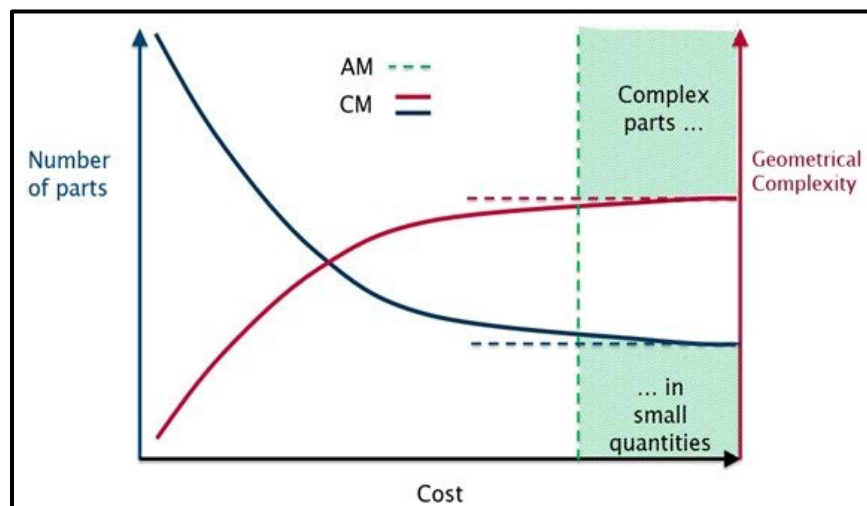
Figure 1. Cost comparison between different manufacturing techniques

B. Additive Manufacturing:

I. History of 3D Printing:

Table 2 Time-line history of AM technology [23]

1980	Hideo Kodama Files the first 3D Printing patent application
1984	Birth of Stereolithography (SLA)
1986	First patented 3D printer
1989	Stratasys Commercialize the first Fused Deposition Modeling (FDM) printer
1992	3D Systems Commercialize the first SLA machine
1995	Fraunhofer Institute develops the first Selective Laser Melting (SLM) machine
2001	EOS Commercialize the first Selective Laser Sintering (SLS) powder-based machine
2002	Arcam Commercialize the first Electron Beam Melting (EBM) machine
2007	Arcam produce the first CE-certified Orthopedic implant
2010	Organovo produces the first 3D printed human blood vessel
2013	First 3D printed robotic human heart
2015	Bio-ink is introduced to the market by Cellink, to print tissue cartilage
2016	Mass production of 3D printed engine parts
2019	World biggest 3D printed building in Dubai by Apis Cor
2021	BICO develops the world's most accurate 3D bioprinter "Quantum X Bio"

II. Overview of 3D Printing:

It might be tough to choose the best 3D printing technique for a certain design. Because of the variety of 3D printing methods and materials available, many procedures are frequently acceptable, with each offering differences in features such as dimensional accuracy, surface quality, and post-processing needs.

III. Classification of 3D printing technologies:

The ISO/ASTM 52900 Standard was developed in 2015 to standardize the terminology and identify the various ways of 3D printing. Seven process categories have been defined.
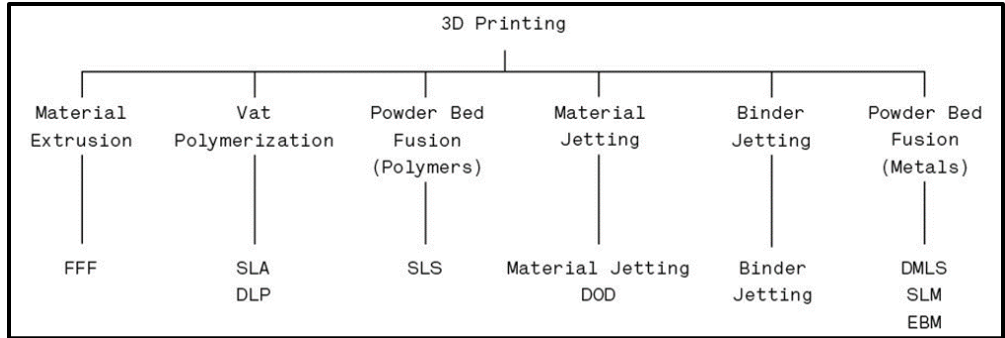
Figure 2. 3D Printing Categories by the ISO52900 standard [24]

IV. The 3D printing process:

i) Producing a 3D file

The first stage in the 3D printing process is to create a digital model. Computer Aided Design is the most popular approach for creating a digital model (CAD). Reverse engineering may also be used to create a digital model by scanning it in 3D.

ii) STL creation and file manipulation

To 3D print an item, a CAD model must be translated into a format that a 3D printer can understand. This is accomplished by first turning the CAD model into a Stereo Lithography (STL) file, which employs triangles (polygons) to represent the surfaces of an item, therefore reducing the sometimes-complicated CAD model. Once created, the file is loaded into a slicer application (which transforms the STL file to G-code) that slices the design into the layers that will be utilized to construct the part.

3. Printing   **4. Removal of prints**   **5. post-processing**
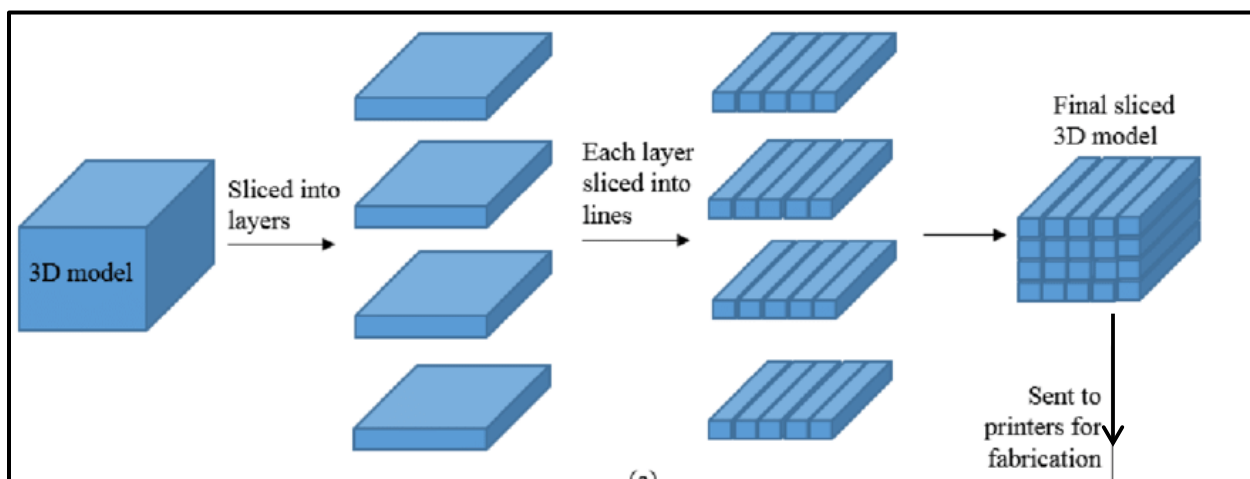
Figure 3. Slicing Process
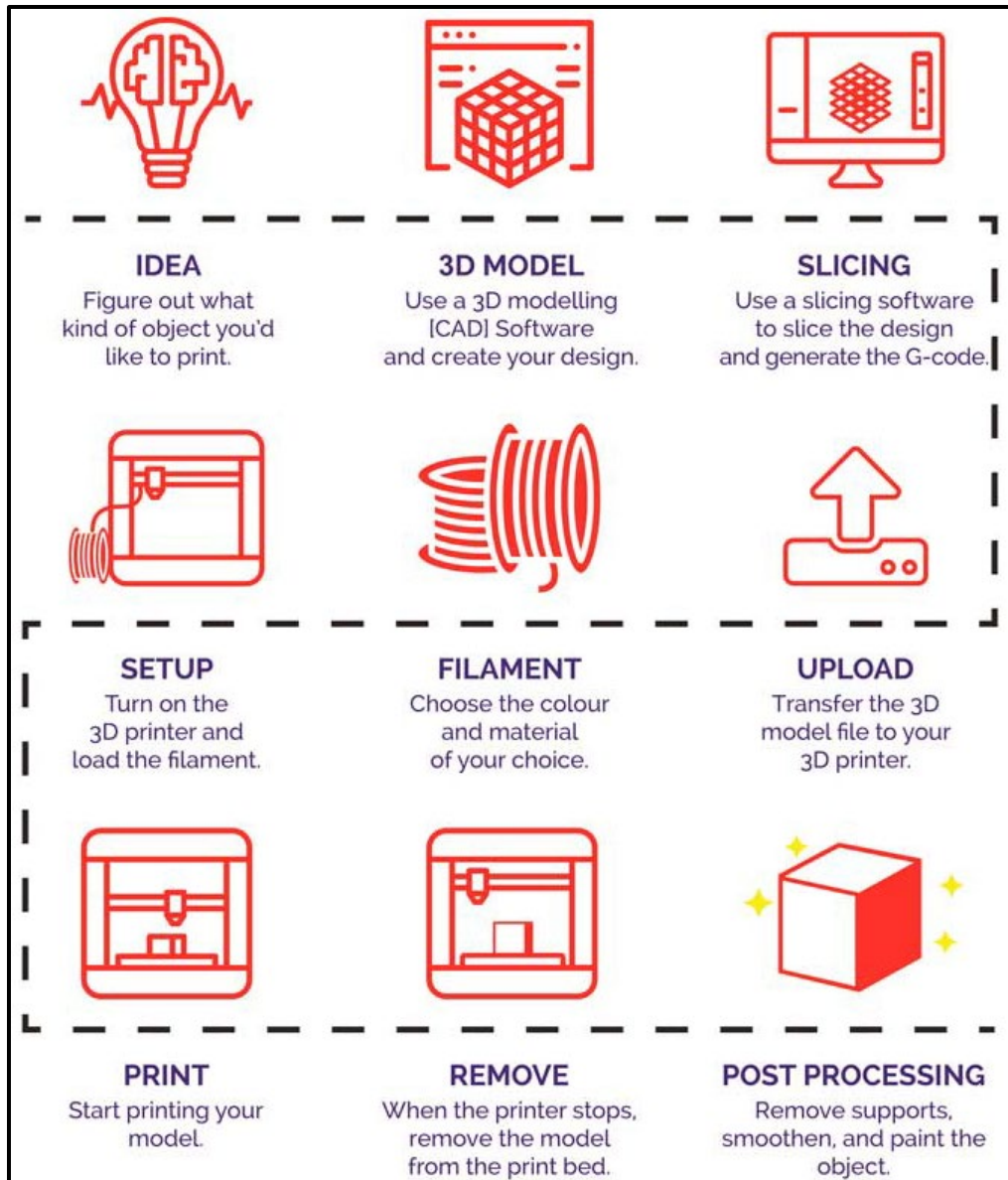
Figure 4. 3D Printing Process

IV. 3D printer's type:

IV.1. Material extrusion (FFF):

Fused Filament Fabrication, or FFF (more often referred to as Fused Deposition Modeling, or FDM), is the most prevalent material extrusion process. A spool of filament is inserted into the printer and passes through the extrusion head. When the printer nozzle reaches the desired temperature, a motor pushes the heated filament through the nozzle, melting it.

The printer then translates the extrusion head in the x and y direction, to deposit the molten material in a precise position where it solidified at the end of the process. Once the layer is finished,

the build platform slides down to start the new layer and the procedure is repeated to utile all operations of building the shape is achieved.
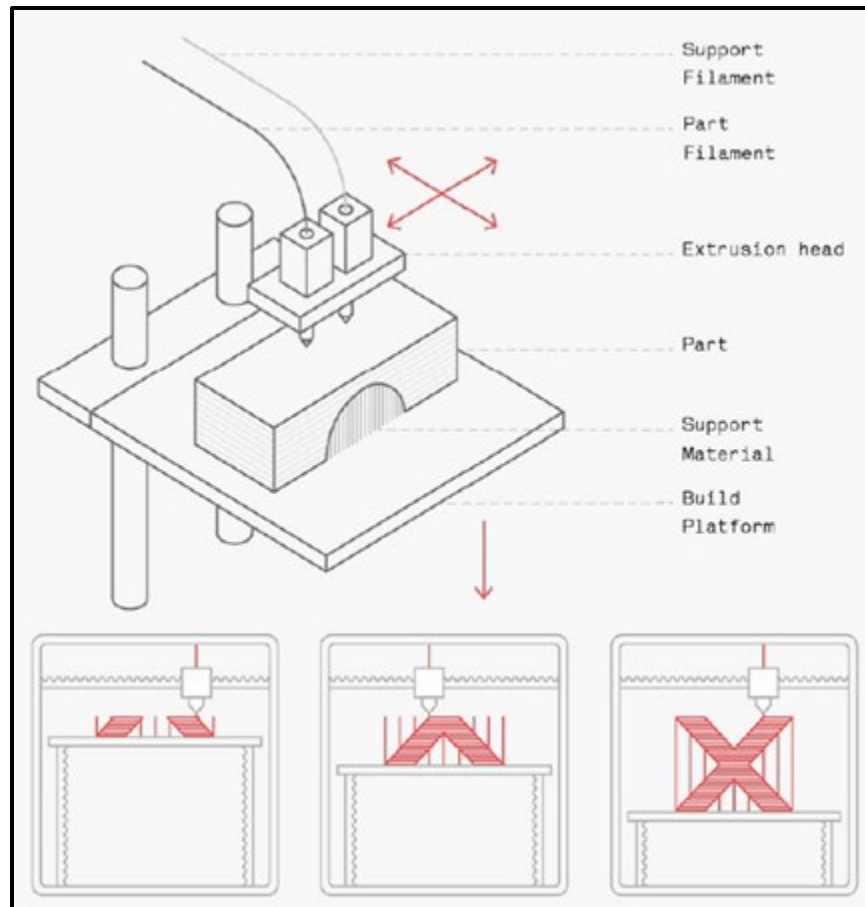
Figure 5. Schematic and the printing process of a FFF printer [25]

IV.2. VAT Polymerization (SLA/DLP):

SLA is well-known for being the first 3D printing method. Charles W. Hull created the term stereo lithography after patenting the technique in 1986 and establishing 3D Systems to market it. The method uses galvanometers or galvos (two mirrors on the x and y axes) to swiftly direct a laser beam over a vat, the print area, curing and hardening resin as it travels. Layer by layer, this procedure deconstructs the design into a sequence of points and lines that are provided to the galvos as a set of coordinates. To cure components, the majority of SLA machines employ a solid-state laser.

Compared to SLA, DLP employs a digital light projector screen to flash a single picture of each layer at once. Because the projector is a digital screen, each layer's picture is made up of square pixels, resulting in a layer made up of little rectangular bricks known as voxels. Light-emitting diode (LED) screens or a UV light source (lamp) guided to the surface of a substrate by a Digital Micro mirror Mechanism cast light onto the resin (DMD "which is a collection of micro

mirrors that regulate where light is projected and produce the light pattern on the build surface"). Which is why DLP may print quicker than SLA since a whole layer is exposed at once rather than tracing the cross-sectional area with a laser pointer.

SLA printers employ a point laser rather than the voxel technique used by DLP printers.

This makes DLP faster than SLA when printing an identical part Since with SLA it takes longer to expose the cross-section of a part because of the 'point laser', while DLP can expose the entire part in a single flash (depending on part size) [25].
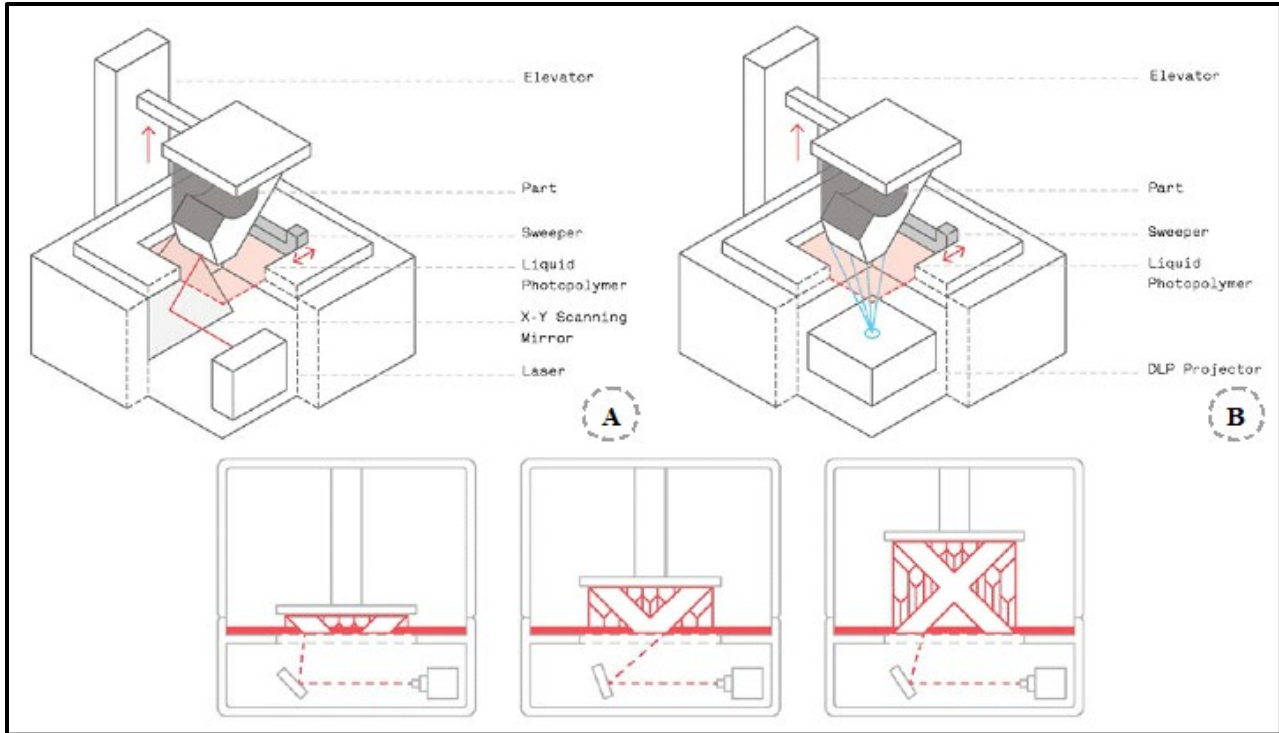
Figure 6. Schematic of an SLA printer Figure B Schematic of a DLP Printer and their printing process

IV.2.1. Bottom-up vs. top-down:

Vat Polymerization machines may manufacture components in two orientations (bottom-up or top-down as illustrated in "Figure 7" SLA and DLP printers are available in both setups, with the design varying according to the manufacturer.
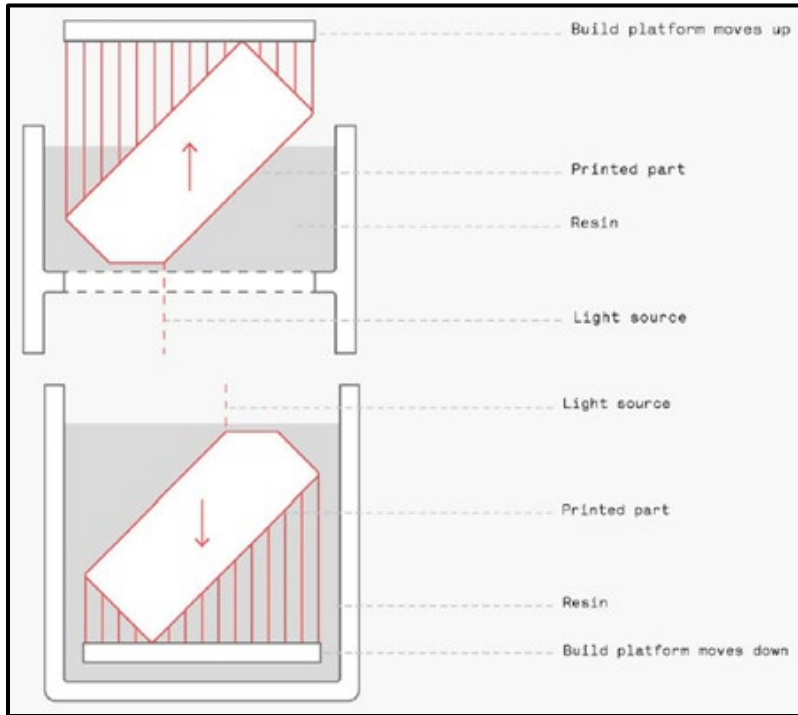
Figure 7. Bottom-up Vs Top-Down Vat Polymerization printing [25]

IV.3. Powder Bed Fusion "Polymers" (SLS):

Powder Bed Fusion procedure using polymer powder is commonly referred to as Selective Laser Sintering (SLS) or simply Laser Sintering (LS) in the 3D printing industry.

The SLS process begins with a container of polymer powder being heated to a temperature slightly below the polymer's melting point. A recoating blade applies a very thin layer of powdered material to a construction platform (usually 0.1 mm). The surface is then scanned by a CO_2 laser beam. The laser sinters the powder selectively and solidifies a cross-section of the component. A pair of galvanometers, like in SLA, concentrate the laser to the correct spot.

When the whole cross-section is scanned, the construction platform lowers in height by one layer thickness. The recoating blade drops a fresh layer of powder on top of the newly scanned layer, and the laser begins to sinter the part's subsequent cross sections onto the previously solidified cross-sections. This procedure is performed until all components are manufactured.
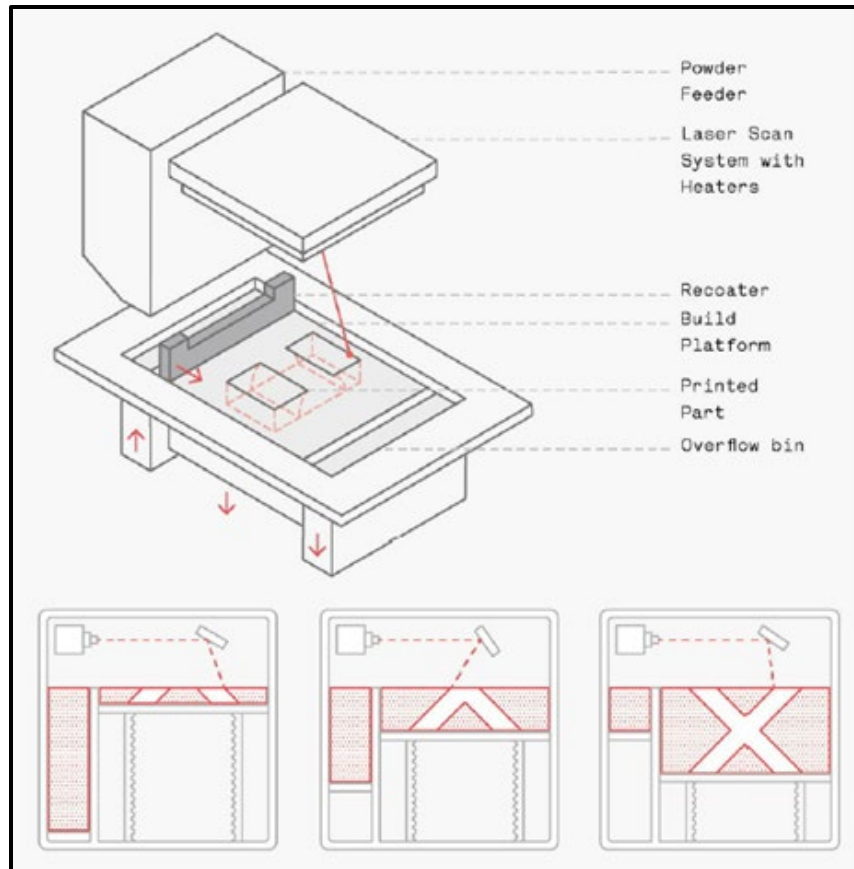
Figure 8. Schematic and the printing process of a SLS printer [25]

IV.4.   Material Jetting (DOD):

The print head sprays hundreds of small droplets of photopolymer, which are subsequently cured (solidified) by a UV laser. After a layer is deposited and cured, the build platform is lowered by one layer thickness, and the process is repeated to manufacture a 3D component. Material Jetting techniques need support, which is printed concurrently during the build from a soluble material that is removed during post-processing.

Particularly Drop on Demand (DOD) printers contain two print jets, one for build materials and the other for dissolvable support material. It follows a predetermined route and jet material in a single moving point to produce the cross-sectional area of a component layer by layer. DOD printers also use a fly-cutter to ensure a completely flat surface before printing the following layer. they are commonly utilized to generate "wax-like" patterns for lost-wax casting/investment casting and mold manufacturing applications.
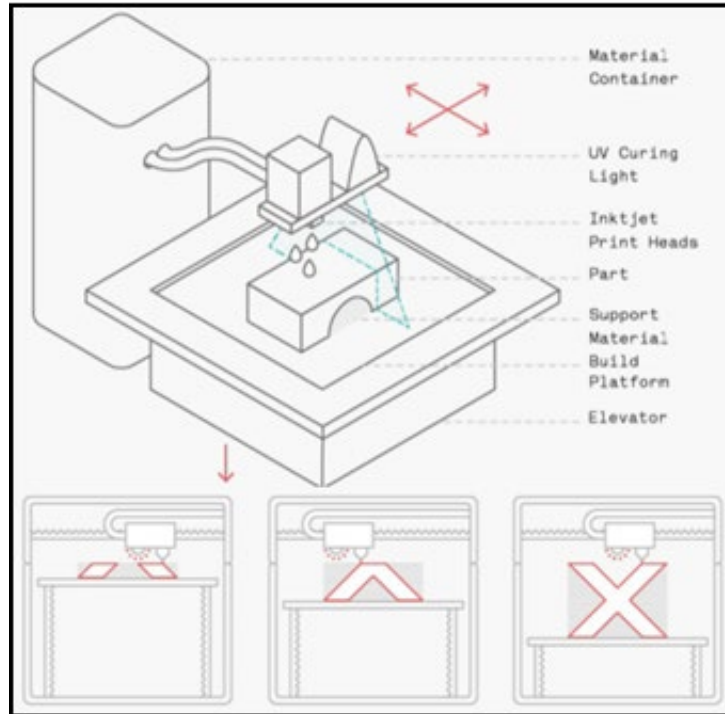
Figure 9. Schematic and the printing process of a DOD printer [25]

IV.5.   Binder Jetting:

Binder jetting is the process of moving a print head over the powder surface and depositing binder droplets that bind the powder particles together to create each layer of the component. After printing a layer, the powder bed is lowered and a new layer of powder is placed over the previously printed layer. It is then left in the powder to cure and strengthen. Following that, the component is withdrawn from the powder bed and the unbound powder is extracted using compressed air. This procedure is continued until a solid component is produced.

2 Types of procedures can be compromised:

- Sand Binder Jetting is a low-cost way of manufacturing sand-based components. The two most prevalent sand printing processes are:

- **Full-color models**: "A printhead initially jets the binding agent, followed by a secondary print head that jets in color, allowing full-color models to be produced".
- **Sand casting cores and molds**: "The cores and molds are removed from the construction area after printing and cleaned to eliminate any loose sand. In most cases, the molds are then immediately ready for casting.

-Creating metal components enables the creation of complex shapes that would be impossible to create using standard manufacturing processes. Only secondary processes, can generate functional metal components.

Such as:

- ❖ **Infiltration:** "metal powder particles are bonded together using a binding agent to produce a green state component. When fully cured, the parts are taken from the loose powder and placed in a furnace, where the binder is burned off, leaving gaps throughout the component. The bronze is then used to enter the voids by capillary action, producing components with great density and strength."
- ❖ **Sintering:** "After printing, green state components are cured in an oven, allowing them to be handled. The parts are then sintered to a high density in a furnace.
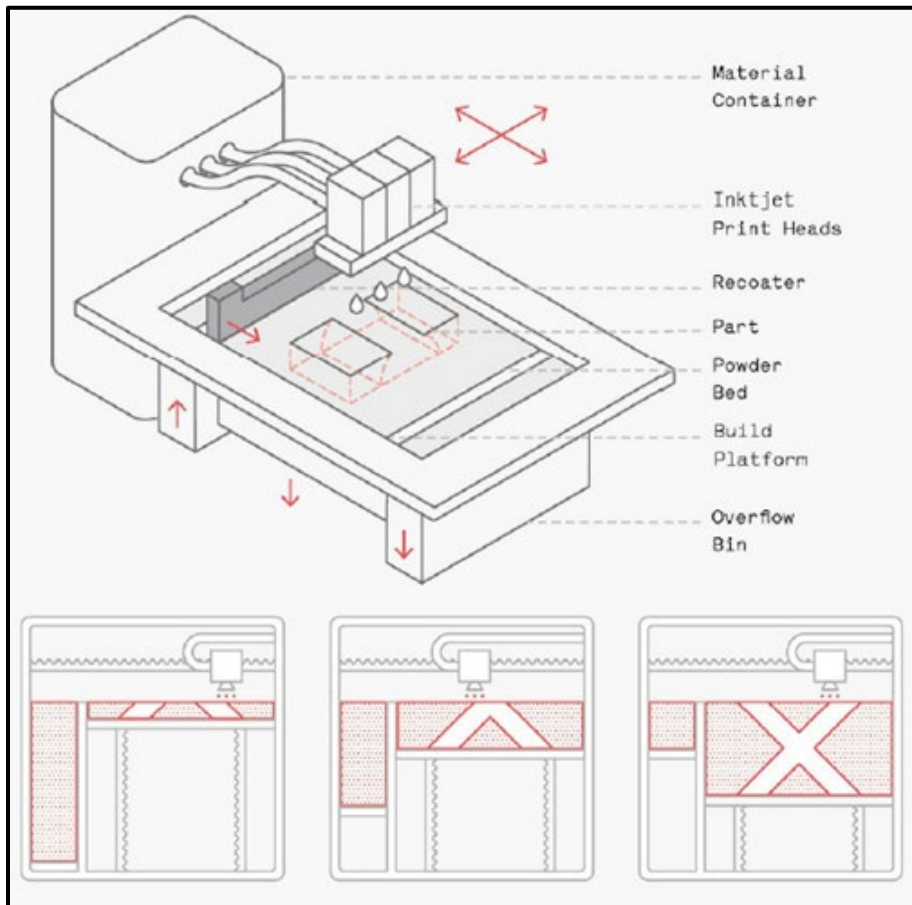
Figure 10. Schematic and the printing process of a Binder jetting printer [25]

IV.6.   Powder Bed Fusion "Metals" (DMLS/SLM), (EBM):

Direct Metal Laser Sintering (DMLS) and Selective Laser Melting (SLM) both produce parts in a manner similar to SLS. The main distinction is that they are used in the manufacture of metal parts. DMLS does not melt the powder, but rather heats it to a point where it can bind together molecularly. SLM employs a laser to achieve a complete melt of the metal powder, resulting in a homogeneous part [25].

Electron Beam Melting (EBM) involves scanning a thin layer of powder with a focused electron beam, causing localized melting and solidification over a specific cross-sectional area. These layers are stacked to form a solid part. Because of its higher energy density, EBM has a generally faster build speed than SLM/DMLS. EBM parts are created in a vacuum, and the process is only applicable to conductive materials.
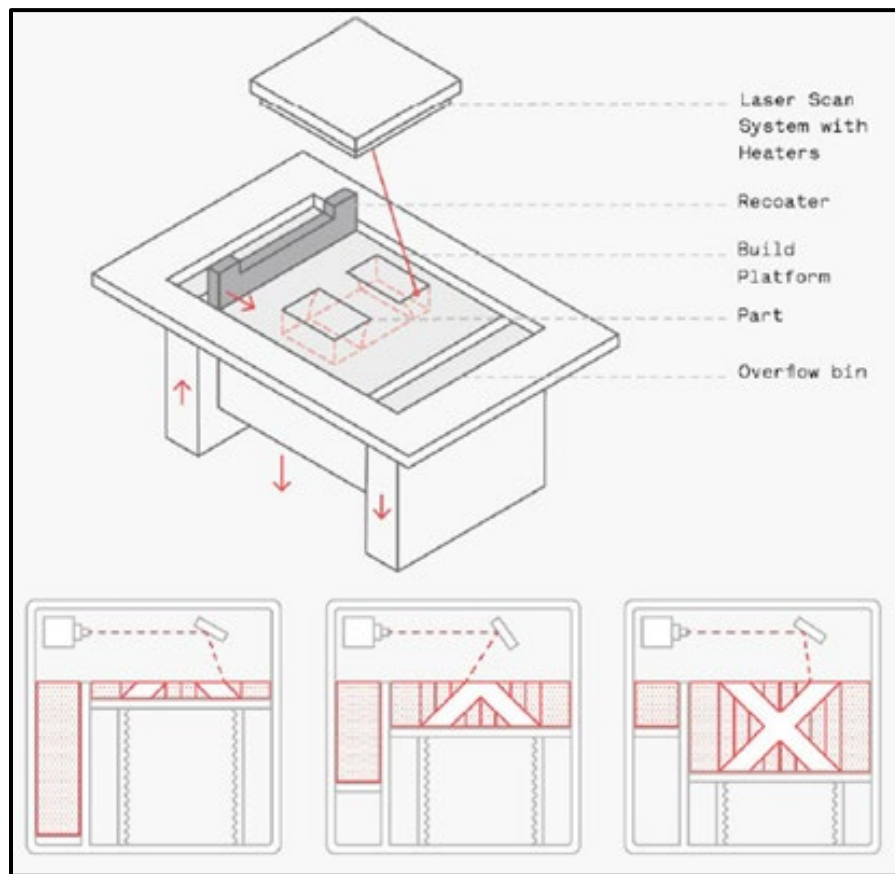
Figure 11. Schematic and the printing process of a Binder jetting printer

V.   Printer characteristics:

V.1.   Material extrusion (FFF):

The user can control the quality of the extruded filament by adjusting the build speed, extrusion speed, and nozzle temperature. The nozzle diameter and layer height play a crucial role in the final resolution definition of the printed part., The smaller nozzle diameter and lower layer height, the smoother the surface and more detailed level of shape are obtained While all parameters influence a part's dimensional precision. Also, some machines utilize automated settings based on the type of material being used in additive manufacturing.

Due to differential cooling, a warping phenomenon takes place. Where various areas of the printed section contract and shrink due to the cooling rate between different layers. A heated bed, as well as strong bed adhesion, are crucial in fixing an FFF component down and reducing the probability of warping or distortion issues [25].

Layer adhesion or bonding is a critical component of the FFF printing process. The extruded filament must bond and solidify with previously printed layers to produce a solid, cohesive component. The filament is pushed against the preceding layers to achieve good adhesion between layers.

Support structure is required especially for any overhanging elements that are shallower than 45 degrees relative to the ground plane, or when there is no layer beneath to print on. the support material is a low-volume, have a lattice structure that can be removed easily after the end of the part printing. Maintaining the 45-degree limit is advised for precise prints with a smooth surface finish.

The drawback of support is that it has an undesirable effect on the quality of the surface If a smooth surface is required, post-processing is usually necessary. In most cases, FFF components are not printed solid. Parts are printed using an interior, low-density structure known as an infill to optimize material and time production. The percentage of infill can be changed depending on the application of a component. The geometry of the infill affects the performance of an FFF component as well. Infill geometries that are commonly used include triangular, rectangular, and honeycomb.

V.2.   VAT Polymerization (SLA)/(DLP):

In contrast to FFF, the majority of printer settings on Vat Polymerization machines are fixed and cannot be altered. Part orientation/support position, layer height, and material are often the sole operator inputs, and they are all set during the slicing step. Most printers automatically modify settings based on the kind of material being used.

The surface quality and precision of a component are governed by layer height and light source resolution (spot size or projector resolution). The majority of Vat Polymerization printers create components with layer heights ranging from 25 to 100 microns [25].

It may be feasible to change out DLP projector lenses to employ a narrower beam for extremely tiny, highly detailed prints. This enables the beam to print fewer layers at a quicker rate and with more resolution.

The position and quantity of support are greatly influenced by the type of printer utilized. Top-down printers have support needs comparable to FFF, with overhanging features like bridges requiring material to hold them up and allow them to be printed properly.

Support for bottom-up printers is more difficult. When the print is removed from the base of the vat during the peeling step, build layers might result in significant stresses. The print may fail if the peeling step is unable to remove the construct from the vat. As a result, components are printed at an angle.

V.3.   Powder Bed Fusion "Polymers" (SLS):

Optimal machine settings are typically set up by the printer manufacturer. Resulting in the machine automatically adjusting to the material used 'heat up process, printing and cooling phases', but a variety of characteristics influence how well a component prints on an SLS machine. The precision and surface quality of a printed item is typically defined by laser spot size and layer height '100 microns as the default (0.1 mm)'. SLS components' surface finishes are generally matte and gritty to the touch. Powder particle geometry and size also play an important influence in establishing a part's characteristics. Finer powders produce a smoother part surface, whilst coarser particles harm surface quality.

How effectively components are packed in the given build volume is one of the most essential variables to consider when preparing an SLS print. The printer has several various bins, the height of which determines the printing time.

SLS, like all 3D printing techniques, builds components layer by layer. Adhesion between layers is critical for achieving a robust, coherent component. The powder particles fuse n numerous directions after being heated initially and then exposed to the sintering laser. As a result, the components are essentially homogenous [25].

V.4.   Material Jetting, (DOD):

Material Jetting printers eject build or support material to make components. The surface quality and minimum feature size of a component are influenced by the size of the jet droplets and the layer height it automatically alters machine settings according to the material being printed.

It is one of the most precise kinds of 3D printing, capable of creating components with layer heights as low as 16 microns, resulting in exceptionally smooth surfaces. Most Material

Jetting machines heat the resin to an optimum temperature (30 ~ 60°C) to regulate the viscosity of the photopolymer during printing, as it is critical that the construction material is in a liquid state.

Material Jetting allows printing components with either matte or glossy settings. Regardless of orientation or structural needs.

All pieces are printed in two separate materials: one for the primary construction material and one for dissolvable support. That is readily removed with gentle agitation resulting in a surface with no sign of support at all. But the support is a printed solid, which requires a considerable quantity of material, increasing manufacturing time and expense

V.5.   Binder Jetting:

The precision and surface quality of the components are determined by the chosen layer height, jetted droplet size, powder size, and geometry. Binder Jetting, like SLS, does not require the printing of support structures since the components are surrounded by powder during the printing process. This shortens post-processing periods and decreases the quantity of material used per print.

V.6. Powder Bed Fusion "Metals" (DMLS/SLM), (EBM):

Laser spot size, powder geometry, and layer height all influence the accuracy and surface quality of DMLS/SLM printed parts. As for Support structures they necessitate the use of support material they are required to connect unsupported geometry to the build platform and act as a heat sink for thermal energy due to the high temperatures involved in the process and the layer-by-layer nature of part construction [25].

VI.   Dimensional accuracy:

Dimensional accuracy refers to how well a printed product fits the source file's dimensions and specifications. It should be taken into account while deciding on a procedure. Even if the printing technology has already been selected, understanding the standard accuracy and typical causes of failure will aid in the design process.

Table 3. Dimensional accuracy for all printing methods

Dimensional accuracy	±0.5%	±0.3-±0.2	±0.1%
Printing Method	FFF lower limit: ±0.5mm SLA/DLP lower limit: ±0.15mm	Binder Jetting ±0.2mm(metal) ±0.3mm (sand) SLS lower limit: ±0.3mm	Material jetting DMLS / SLM

VII.   3D Printing Materials:

3D printing empowers parts prototyping and manufacturing, for a wide range of applications quickly and cost-effectively. But choosing the right 3D printing process is just one side of the coin. Ultimately, it'll be largely up to the materials to enable the creation of parts with the desired mechanical properties, functional characteristics, or looks [25].

VII.1.   Material extrusion (FFF):

In general, thermoplastics are the best when looking for good mechanical properties such as PEEK and PEI they have good mechanical properties but are typically produced using industrial equipment that allows better control over the print environment. ABS and PLA are easy to print with but are Susceptible to Warping, PETG got High impact & chemical resistance, TPU and Nylon (PA) is commonly used for its Flexible and rubber-like parts and its good elongation.

VII.2.   VAT Polymerization (SLA/DLP):

Vat Polymerization methods create components from thermoset photopolymers. Photopolymer resins have a limited shelf life as well (typically one year, if stored properly).

When utilizing Vat Polymerization to create components, it is important that the pieces be appropriately cured under UV light after printing. This will guarantee that they attain their best characteristics "Biocompatibility, Transparency, Temperature resistance, Rubber-like flexibility"

VII.3.   Powder Bed Fusion "Polymers" (SLS):

Low thermal conductivity materials are best suited for Powder Bed Fusion because they display more stable behavior during the sintering process. To create components, the polymer side of Laser Sintering nearly entirely uses one type of thermoplastic polymer known as polyamide that offers great long-term stability and chemical resistance, with nylon being the most common

commercial polyamide when combined with other materials such as aluminum, glass, carbon, and graphite to produce a composite powder with better mechanical properties, heat/chemical resistance, or appearance [25].

VII.4.   Material Jetting (DOD):

Material Jetting technology necessitates materials with low viscosity that can be properly blasted in droplet form. Material Jetting, unlike other 3D printing methods, always requires two distinct resins while printing; one for the main construction material of the item and another for support material.

VII.5.   Binder Jetting:

Binder Jetting technology uses a powder and a binding agent to create parts. Powders are available in a variety of materials such as "Sandstone, Stainless steel-bronze matrix that got excellent mechanical properties, Tungsten Used for the production of cutting tools, carbide and Inconel alloy with good temperature resistance",100% of the unbounded powder can be recycled.

VII.6.   Powder Bed Fusion "Metals" (DMLS/SLM), (EBM):

DMLS/SLM technology, can produce parts from a variety of metals including aluminum, ("stainless steel, titanium" due to their relatively low thermal conductivity), cobalt-chromium, and Inconel. It's also used to make jewelry out of precious metals like gold, platinum, palladium, and silver. [25]
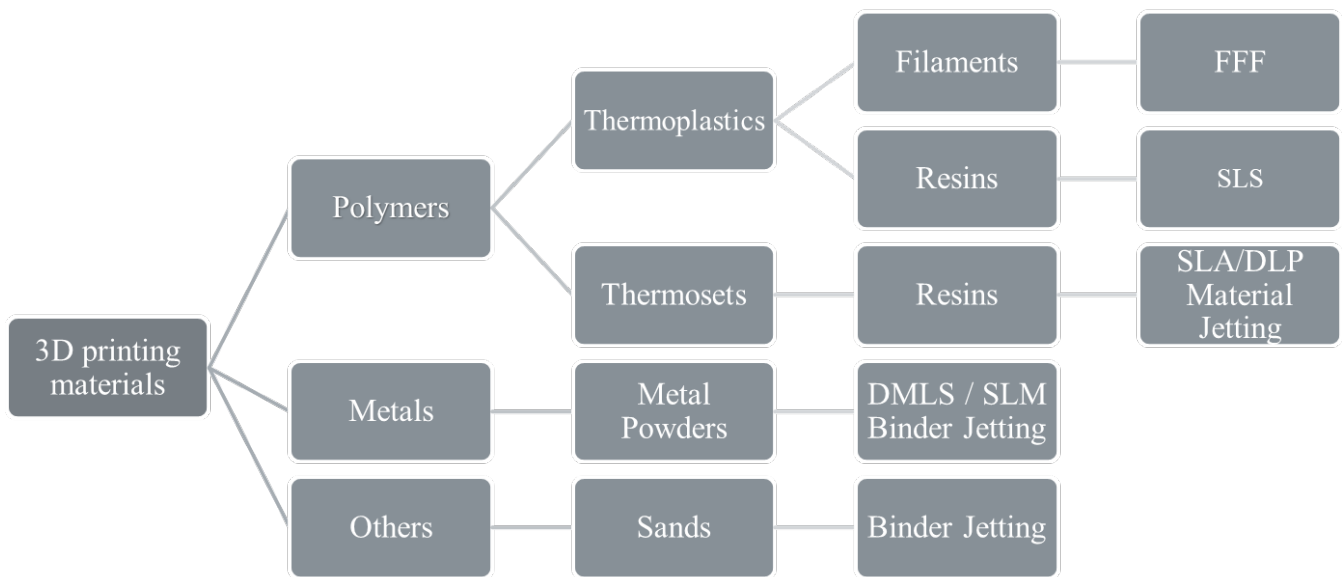
Figure 12. 3D Printing Materials Groups

VIII.   Post processing:

Parts manufactured using 3D printing technology often need some kind of post-production treatment. Post-processing is a key phase in the 3D printing process. In 3D printing, post-processing refers to any procedure or task that must be performed on a printed item, as well as any technology used to further enhance the product. Post-processing 3D printed components choices include removing support or superfluous material, washing and curing, sanding or polishing a model, and painting or dyeing. As such, the following post-processing techniques can be used in many combinations depending on the printing process [25].

- **Support Removal**: If support is required, it must be removed after printing whether it is cut or broken off "FFF SLA SLM/DMLS" or soaked in sodium hydroxide solution "Material jetting"
- **Surface Finish:** Sanding is required if a smooth surface is needed and the parts are going to be coated a grit sand paper and a solution to wipe/rinse with is used to achieve that "Material jetting SLA FFF". Media tumblers (small chips that vibrate on the outer surface) erode the part to a polished state "SLS/SLM". Machining, electro polishing is employed to improve the surface state; micro machining is operated on demanding surfaces to reduce friction "SLM/DMLS".
- **Powder removal:** Loose powder is removed with compressed air jets then the surface has to be cleaned via plastic bead blasting to remove the prints for a smoother surface "Binder Jetting, SLS, and SLM/DMLS".
- **Improving Properties:** Metal Plating is where part is cleaned and coated with a conductive layer 'nickel, gold, stainless steel, chrome' then goes through standard metal coating process to improve strength, electrical conductivity, and hardness of the parts "FFF, SLS, DMLS/SLM and Material/Binder Jetting" .
- **Post Coating/Curing:** Polishing is applied first to prepare for the Coating and Priming "SLA FFF". Parts are coated with a lacquer or an epoxy coat, which primes the surfaces resulting in a smooth surface for painting improving wear resistance, surface hardness, and water-tightness, locking paint in and limiting smudges on the surface. Increasing its lifespan and protecting it from exposure "SLA, FFF, SLS, Material Jetting".
- **Dyeing:** Parts are immersed in a hot dye color bath with the desired color to ensure full internal and external coverage "SLS and Material Jetting.

IX.   Applications:

One of the reasons for Additive manufacturing new upswing in usage is that it is a simple application that will be applied in applications in all sorts of areas. In its earlier years, 3D printing demonstrated higher entry prices. 3D printer models and fabrics were costly. In past years, with improvements and fluctuations in these technologies of both these machines and materials employed at them, prices have been falling down, making 3-D printing more convenient and cost-

effective, in industry and education. In fact, 3D printing has become so popular that it is now being used in many industries such as describbed in the graphs below:
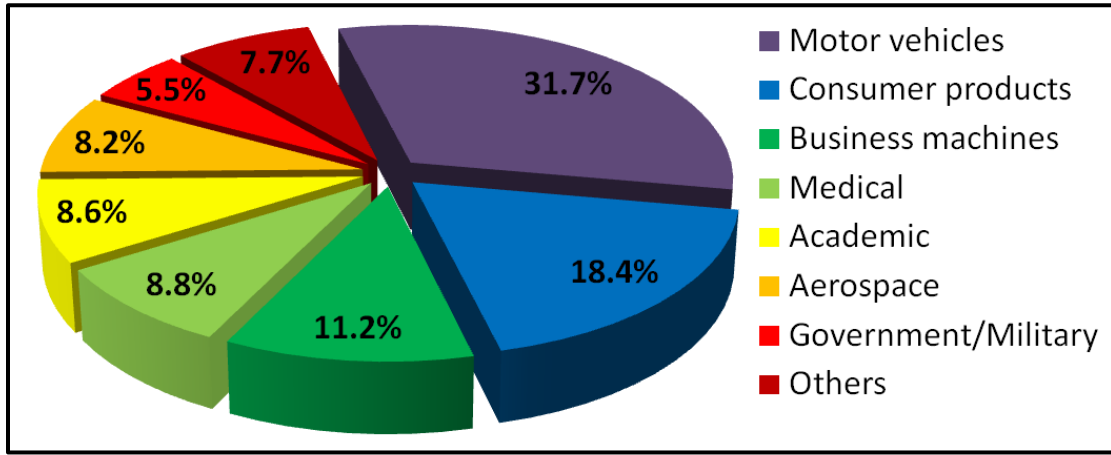
Figure 13. Principal fields of application of 3d printing [Cotteleer and Joyce, 2014] [26]

Below are some applications listed by printers type:

IX.1.   FFF Applications:

- Investment casting patterns
- Electronics housings
- Jig and fixtures
- Form and fit testing
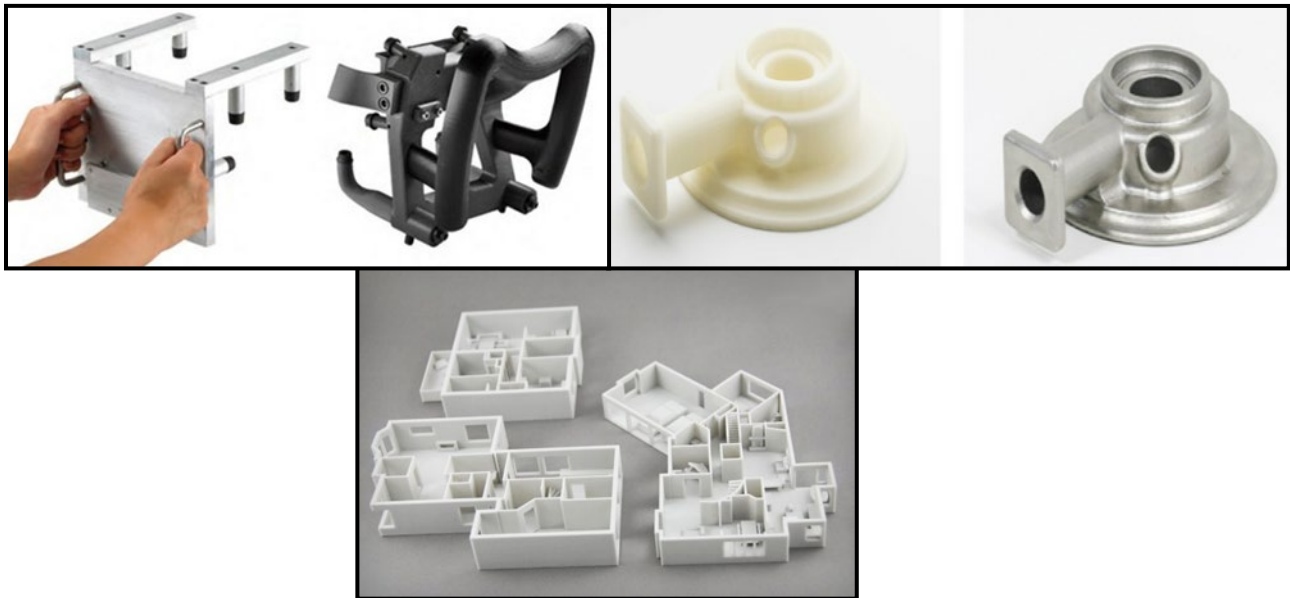
Figure 14. Top Left « Printing of Jigs And Fixture » ,Top Right « printed cast pattern and final metal investment cast , Bottom « House architecture Prototype »

IX.2.   SLA/DLP Applications:

- Injection and mold-like prototypes
- Jewelry (investment casting)
- Dental applications
- Hearing aids
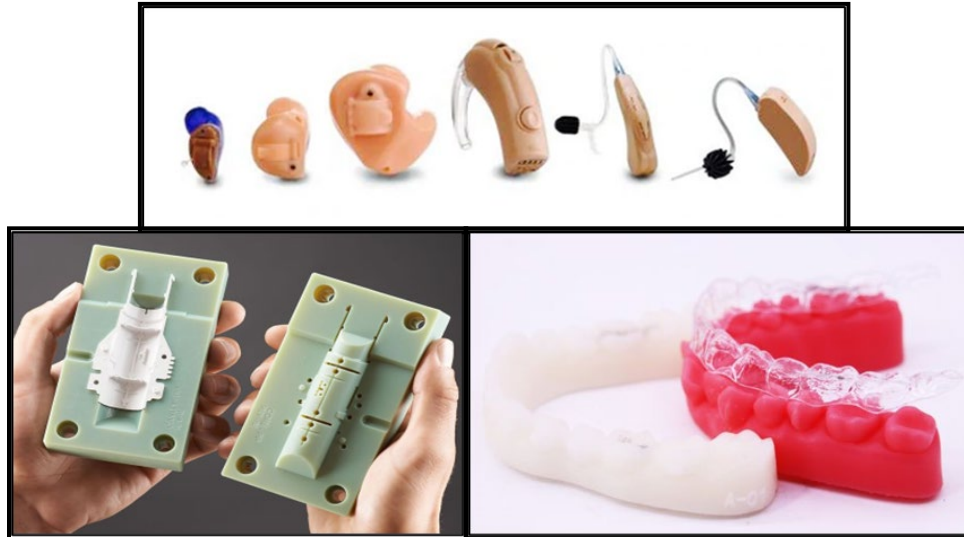
Figure 15. Top « SLA Printed Hearing Aids » , Bottom left «printed injection mold » bottom right « Printed personalized dental mold »

IX.3.   SLS Applications:

- Functional parts
- Low run part production
- Complex ducting (hollow sections)
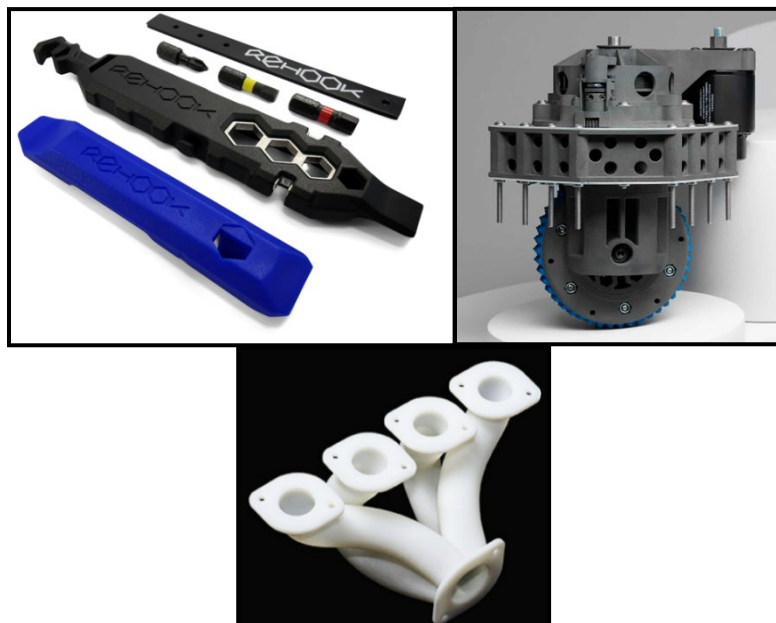
Figure 16. Top left «printed bike chain repair kit 'REHOOK' » Top Right « FormLabs Fuse 1 full functionning engine » , Bottom « functional ducting used in automotive application »

IX.4. Binder jetting Applications:

- Full-color models
- Sand casting
- Functional metal parts
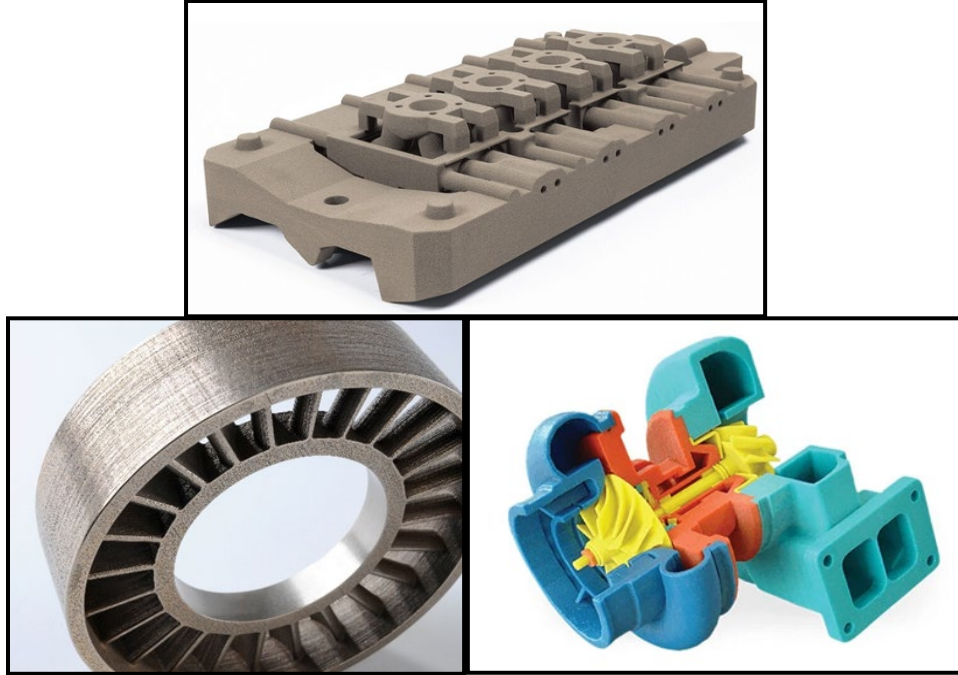
Figure 17. Top « multi-part sand cast assembly used to cast an engine block » , Bottom left « oil and gas stator printed from stainless steeland infiltrated with bronze » , Bottom Right « a full Color Jetting Printed engine »

IX.5. DOD Applications:

- Full color Visual prototypes
- Medical models
- Injection mold-like prototypes
- Low-run injection molds

Figure 18.Top Left «Low Run Injection Molded Sensor Housings », Top Right «Steel Base Injection mold» Bottom « Full Model of a human skull »

IX.6.   SLM/DMLS Applications:

● Waveguides making
● Medical applications
● Aerospace and automotive applications

Figure 19. Top « prinrted Aluminium Waveguide » , Bottom Left « printed Hip Implant » , Bottom Right « tesla roadster space x with 100% 3d Printed 'SuperDraco thrusters' »

X.   Benefits and limitations:

Manufacturers have recognized the benefits of making small batches of sophisticated items since the emergence of 3D printing in the 1980s. With new technologies being released on an ongoing basis and so many industries shifting to additive manufacturing in recent years, more and more benefits are being exposed on a regular basis. Including the following for each printing technique previously described: for the FFF printing functional parts while being low cost is a main win. Having the ability of fine feature details with a smooth surface is what SLA/DLP printers are characterized with. Functional yet complex geometrical parts with good mechanical properties is why SLS printers are used for end-use parts manufacturing. Material jetting offers three major advantages, best surface finish, full color and multi-material printing not to mention that is the most precise of 3D printing methods.

One of the main advantages of Binder jetting is the ability of printing large build volumes even in metal materials while maintaining the low cost. The DMLS/SLM process's strength lies production of complex, bespoke parts made of well-established metal materials, which makes them the strongest functional parts out of all the processes.

Unfortunately, even with all the futuristic and ideal advantages of additive manufacturing, as every other process and technology comes its drawback that can be shortened to: being brittle and not suitable for mechanical parts for SLA/DLP and Material jetting with the latter being more expensive for visual purposes. Having limited dimensional accuracy for even small parts, not to mention the bad surface finish resulted from print layers being visible is the FFF printer main drawback. The binder jetting printer weakness lies in its mechanical properties being not as good as metal powder bed fusion. The main constraints for the DMLS/SLM and the SLS printers are the cost for it being the highest of all the technologies, and the long lead times for the latter.

All of this show that additive manufacturing has a potential, but also still have challenges that must be addressed before AM achieves widespread adoption and more financial challenges.
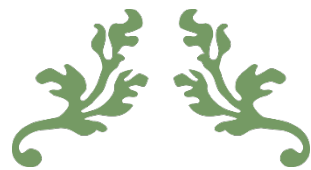
Chapter II

Factorial Design and Desirability Function

I.   INTRODUCTION:

The traditional experimental methodology, for analyzing a large number of parameters, entails fixing the levels of all variables but one and measuring the system's response for various values of this variable, which necessitates a thorough examination of the system. This necessitates doing a large number of tests. For example, the experimenter needs to do $4^9 = 262144$ trials using 9 variables at 4 levels (i.e., using 4 different values for each variable). It is difficult to conduct such a vast number of experiments for many problems.

In this chapter, we'll look at how to present experimental designs, and their two primary categories that exist so that they can allow exploitation of a large sum of parameters while doing a smaller number of fixed and known tests on site.

II.   Presentation of the experimental designs:

II.1.   Historical Overview:

The experimental designs are based on the use of mathematical and statistical approaches to experimentation. Agronomists were the first to confront the problem of trial organization.

They needed to investigate a large number of parameters and couldn't expand the number of experiments. Furthermore, the length of the experiments was a significant constraint. Fisher, [27] and [28], proposed a method in which numerous factors were studied at the same time for the first time in 1925. Statisticians and mathematicians adopted and expanded on this strategy, creating tables of experiments to explore a variety of parameters.

This concept was taken up and expanded by statisticians and mathematicians, who constructed tables of experiments that allowed for a significant reduction in the number of trials to be performed while maintaining the test campaign's significance. Following the study of Dr. Taguchi, [29], large organizations were interested in this method as part of a quality approach. In the 1960s, he was a key figure in the spread of the use of design of experiments in industry in Japan. This strategy has been established in most fields of activity in recent years due to the relevance of the information presented.

II.2.   Principle:

We will be able to achieve our needs using the design of experiments technique. Indeed, the premise behind it is to change the levels of one or more components (variables, discrete or continuous) at the same time in each trial. This will allow for a significant reduction in the number of experiments required while increasing the number of factors investigated, as well as the detection of interactions between factors and optima in relation to a response, i.e., "a quantity used as a criterion, and the easy modelling of the results". The goal of employing experimental designs

is to reduce the number of experiments required while maintaining precision in the outcomes. Experimental design is the subject of many books.

The one produced by the Experiment Association [30] presents experimental designs in a clear manner and proposes a very comprehensive commented bibliography to help the experimenter discover the knowledge they need.

There are many distinct designs available right now. Each one facilitates the solution of specific difficulties due to its qualities. However, experimental designs can be classified into two categories:

- Designs for examining (estimating and comparing) the effects of parameters;
- Designs for researching (estimating and comparing) the effects of variables.

Various methods for adjusting the parameters to produce the best results.

The most important concept that should guide the experimenter's approach is that a design of experiments is used to solve a specific problem. As a result, the design that will offer the information requested must be chosen or constructed. As a result, using the same design to adequately analyze the effects of the parameters while pursuing an optimum will be impossible.

- ❖ A methodological approach must be followed in order to acquire useful information:
- ❖ definition of the objectives and criteria,
- ❖ definition of the factors to be studied and the experimental field,
- ❖ construction of the experimental plan,
- ❖ experimentation,
- ❖ analysis of the results,
- ❖ possible conduct of additional tests,
- ❖ validation of results,
- ❖ Conclusion of the study.

At the conclusion of this approach, one can draw conclusions based on the plans' outcomes. For the two sorts of plans indicated above, each of these factors will be discussed in detail.

III.   Study of the effects of the factors:

The first section is devoted to the description of experimental designs with the goal of estimating and comparing the impact of the elements under consideration. Various designs exist that allow such a study to be conducted, and many works describe how to apply them: [31], [32], [33], and [34]. Only the factorial experimental designs, which are the simplest and most widely used and have produced good results for the tuning of experimental phase, will be discussed here.

III.1.   Complete factorial designs:

The factorial designs, or experimental designs with two levels per factor, will be shown first. They're the most popular because they're the easiest and quickest to set up. First and foremost, we'll go over the whole factorial designs. These are labeled 2^k because they have two levels and k factors. All of the experiments must be carried out in a full factorial design, as in the standard technique. 2^k experiments are required for an ideal full factorial design with k factors. The principle is then to distribute the trials in the experimental domain as efficiently as possible.

Consider the following example: a complete factorial design with two factors, note: 2^2. The optimal technique is to choose measurement locations at the extremes of the experimental region, which increases precision and takes just four trials (see Figure 20).
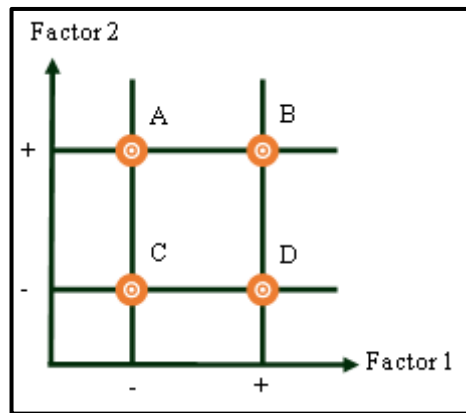
Figure 20. Location of the experimental points in the experimental area

The Yates notation will then be used to specify the levels of the factors, with the value -1 representing the low level and value+1 representing the high level. By modifying the unit of measurement and origin, this amounts to employing decreased center variables.

After that, the experience matrix "Table 4" can be defined. It enables the trials to be gathered in a table. Each column of this table represents a factor, and each row represents an experiment. We associate the criterion that we wish to improve with each experiment. All possible combinations of the two factors appear to be tried.

Table 4. Experience matrix for a full factorial design with two factors

Number of essays	Factor	Factor 2	Interaction ½	Medium	Criterium
1	-	-	+	+	Y1
2	+	-	-	+	Y2
3	-	+	-	+	Y3
4	+	+	+	+	Y4
Impact	E1	E2	E3	M	

The effect of the various elements, i.e., "the influence they have on the criterion", can be determined using this table from the set of responses received for the given criterion. The difference between the means of the responses (criterion) at the high level and the mean at the low level is the effect of a factor by definition. The influence of factor 1, stated El, is calculated using Equation 2.1:

$$E1 = \frac{-y1+y2-y3+y4}{4} \quad (2.1)$$

By multiplying the transpose of the column associated with the factor considered with the column of the criterion acquired for each of the experiments and dividing by the number of trials, it is feasible to directly derive the value of the effects from the matrix of experiments.

For designs with more than two levels per factor, this formula (equation 2.2) can be generalized. The Yates notation is no longer applicable in this situation. The number of levels per factor is given by Niv. The various levels are then numbered in increasing sequence, with 1 being the lowest and Niv being the highest. As a result, Eli denotes the average effect of component 1 at level I.

$$E1_i = \text{Average of responses at level I - Overall average} \quad (2.2)$$

Let Me be the overall mean. In the example, it takes the value:

$$M = \frac{y1+y2+y3+y4}{4} \quad (2.3)$$

It is also feasible to compute the effect of the interactions between the different elements on the criterion, that is, the effect on the criterion when some factors are in a specific configuration. When factors 1 and 2 are at the same level, E12 shows the effect of their interaction. In the event that they aren't zero,

The interactions' influence is added to the factors' effect. The elements of the column indicating the intended interaction can be simply determined using the Yates notation in the experience matrix, "Table 3", by multiplying the columns of the factors evaluated. As a result, the terms of the columns of factors 1 and 2 are multiplied by two for interaction 12. The interactions' effect is then calculated in the same way:

$$E12 = \frac{y1-y2-y3+y4}{4} \quad (2.4)$$

The formula can be generalized to the case where each factor has more than two levels. When factor 1 is at level I and factor 2 is at level j, $E1_i2_j$ reflects the interaction effect. Then comes the following:

$$E1_i2_J = \text{Average of responses when (E1(i), E2(j)) - M} - E1_i - E2_J \quad (2.5)$$

An interaction between two factors is referred to as a second-order interaction, while an interaction between n factors is referred to as an n-order interaction.

It is feasible to interpret the experimental designs' outcomes based on the effects calculations. Consider "Table 4", which is a two-factor complete factorial design. The goal is to optimize the chosen criterion. For the test campaign, for example, the following responses were chosen:

$$\begin{cases} Y_1 = 60 \\ Y_2 = 30 \\ Y_3 = 110 = y \text{ centre} \\ Y_4 = 120 \end{cases} \quad (2.6)$$

The following effects and averages are then obtained

$$\begin{cases} E_1 = -5 \\ E_2 = 35 \\ E_3 = 10 = E \text{ Impact} \\ E_4 = 80 \end{cases} \quad (2.7)$$

Because the implemented plan is a full plan, all of the tests have been completed (which will not always be the case, as stated below), and it is sufficient to search for which test the criterion is the highest in order to determine the optimum setting. This is, without a doubt, test number four. However, assessing the impacts obtained by the designs can help find the best combination of factor levels in the direction of maximizing the criterion. Factor 1 has a negative effect, but factor 2 has a beneficial effect. We should be able to identify the ideal answer by setting factor 2 to a high level and factor 1 to a low one.

This is not the case, however. In fact, the effect of the interaction between the two factors is bigger than the influence of factor 1 in absolute value. Because this one is positive, the two components must be at the same level for the interaction to work in the direction of increasing the criterion. Because the influence of factor 2 is greater than that of factor 1, the levels of factor 2 and the interaction will be fixed, and the effect of factor 1 will be imposed. As a result of the study, the combination of trial 4 is determined to be the best setting.

Full factorial designs can be used to create designs with three or more layers. Equations 2.3 and 2.5, which are generalized formulas for calculating effects, are sufficient. These designs take more trials than factorial designs, but they can produce more refined findings.

Full designs aren't particularly interesting in and of themselves because they necessitate a big number of trials, but they do establish the framework for the production of other sorts of designs that necessitate a much smaller number of trials.

III.2.   Mathematical model:

The experience matrices are a mathematical representation of how the effects are organized. It is about the model's matrix, which will be referred to as X in the following. Using "Table 4" as an example, it is then time for X:

$$X = \begin{pmatrix} -1 & -1 & 1 & 1 \\ 1 & -1 & -1 & 1 \\ -1 & 1 & -1 & 1 \\ 1 & 1 & 1 & 1 \end{pmatrix} \qquad (2.8)$$

The effects can thus be directly calculated:

$$E = \frac{1}{4}X^tY \quad (2.9)$$

The first concept of the designs, as previously said, is to creatively arrange the experimental sites in order to acquire the best possible precision on the outcomes in the fewest feasible trials. The Hadamard matrices are the best matrices of the model in terms of precision on the effects for factorial designs. This argument will be discussed in more detail later.

H is a Hadamard matrix if and only if:

❖ H is a square matrix of dimension N_H,
❖ - ∀(i, j) ϵ [1 N_H]:   H (i, j) ϵ {- 1, 1},
❖ it respects the relation:

$$H^T H = N_H I_{N_H} \qquad (2.10)$$

With I_{NH} identity matrix of dimension N_H.

The condition of existence of a Hadamard matrix is that N_H= 4[4]. Such a matrix is orthogonal which explains why the vector of effects is a linear combination of the responses.

We must examine the variance of the effects to explain the precision provided by such model matrices. Using the example of "Table 4", it appears that each effect is calculated using the measurements of the responses from all four trials in equation 2.3. Let CT denote the standard deviation (also known as error in this section) of each trial's response. The variance of component 1's influence, $V_{(E1)}$, is then calculated as follows:

$$V_{(E1)} = \frac{1}{4}\left(V_{(y1)} + V_{(y2)} + V_{(y3)} + V_{(y4)}\right) = \frac{1}{16}(\sigma^2 + \sigma^2 + \sigma^2 + \sigma^2) = \frac{\sigma^2}{4} \quad (2.11)$$

The error on the effect of factor 1, σ_{Ei} is then:

$$\sigma_{E1} = \sqrt{V_{(E1)}} = \frac{\sigma}{2} (2.12)$$

Because all of the measured responses were taken into account in the computation, the best feasible accuracy was achieved. The Hadamard matrices, which calculate the effects by taking into account all of the measurements, provide for the best possible precision for a given number of tests (multiple of four), [31] and [35].

The results can then be extrapolated to other situations. If the response error is σ and n trials are conducted using a Hadamard type model matrix, the following error σ_E on the influence of a factor or interaction results:

$$\sigma_E = \sqrt{V_{(E)}} = \frac{\sigma}{\sqrt{n}} \ (2.13)$$

It is therefore advised that such matrices be used in factorial designs, as they impose a constraint on the shape and size of the table of experiments, as well as the number of trials to be done.

III.3.   Fractional factorial designs:

When there are more than a few components to analyze, full factorial designs are quite greedy in terms of number of experiments, as seen in the previous section. Indeed, two-level 2^k trials with k factors are required. Fractional factorial designs, which are based on the concept of complete factorial designs, can be used to reduce the number of tests. To limit the number of experiments, the approach entails tolerating a degree of indeterminacy in the influence of the components. The tests are then structured in the experimental domain to conduct the fewest number of trials possible while achieving the highest level of precision. The following section will show an example of fractional factorial designs at two levels.

The goal is to reduce the number of trials by employing a complete design of lower order than the number of elements to be researched and studying the additional factors using the interactions between the factors of this full design. 2^{k-p} represents the difference between the number of factors studied and the number of factors in the full design used in such two-level fractional factorial designs, where k represents the number of factors studied and up represents the difference between the number of factors studied and the number of factors in the full design used. Using "Table 4" as an example, it is feasible to investigate a third component, whose influence will be added to that of the interaction between factors 1 and 2 in column 3. "Table 5" shows a design like this, which is labeled 2^{3-1}.

Table 5. Experience matrix for a two-factor fractional design

Number of essays	Factor 1	Factor 2	Factor 3 = Interaction ½	Medium	Criterium
1	-	-	+	+	Y1
2	+	-	-	+	Y2
3	-	+	-	+	Y3
4	+	+	+	+	Y4
Impact	E1	E2	l3	M	

The effect of the factor 3 (E_3) and the interaction (E_{12}) are then aliased and it comes:

$$l_3 = E_3 + E_{12} \ (2\ .14)$$

l3, called alias or contrast, is then the main effect E_3 increases by the interaction E_{12}.

The number of extra elements that can be investigated is determined by the number of interactions and the overall design size. The greatest number of factors that can be researched as a

function of the number of primary factors that are the factors in the basic full design is shown in "Table 6"

Table 6. Fractional designs and number of factors studied

Basic plan	Number of main factors	Number of factors that can be aliased	Maximum number of factors studied
2^2	2	1	3
2^3	3	4	7
2^4	4	11	15

Let k be the number of factors in the basic complete design considered. The number of interactions of order q is then given by:

$$N_{interactions\ of\ order\ q} = C_k^q = \frac{k!}{q!(k-q)!} \ (2.15)$$

The maximum number of factors that can be aliased is therefore:

$$N_{nombre\ maximum\ de\ facteurs\ alias} = \sum_{q=2}^{k} C_K^q = 2^k - k - 1 \ (2.16)$$

Calling the effect of a single factor a first-order interaction, the interaction between two factors a second-order interaction and so on, the maximum number of factors that can be studied is given by the following relationship:

$$N_{maximum\ number\ of\ factors\ studied} = \sum_{q=2}^{k} C_K^q = 2^k - k - 1 \ (2.17)$$

One of the criteria for choosing the basic two-level full factorial design therefore depends on the number of factors one wishes to study.

III.4.   Analysis of variance:

The non-replicability of the measured outcomes is an inherent challenge of the experiment. This issue can stem from a variety of sources, causing the final result to be skewed. The issue is deciding whether or not a result is influential.

The issue is deciding whether or not a result is influential. It will have to calculate the error in the calculations of the various effects.

The first step in minimizing the influence of measurement derivatives under the constraint of fluctuating external conditions is to perform the tests in a random order.

In a second phase, the mistake committed on the outcomes must be quantified, and the experimental error retained for the analysis of the results must be chosen, allowing statistical techniques to be used to exploit the plan's results. The paper [38] contains the mathematical parts as well as the many tables needed in the statistical analysis.

III.5.   Estimating the experimental error on an effect:

The value of the experimental error Δx committed on the response is assumed to be known and to have a normal distribution (Gaussian curve). This distribution, shown in "Figure21", can be defined by two quantities, the mean $\bar{Y}$ and the standard deviation σ.

The probability density f of a continuous random variable x of mean μ and standard deviation σ can be defined by:

$$f(x) = \frac{1}{\sigma\sqrt{2\pi}} e^{-\frac{1}{2}\left(\frac{x-\bar{\mu}}{\sigma}\right)^2} \quad (2.18)$$

The real value of the response is then defined as a confidence interval in which the actual value has a high possibility of being found. As the size of the confidence interval grows, so does the probability.

The real value of a normal distribution derived from a Y_i measure is:

- 68% chance of being in the $Y_i \pm \sigma$ interval,
- 95% chance of being in the $Y_i \pm 2\sigma$ interval,
- 99.9% chance of being in the range $Y_i \pm 3\sigma$ interval.
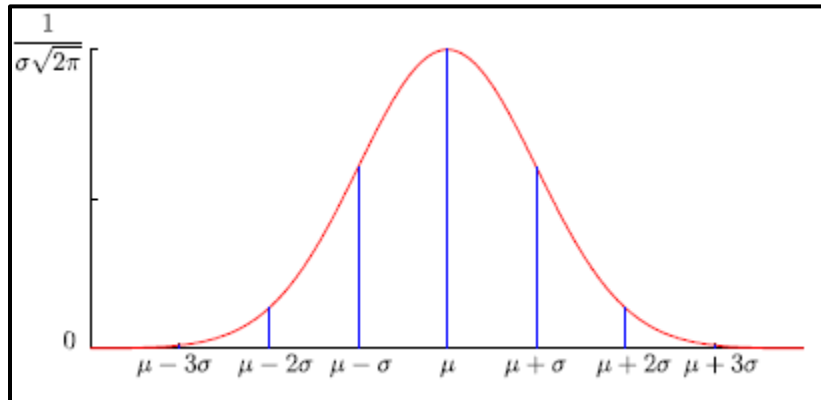
Figure 21. Normal distribution

Assuming the measurement error Dy is equal to the standard deviation, the precision of the effects depends on the number n of trials considered, i.e.:

$$\Delta E = \frac{\Delta y}{\sqrt{n}} = \frac{\sigma}{\sqrt{n}} \quad (2.19)$$

The experimenter will select the confidence interval corresponding to a percentage error based on his needs. The most common error [31] amounts to roughly one standard deviation, or two out of three odds of not being wrong.

It should be highlighted, however, that there are more unfavorable circumstances than the one in which the distribution of measurements is known and confidence intervals can be calculated. Indeed, estimating the experimental error will frequently be required to establish whether effects are important.

III.6.   Estimation of the experimental error:

The knowledge of the experimental error is therefore very important and when it is not known, it must be estimated.

A first solution consists in carrying out several measurements at the same point of the experimental domain (often the center) by assuming an iso-distribution on this one. This approach leads to an estimate of the standard deviation σ:

$$s = \sqrt{\frac{1}{N-1} \sum_{i=1}^{N} (y_i - \bar{y})} \quad (2.20)$$

With:

- N: number of measurements made,
- Y_i: measurement of the response number i,
- $\bar{Y}$: average of the responses Y_i

Because of the small number of trials, the error estimate distribution resembles a student curve, which is a flattened Gauss curve. To avoid being wrong, it will be required to raise the size of the confidence intervals. However, as the number of trials rises, the precision improves and the student curve converges to the Gauss curve. "Table 7" shows the values of the student variable t_α^v with v degrees of freedom and a likelihood of exceeding an in absolute value:

$$P\{T > |t_\alpha^v|\} = \alpha \quad (2.21)$$

"Figure 22" shows this probability.
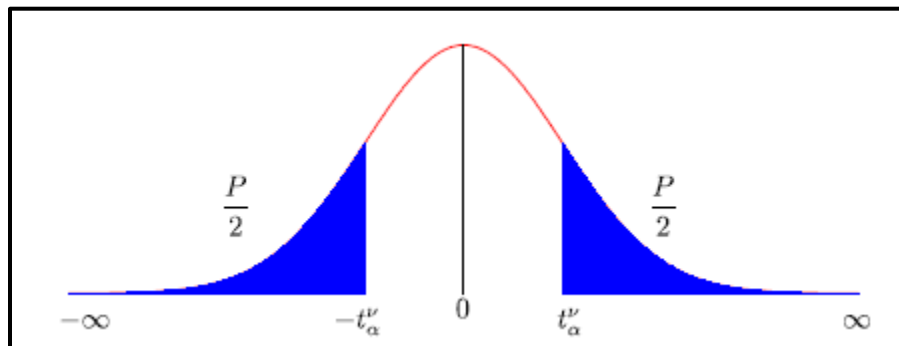
Figure 22. Distribution table of Student's law

Table 7. Student's Table

A	1	2	3	4	9	19	∞
				V			
0.3	1.96	1.38	1.25	1.19	1.1	1.06	1.03
0.1	6.31	2.92	2.35	2.13	1.83	1.73	1.64
0.05	12.71	4.3	3.18	2.78	2.26	2.09	1.96
0.01	63.66	9.92	5.84	4.6	3.25	2.86	2.58

The number of measurements N is related to the number of degrees of freedom v by the relation 2.22:

$$v = N - 1 \qquad (2.22)$$

The multiplicative coefficients to be applied to the estimation of the standard deviation are then obtained according to the number of measurements performed and the desired precision. Thus, a confidence interval with a probability α is defined by $\pm t_\alpha^v$ x s around the considered value of the considered value.

The second option is to repeat each of the n trials of the experimental design N times. The previous sections showed that, depending on the number of experiments n, the standard deviation on the effects is a fraction of the standard deviation on the response using Hadamard matrices:

$$\sigma_E = \frac{\sigma}{\sqrt{n}} \qquad (2.23)$$

Let N be the number of repetitions of each experiment. By performing N repetitions for each experiment i, we improve the estimate i_s of the standard deviation on the measured response. By noting $y_{am,}$ the measure of the j^{et} repetition of the experiment i and Y_i the average of the N repetitions of the i^{tch} experiment, we can then define the variance s_i^2:

$$s_i^2 = \frac{1}{N-1} \sum_{j=1}^{N} (y_{i,j} - \bar{y}_i)^2 \qquad (2.24)$$

It is feasible to define the estimate of the standard deviation throughout the entire domain, s, based on the widely recognized assumption [30] that the iso-variance on the answer is guaranteed over the entire experimental domain and that the mistakes on the result are independent. Equation 2.25 follows:

$$s = \sqrt{\frac{\overline{s_i^2}}{n}} = \sqrt{\frac{\sum_{j=1}^{N} s_i^2}{n * N}} \qquad (2.25)$$

Let us then estimate the standard deviation on the effects, see equation 2.26:

$$s_E = \frac{s}{\sqrt{N * n}} \qquad (2.26)$$

It is then possible to define the confidence interval. The estimate of the standard deviation will therefore be weighted by the value of the student's variable at n x (N - 1) degrees of freedom for a probability in absolute value α : $t_{\alpha}^{n*(N-1)}$

The precision of the effects obtained will be improved by repeating the trials of the table of experiments in this manner. However, such an improvement in trials is contingent on a higher cost.

Factorial designs allow researchers to investigate the effects of various variables on one or more criteria and determine an optimal solution. However, the value of the levels chosen for each of the parameters during the study determines the best point. The response surface approach, described in the following section, will allow you to model the evolution of the criterion between various levels in order to arrive at an optimal point that is independent of them.

IV.   Response surfaces:

In this part, the experimental designs allowing to adjust the parameters to reach an optimum between the levels of the factors will be presented. The principle here is to model the experimental response surface, i.e., "the evolution of the criterion on a bounded universe of discourse of the variables and to seek the optimum of the estimated surface". Here again, many references on the subject exist: [30], [39] and [49]. Among the numerous types of designs allowing to build response surfaces, we to construct response surfaces, we will only present and use here the centered composite here only the centered composite designs.

IV.1.   Model Definition:

The designs we have presented previously allow us to study and compare the effects of factors on a response. The objective is now to obtain a so-called optimal setting of these parameters over the range of variation of these parameters with respect to the selected criterion. It is therefore desirable to be able to search for these coefficients "between" the levels given to the variables. Reduced centered variables will again be used, taking values in the interval [-1, 1] on the experimental domain studied in relation to the center of the latter. The following coding relation is used to transform the value u ϵ [c_{umin}, x_{max}) of the factor U where c_{umin} and x_{max} represent the extreme values of U on the experimental domain into the reduced centered variable x ϵ [-1, 1]:

$$x = \frac{u - \dfrac{u_{min} + u_{max}}{2}}{\dfrac{u_{max} - u_{min}}{2}} \qquad (2.27)$$

It will now be necessary to position the tests judiciously within the experimental domain in order to be able to model the studied experimental surface in a reduced number of experiments. To do this, there are many types of designs, each of which provides each providing answers to different types of problems [30]. The first question is based on the type of model that will be used to estimate the experimental surface. It will then be necessary to choose the design accordingly and to carry out a statistical analysis of the model obtained in order to check whether the regression surface gives a usable approximation of the real phenomenon. Finally, the obtained surface will be analyzed in order to find the optimal setting for the chosen problem. This analysis will be all the easier if the choice of the model is judicious. Thus, a slight loss of information at the level of the correlation, i.e., the adequacy between the model and the real response, could be interesting in terms of exploitation of the model if it is easily exploitable.

Consequently, the assumption that the response surface can be estimated by a particular form of modeling: a quadratic form is commonly adopted, [39] and [40]. This choice is based on the fact that this model is well known and easy to exploit and that its particular form, based on polynomials of the second degree, is applicable to of the second degree, is applicable to many problems. Indeed, it is always possible to define in the vicinity of a point a development in series of any function. By posing η the estimate of the value of the response studied for a given operating point, β_m and β_{Mn} the coefficients of the polynomial and x_i the variable associated with the factor l, l $\in$ [1- k], the general form of the model can be defined:

$$\eta = \beta_0 + \sum_{i=1}^{k} \beta_i * x_i + \sum_{i=1}^{k} \beta_{ii} * x_i^2 + \sum_{i=1}^{k-1} (\sum_{j=i+1}^{k} \beta_{ij} * x_i * x_j) \qquad (2.28)$$

We then have p unknowns which are the coefficients β of the model:

$$p = \frac{(k + 2)!}{k! \, 2!} = \frac{(k + 1)(k + 2)}{2} \qquad (2.29)$$

It will thus be necessary to carry out a number of experiments higher or equal to the number p of unknowns to estimate them. It thus appears that it will be necessary to limit the number of factors studied number of factors studied, the number of necessary tests increasing in a factorial way with it. factorially with it. In practice, the designs allowing the study of the response surfaces response surfaces are often used in addition to an initial study of the effects of the factors of the factors which allows to select the parameters used to model the experimental surface, i.e., the experimental surface, i.e., the most influential factors.

IV.2. Centered composite planes:

We chose the centered composite designs, [39] and [40], for the study of response surfaces. They have the advantage of being easy to construct because they are built by adding measurement points to a complete factorial design. The designs for the study of a response surface are often used after

a study of the effects of the factors, it is then sufficient to carry out only a few additional experiments to estimate the response surface of the criterion studied.

However, they are rather greedy in terms of number of trials compared to other types of designs [30], but this number remains reasonable when the number of factors studied remains low (between 2 and 4 parameters). Another disadvantage is that this type of design requires 5 levels per factor and that it can sometimes be physically difficult to realize them. A very complete presentation of these designs is given in [30]. A centered composite design is defined by:

- ❖ A full factorial design 2^k,
- ❖ n_0 repetitions in the center of the experimental domain, dedicated to statistical analysis,
- ❖ Two-star points per parameter and positioned on the axes of each of them at a distance from the center of the domain. These points contribute to the evaluation of the quadratic terms of the polynomial model, i.e., they give information about the curvature of the response surface.

"Figure 23" shows an example of a centered composite design for the study of two parameters (the additional tests giving information about the surface curvature are placed outside the experimental domain).

The total number of trials to be conducted, N, will depend on the number of factors k studied and the number of repetitions in the center of the domain, n_0:

$$N = 2^K + 2 * K + n_0 \qquad (2.30)$$
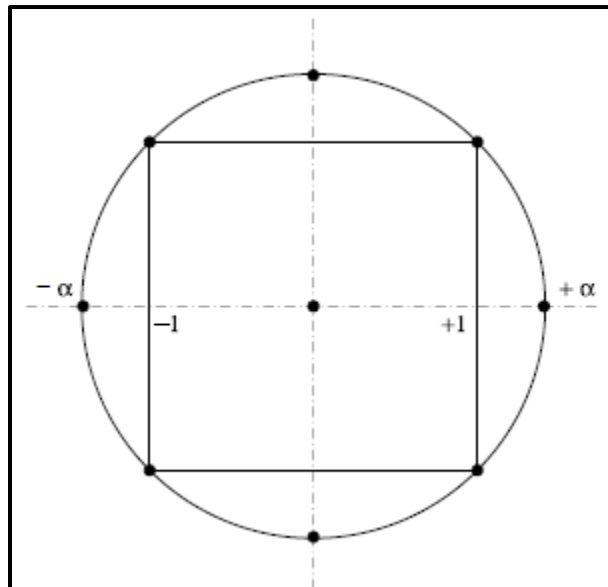
Figure 23. Centered composite design for the study of two factors

The number of repetitions in the center and the value to be given to a will depend on the properties that will be attributed to the design, as presented a little further on. To illustrate the construction of a centered composite design, the example of 3 factors design, will be presented. First, the experience matrix, ξ, will be defined in equation 2.31. It defines the levels of each of the parameters at each experiment. Each column of the matrix is associated with a factor.

$$\varepsilon = \begin{pmatrix} -1 & -1 & -1 \\ +1 & -1 & -1 \\ -1 & +1 & -1 \\ +1 & +1 & -1 \\ -1 & -1 & +1 \\ +1 & -1 & +1 \\ -1 & +1 & +1 \\ +1 & +1 & +1 \\ +\alpha & 0 & 0 \\ -\alpha & 0 & 0 \\ 0 & +\alpha & 0 \\ 0 & -\alpha & 0 \\ 0 & 0 & +\alpha \\ 0 & 0 & -\alpha \\ 0 & 0 & 0 \end{pmatrix} \qquad (2.31)$$

For the simplicity of the representation, n_0 is here temporarily fixed at 1. then determine the value to give to it, as well as to α

From this matrix of experiments, it is possible to define the matrix of the model allowing to calculate the coefficients of the model. With k = 3 factors studied, a 3-dimensional space with p = 10 unknowns is obtained. Let β be the vector of coefficients defined by:

$$\beta = \begin{pmatrix} \beta_0 \\ \beta_1 \\ \beta_2 \\ \beta_3 \\ \beta_{11} \\ \beta_{22} \\ \beta_{33} \\ \beta_{12} \\ \beta_{13} \\ \beta_{23} \end{pmatrix} \qquad (2.32)$$

The following equation of the model then comes, (2.33), application for 3 unknowns of equation 2.28:

$$\eta = \beta_0 + \sum_{i=1}^{3} \beta_i * x_i + \sum_{i=1}^{3} \beta_{ii} * x_i^2 + \sum_{i=1}^{2} (\sum_{j=i+1}^{3} \beta_{ij} * x_i * x_j) \qquad (2.33)$$

To calculate these coefficients by the least square's method, the model matrix, X, equation 2.34, will be used. This matrix extends the experiment matrix by defining in each column the levels of each of the coefficients of the model equation for each trial. These new columns are calculated by multiplying the columns of the experiment matrix.

$$
X = \begin{pmatrix}
1 & -1 & -1 & -1 & 1 & 1 & 1 & 1 & 1 & 1 \\
1 & 1 & -1 & -1 & 1 & 1 & 1 & -1 & -1 & 1 \\
1 & -1 & 1 & -1 & 1 & 1 & 1 & -1 & 1 & -1 \\
1 & 1 & 1 & -1 & 1 & 1 & 1 & 1 & -1 & -1 \\
1 & -1 & -1 & 1 & 1 & 1 & 1 & 1 & -1 & -1 \\
1 & 1 & -1 & 1 & 1 & 1 & 1 & -1 & 1 & -1 \\
1 & -1 & 1 & 1 & 1 & 1 & 1 & -1 & -1 & 1 \\
1 & 1 & 1 & 1 & 1 & 1 & 1 & 1 & 1 & 1 \\
1 & +\alpha & 0 & 0 & +\alpha^2 & 0 & 0 & 0 & 0 & 0 \\
1 & -\alpha & 0 & 0 & +\alpha^2 & 0 & 0 & 0 & 0 & 0 \\
1 & 0 & +\alpha & 0 & 0 & +\alpha^2 & 0 & 0 & 0 & 0 \\
1 & 0 & -\alpha & 0 & 0 & +\alpha^2 & 0 & 0 & 0 & 0 \\
1 & 0 & 0 & +\alpha & 0 & 0 & +\alpha^2 & 0 & 0 & 0 \\
1 & 0 & 0 & -\alpha & 0 & 0 & +\alpha^2 & 0 & 0 & 0 \\
1 & 0 & 0 & 0 & 0 & 0 & 0 & 0 & 0 & 0
\end{pmatrix}
\qquad (2.34)
$$

Then comes the information matrix. $(^{\mathrm{T}}X\,X)$ (2.35), which defines the properties and qualities of the experimental design.

$$
(^{t}XX) = \begin{pmatrix}
N & 0 & 0 & 0 & a & aa & 0 & 0 & 0 \\
0 & a & 0 & 0 & 0 & 0 & 0 & 0 & 0 \\
0 & 0 & a & 0 & 0 & 0 & 0 & 0 & 0 \\
0 & 0 & 0 & a & 0 & 0 & 0 & 0 & 0 \\
a & 0 & 0 & 0 & c & bb & 0 & 0 & 0 \\
a & 0 & 0 & 0 & b & cb & 0 & 0 & 0 \\
a & 0 & 0 & 0 & b & bc & 0 & 0 & 0 \\
0 & 0 & 0 & 0 & 0 & 0 & b & 0 & 0 \\
0 & 0 & 0 & 0 & 0 & 0 & 0 & b & 0 \\
0 & 0 & 0 & 0 & 0 & 0 & 0 & 0 & b
\end{pmatrix}
\qquad (2.35)
$$

With:

$$
\begin{cases}
N = 2^k + 2k + n_0 = 14 + n_0 \\
a = 2^k + 2\alpha^2 = 8 + 2\alpha^2 \\
b = 2^k = 8 \\
c = 2^k + 2\alpha^4 = 8 + 2\alpha^4
\end{cases}
\qquad (2.36)
$$

This matrix leads to the dispersion matrix $(^{\mathrm{T}}x)^{-1}$ used in the least squares method to estimate the parameter vector β. This matrix takes the form described in equation 2.37

$$(^tXX)^{-1} = \begin{pmatrix} D & 0 & 00 & C & CC & 0 & 00 \\ 0 & E & 00 & 0 & 00 & 0 & 00 \\ 0 & 0 & E0 & 0 & 00 & 0 & 00 \\ 0 & 0 & 0E & 0 & 00 & 0 & 00 \\ C & 0 & 00 & A & BB & 0 & 00 \\ C & 0 & 00 & B & AB & 0 & 00 \\ C & 0 & 00 & B & BA & 0 & 00 \\ 0 & 0 & 00 & 0 & 00 & F & 00 \\ 0 & 0 & 00 & 0 & 00 & 0 & F0 \\ 0\,0 & 0 & 00 & 0 & 00 & 0 & F \end{pmatrix} \qquad (2.37)$$

With:

$$\begin{cases} A = \dfrac{-N*b-a^2}{-2N*b^2+3a^2(b-c)+N*c(b+c)} \\[2mm] B = \dfrac{N*b-2a^2+N*c}{-2N*b^2+3a^2(b-c)+N*c(b+c)} \\[2mm] C = \dfrac{-a}{2N*b-3a^2+N*c} \\[2mm] D = \dfrac{2b+c}{2N*b-3a^2+N*c} \\[2mm] E = \dfrac{1}{a} \\[2mm] F = \dfrac{1}{b} \end{cases} \qquad (2.38)$$

From the information and dispersion matrices, it is necessary to look for the values to assign to α and n_0 to obtain interesting properties. In the case of fractional factorial designs, the orthogonality condition was sought to improve the precision of the effects. For the centered composite designs, it will not be possible to ensure this property, the diagonal terms of the matrix of information (corresponding to the additional points giving information on the curvature of the surface) cannot be cancelled. Other conditions on these two parameters will then be sought to ensure certain properties such as pseudo-orthogonality, is variance by rotation or uniform precision.

The property of pseudo-orthogonality consists in approximating the dispersion matrix to a diagonal matrix by canceling the terms noted B. It is possible to show,[30], that to cancel these coefficients, one must choose α and n_0 such that:

$$\alpha = \left(\frac{2^k(\sqrt{2^k+2k+n_0}-\sqrt{2^k})^2}{4} \right)^{\frac{1}{4}} \qquad (2.39)$$

A second interesting property isovariance by rotation. The FD X 06-080 standard, [AFN89] defines it as follows:

"An experimental setup exhibits rotational is variance properties when the variance function depends only on the distance to the center of the experimental domain. Thus, no direction is favored."

The condition of isovariance by rotation is given by the condition in Eq. 2.40 [30]:

$$\alpha = \sqrt[4]{2^k} \qquad (2.40)$$

The last property that will interest us, the notion of uniform precision, is also defined by the FD X 06-080 standard, [AFN89]:

"An experimental device has uniform precision properties if the variance function is practically constant within a sphere having the same center as the experimental domain. It can only be obtained if isovariance by rotation is already assured."

It is possible to show that the condition of uniform precision is:

$$n_0 = \frac{(k+3) + \sqrt{9k^2 + 14k - 7}}{4(k+2)} (\sqrt{2^k} + 2)^2 - 2^k - 2k \qquad (2.41)$$

Since rotational isovariance depends only on α, it is possible to associate either pseudo-orthogonality or uniform precision with this property. On the other hand, the two latter are incompatible because the uniform precision is inseparable from isovariance by rotation, [30]. "Table 8" gives the values to be given to α and n_0 to obtain the different properties.

In the following, the properties of isovariance by rotation and uniform precision will be preferred in order to keep a quasi-constant variance on the experimental domain. Experimental domain. The statistical analysis will be all the easier. For $k = 3$ factors.

Table 8. Conditions of isovariance by rotation, pseudo-orthogonality and uniform precision

Factors Numbers								
	K=2		K=3		K=4		K=5	
2^k	4		8		16		32	
2k	4		6		8		10	
α (rotational isovariance)	1.414		1.682		2		2.378	
N₀ (pseudo-orthogonality)	8		9		12		17	
N₀ (uniform precision)		5		6		7		10
N= 2ᵏ+2k+n₀	16	13	23	20	36	31	59	52

It comes then:

$$\begin{cases} \alpha = 1.682 \\ n_0 = 6 \end{cases} \qquad (2.42)$$

From the matrix of experiments, the tests can now be performed and lead to the measurement of the response vector Y:

$$^tY = (y_1 \ y_2 \ y_3 \ \dots y_N \qquad (2.43)$$

IV.3. Analysis of results:

The exploitation of the results will pass by the use of the least squares method. This method allows us to estimate the vector of parameters β by minimizing the square of the residuals. Let $\hat{\beta}$ be the estimate of β.

$$\hat{\beta} = \begin{pmatrix} \widehat{\beta_0} \\ \widehat{\beta_1} \\ \widehat{\beta_2} \\ \widehat{\beta_3} \\ \widehat{\beta_{11}} \\ \widehat{\beta_{22}} \\ \widehat{\beta_{33}} \\ \widehat{\beta_{12}} \\ \widehat{\beta_{13}} \\ \widehat{\beta_{23}} \end{pmatrix} \qquad (2.44)$$

The existence of residuals during estimation implies the introduction of an error between the real response and the estimated response. Let the vector of these errors be:

$$^tE = (e_1 \ e_2 \ e_3 \ \dots e_N \ ) \qquad (2.45)$$

Then comes the following matrix system by noting Y the estimate of the response vector:

$$Y = X * \hat{\beta} + E = \hat{Y} + E \qquad (2.46)$$

The estimation of the coefficients is then directly obtained by using the matrices defined above and thus with the properties of isovariance by rotation and uniform precision:

$$\hat{\beta} = (^tXX)^{-1} * (^tX) * Y \qquad (2.47)$$

Let then be the residues, E:

$$E = Y - \hat{Y} \qquad (2.48)$$

The results obtained can then be represented graphically in order to compare the measured points and the estimated responses. To do this, it is necessary to plot the model's adequacy graph. The measured responses are placed on the abscissa and the estimated responses on the ordinate, figure 24. If the scatterplot is aligned with the line of equation y = x, the descriptive quality of the

model will a priori be rather good. Figure 24 gives an example of a goodness-of-fit plot for the study of the IAE of the output voltage of a sine wave absorber
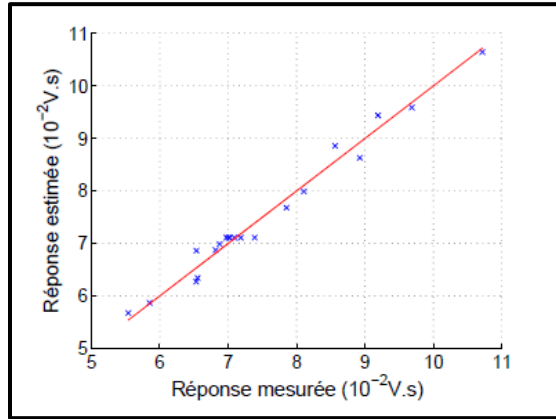
Figure 24. Example of a model adequacy graph

By this graphical representation a first estimator of the descriptive quality of the model is then of the model is then obtained. It is then easy to plot the modeled response surface as a function of the variables studied. Figure 25 represents as an example the evolution of the criterion as a function of two parameters.
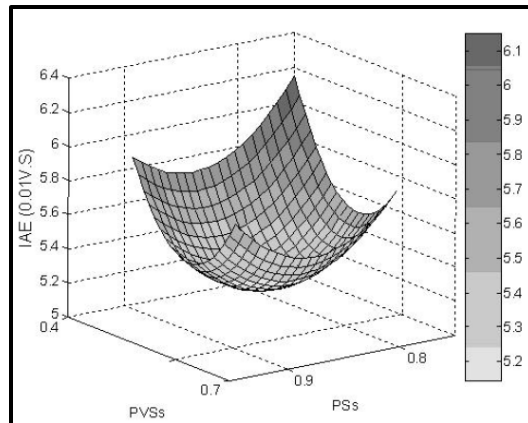
Figure 25. Example of a response surface estimation

There are other representations, such as iso-response curves giving the zones in which the criterion takes a same value. However, such representations are difficult to use directly when the number of parameters studied is greater than two. In any case, before exploiting the model obtained, it is necessary to carry out a statistical study of it.

IV.4.   Statistical analysis of results:

A series of statistical tests will now be conducted to judge the quality of the model. A detailed presentation of statistical tests applied to regression methods can be found in [41] and [42]. This study can be decomposed into three steps:

- The global analysis of the system,
- The study of the coefficients of the model,
- The analysis of the residuals.

The objective of the global analysis of the results is to define the descriptive quality of the model by means of an analysis of variance table (ANOVA table). For To do this, several variables must be defined beforehand.

Let SCT be the total sum of squares, i.e., the sum of the squares of the differences between the response measures and their mean:

$$SCT = \sum_{i=1}^{N} (y_i - \bar{y})^2 \qquad (2.49)$$

This sum can be decomposed as a sum of two terms, SCM, the sum of squares due to the regression or variation explained by the model and SCE, the sum of squares of the residuals or variation unexplained by the model:

$$SCT = SCE + SCT \qquad (2.50)$$

SCM is the sum of the squares of the errors between the estimated responses and the mean of the measured responses:

$$SCM = \sum_{i=1}^{N} (\hat{y}_i - \bar{y})^2 \qquad (2.51)$$

SCE is the sum of the square of the differences between the measured and estimated responses:

$$SCE = \sum_{i=1}^{N} (y_i - \hat{y}_i)^2 \qquad (2.52)$$

A statistical test to reject the hypothesis (H$_0$) that the model does not describe the variation of the trials will now be performed. When this hypothesis is verified, it is possible to show [41] that the F$_c$ statistic described in equation 2.53 follows a Fisher distribution with respectively (p-1) and (N - p) degrees of freedom

$$F_C = \frac{SCM}{SCE} \qquad (2.53)$$

Thus, the hypothesis (H0) is rejected with probability α if:

$$F_C > F_{(a,p-1,N-p)} \qquad (2.54)$$

In equation 2.54, $F_{(a, p-1, N-p)}$ is the (1- a) quantile of a Fisher distribution with (p-1) and (N-p) degrees of freedom.

These data lead to the construction of the ANOVA "Table 11", summarizing these different results. It is thus possible to conclude about the capacity of description of the variations of the tests of the model. The next point consists of defining the percentage of total variation explained by the model by means of the coefficient of determination R^2, taking values in the interval [0 1]:

$$R^2 = \frac{SCM}{SCT} = 1 - \frac{SCE}{SCT} \qquad (2.55)$$

Table 9. ANOVA Table: Regression Analysis

Source of variation	Degrees of freedom	Sum of squares	Average of squares	F_C
Regression	p-1	SCM	$\dfrac{SCM}{P-1}$	$\dfrac{SCM}{SCE}$
Residual	N-p	SCE	$\dfrac{SCE}{N-p}$	
Total	N-1	SCT		

When $R^2 = 1$, the Y_i estimates coincide with the measurements while for $R^2 = 0$ the data are not aligned at all. The coefficient of determination thus indicates the degree of alignment of the data with the regression model. Thus, for $R^2 = 0.8$, 80% of the variation of the trials is explained by the model.

However, in the presence of several explanatory variables, which is often the case for multiple regressions, the coefficient of determination naturally increases and does not allow for a significant comparison of different models [41] It is therefore usual to introduce and use the adjusted R^2 criterion, R^2 criterion, which is maximal when the error estimator. s^2, equation 2.56, is minimal.

$$s^2 = \frac{SCE}{N-p} \qquad (2.56)$$

R^2 criterion is defined by:

$$R^2_{criterion} = 1 - \frac{\dfrac{SCE}{N-p}}{\dfrac{SCT}{N-1}} \qquad (2.57)$$

The quality of the model will therefore be all the better if R^2 criterion is close to î.

The different parameters of the model can also be analyzed statistically. The null hypothesis (H_0) is then investigated for each of the coefficients, according to which they are harmful. To do this, the t_{ic} statistic which depends on the estimate of the standard deviation of $\hat{\beta}(\iota)$, $s(\widehat{\beta(\iota)})$ is then calculated:

$$t_c = \frac{\hat{\beta}(i)}{s(\widehat{\beta(\iota)})} \qquad (2.58)$$

However, this standard deviation is estimated from the diagonal terms c_{ii} of the dispersion matrix $(^tXX)^{-1}$:

$$s(\widehat{\beta(\iota)}) = \sigma\sqrt{c_{ii}} \qquad (2.59)$$

Let the variance of the residuals, σ_r^2, be the estimate of the experimental variance

$$\sigma_r^2 = \frac{SCE}{N-p} \qquad (2.60)$$

This leads to the calculation of t_{ic}

$$t_c = \frac{\hat{\beta}(i)}{\sigma_r\sqrt{c_{ii}}} \qquad (2.61)$$

It is possible to show that, under (H_0), tic follows a student's law with ($N - p$) degrees of freedom [41]. The property (H_0) will then be rejected at the level of significance level α if:

$$|t_c| > t_{\frac{\alpha}{2},N-p} \qquad (2.62)$$

In equation 2.62, the critical value $t_{\frac{\alpha}{2},N-p}$ is the $(1 - \frac{\alpha}{2})$ quantile of a student's law with ($N-p$) degrees of freedom. It is then possible to determine which coefficients should be kept. (2.62)

Finally, the normality of the errors will be tested. To do this, the QQ-plot of the residuals gives information about the distribution of the residuals [41]. It is a question of ordering the residuals E in an increasing manner. Let $\tilde{E}$ be the vector of errors with $\widetilde{e_1}$ the smallest residual and $\widetilde{e_N}$ the largest:

$$\tilde{E} = (\widetilde{e_1} \ \widetilde{e_2} \ \widetilde{e_3} \ ... \widetilde{e_N}) \qquad (2.63)$$

To each of these residues $\widetilde{e_\iota}$ is then associated the $\frac{i}{N+1}$ quantile q_i of a normal distribution. The quantile function of a random variable is the inverse of its distribution function. For a normal distribution, the values of the quantile function are tabulated. The plot with quantiles q_i on the x-axis and ordered residuals $\tilde{E}$ on the y-axis can then be drawn. "Figure 26" shows an example of the distribution of these residuals for the same case as above.

If the residuals are normally distributed (as is assumed), the points should be aligned. The distribution on the example is therefore satisfactory.

IV.5. Search for the optimum:

The search for the optimum consists in analytically determining its coordinates and its nature on the experimental domain studied, from the model obtained. The quadratic form of this one is recalled equation 2.64 for k parameters:

$$\eta = \beta_0 + \sum_{i=1}^{k} \beta_i * x_i + \sum_{i=1}^{k} \beta_{ii} * x_i^2 + \sum_{i=1}^{k-1} (\sum_{j=i+1}^{k} \beta_{ij} * x_i * x_j) \qquad (2.64)$$

This can then be written in the following matrix form by noting x the vector of variables:

$$\eta = b_0 + {}^t x * b + {}^t x * B * x \qquad (2.65)$$
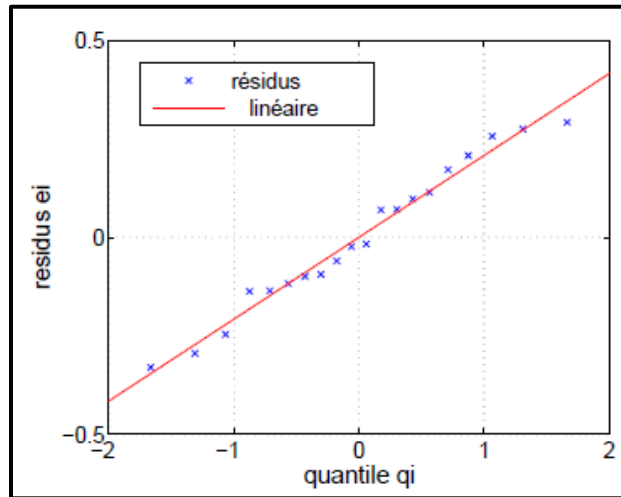
Figure 26. Example of residual analysis

Whatever the number of variables in the model, the coefficient b_0 is defined as follows:

$$b_0 = \beta_0 \qquad (2.66)$$

For a model taking into account k variables, the coefficients of equation 2.65 are, on the one hand for the vector b:

$${}^t b = (\beta_1 \quad \beta_2 \quad ... \quad \beta_{k)} \qquad (2.67)$$

On the other hand, the matrix B is symmetric and of the following form:

$$B = \begin{pmatrix} \beta_{11} & & \dfrac{\beta_{12}}{2} & \dfrac{\beta_{1K}}{2} \\ & \beta_{22} & & \dfrac{\beta_{2K}}{2} \\ symmetrical & & & \dfrac{\beta_{K-1,k}}{2} \\ & & & \beta_{kk} \end{pmatrix} \qquad (2.68)$$

The vector x groups the variables of the model:

$$t_x = (x_1 \quad x_2 \quad \dots x_k) \quad (2.69)$$

The determination of the stationary point, xj, of the quadric form is then obtained by solving the following equations:

$$\forall_i \in [1 \quad k], \qquad \frac{\partial \eta}{\partial x_i} = 0 \qquad (2.70)$$

Equation 2.70 then gives:

$$\begin{cases} \dfrac{\partial \eta}{\partial x_1} = \beta_1 + 2\beta_{11} * xs_1 + \displaystyle\sum_{i=2}^{k} \beta_{1i} * x_i = 0 \\[3mm] \dfrac{\partial \eta}{\partial x_2} = \beta_2 + 2\beta_{22} * xs_2 + \displaystyle\sum_{i \neq 2}^{k} \beta_{2i} * x_i = 0 \\ \quad . \\ \quad . \\ \quad . \\ \dfrac{\partial \eta}{\partial x_k} = \beta_k + kk * xs_k + \displaystyle\sum_{i \neq k}^{k-1} \beta_{ki} * x_i = 0 \end{cases} \qquad (2.71)$$

Thus, in matrix form, equation 2.71 becomes:

$$b + 2B * xs = 0 \qquad (2.72)$$

The following relationship is immediately established, giving the coordinates of the point stationary point:

$$xs = -\frac{1}{2} B^{-1} b \qquad (2.73)$$

The coordinates of the stationary point being known, it is then necessary to study its nature (maximum, minimum, inflection point).

Desirability:

In the previous sections, it has been shown that the design of experiments was an interesting tool for the study of a criterion. However, it is quite possible to use the same methodology for the study of several criteria while implementing only one design of using only one experimental design. For that, the notion of desirability, which allows to aggregate in a single composite criterion several other criteria, will be used. This notion was introduced by E.C. Harrington [44] in 1965 and was then developed thereafter, in particular by G. Derringer, [45] and [46].

It allows to gather criteria having different units through elementary desirability functions, adimensional and varying between 0 and 1. A desirability of 0, i.e., an elementary desirability taking the value a desirability of 0, i.e. an elementary desirability taking the value of 0, represents an unacceptable configuration for the selected property, whereas a desirability taking the value of 1 indicates that an improvement of the selected property will not improve the studied product and thus represents the maximum desired for the criterion.

To each criterion Y_i (i^{tch} criterion) considered, an elementary desirability functions d_i will thus be associated. There are many functions of different types to transform the criteria into elementary desirability functions. We will retain here for the framework of our work the following transformation, presented in figure 27 which has the advantage of transposing easily in mathematical terms the management of properties, [46].

$$d_i = \begin{cases} 0 & \leftrightarrow Y_i \leq Y_{i,p} \\ \left[\dfrac{Y_i - Y_{i,p}}{Y_{i,c} - Y_{i,p}} \right]^{r_i} & \leftrightarrow \quad Y_{i,p} < Y_i < Y_{i,c} \\ 1 & \leftrightarrow Y_i \geq Y_{i,c} \end{cases} \qquad (2.74)$$

With:

- $Y_{i,p}$: floor value below which the criterion is not suitable ($d_i = 0$).
- $Y_{i,c}$: target value above which the criterion is very satisfactory ($d_i = 1$),
- r_{ig}: parameter modifying locally the importance of an increase of the criterion for the considered elementary desirability.

For $r_{ig} > 1$, only an improvement of the criterion around 1a, target value will be influential, whereas for $r_{ig} < 1$ it is the improvement of the criterion around the bottom value which will be significant.
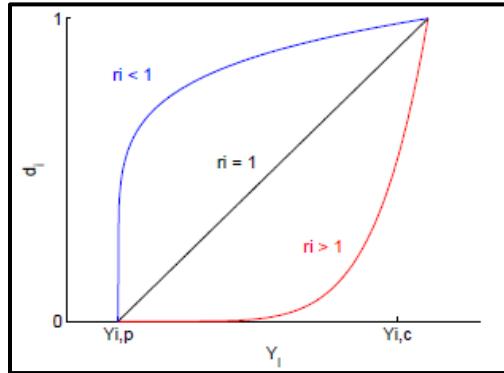
Figure 27. Desirability

The set of elementary desirability functions is then assembled into a composite desirability, D, defined by:

$$D = \left[\Pi d_i^{\omega_i}\right]^{\frac{1}{\sum \omega_i}} \quad (2.75)$$

The ω_i parameters allow to weight the relative importance of the different elementary desirability in the global criterion, i.e., to privilege the importance of some of the criteria.

It is of course quite possible to adapt the proposed mathematical transformation to the problem under study, in particular by reversing the positions of the target and floor values.

By means of this method, it will thus be possible to implement simply design of experiments for the study of composite criteria without having to increase the number of tests to be carried out. The methodology of the design of experiments can thus constitute an effective tool to carry out a complete study leading to an optimal setting of parameters for a multi-criteria objective.

Chapter III

Optimization Algorithms and MANFIS

I. Introduction:

One of the difficult issues that underpin a wide range of machine learning methodologies, from logistic regression model fitting to artificial neural network training is determining the appropriate approach, and this is where optimization comes in since it is a valuable tool for decision making and understanding physical systems. An optimization problem is a mathematical task of selecting the best solution among all available options. This chapter will go through several optimization issues and algorithms for solving them.

II. Optimization:

A branch of applied mathematics whose ideas and methods are used to answer quantitative issues in fields such as physics, biology, engineering, and economics. Questions of maximizing or minimizing functions that arise in diverse areas can be answered using the same mathematical methods. The objective of a common optimization issue is to identify the values of controllable elements controlling the behavior of a system that maximizes production or reduces waste. The simplest issues include functions (systems) of a single variable (input factor) and may be addressed using differential calculus [47].

II.1.   Optimization methodology:

a. Model Construction:

The first stage in the optimization process is to build a suitable model; modeling is the process of defining and describing the problem's objective, variables, and constraints in mathematical terms.

- ➢ An objective is a quantifiable measure of the system's performance that we aim to decrease or maximize.
- ➢ The variables or unknowns are the system components for which we seek to determine values.
- ➢ The constraints are the functions that explain the connections between the variables and specify the variables' possible values.

b. Determining the Problem Type:

The second phase in the optimization process is selecting which optimization category the model belongs to.

III.   Types of Optimization Problems:

Because techniques for addressing optimization issues are adapted to a certain type of problem, categorizing an optimization model is a key stage in the optimization process. Below are listed a few different sorts of optimization problems [48].

a) <u>Continuous Optimization versus Discrete Optimization:</u>

Models with discrete variables result in discrete optimization problems, whereas models with continuous variables result in continuous optimization problems. Continuous optimization issues are typically easier to solve than discrete optimization problems; the smoothness of the functions implies that the values of the objective function and constraint function at a spot xx may be exploited to extrapolate information about points in XX's area. Because many discrete optimization techniques yield a succession of continuous subproblems, continuous optimization algorithms are significant in discrete optimization.

b) <u>Unconstrained Optimization versus Constrained Optimization:</u>

Unconstrained optimization issues emerge directly in many practical applications; they also develop as a result of the reformulation of constrained optimization problems in which the constraints are replaced by a penalty element in the objective function. Constrained optimization issues come from applications with explicit variable restrictions. The variables' constraints might range from basic boundaries to systems of equalities and inequalities that describe intricate interactions between the variables.

Constrained optimization problems are characterized further based on the nature of the constraints (e.g., linear, nonlinear, convex) and the smoothness of the functions (e.g., differentiable or non-differentiable).

c) <u>None, One, or Many Objectives:</u>

The purpose of a feasibility problem is to discover values for variables that fulfill the restrictions of a model with no specific goal to optimize. Complementarity issues are common in engineering and economics. The objective is to identify a solution that meets the complementarity requirements.

When optimum judgments must be made in the context of trade-offs between two or more competing objectives, multi-objective optimization issues arise. In reality, issues with multiple objectives are frequently recast as single-objective problems by producing a weighted mixture of the distinct objectives or by substituting restrictions for parts of the objectives.

d) <u>Deterministic Optimization versus Stochastic Optimization:</u>

It is assumed in deterministic optimization that the data for the given issue are accurate. However, for many real-world issues, the data is inaccurate for several reasons. The first explanation is due to an inaccuracy in measuring. The second and more basic reason is that certain data reflect future knowledge that cannot be known with confidence.

The uncertainty is integrated into the model in optimization under uncertainty, also known as stochastic optimization. When the parameters are only known within specific limitations, robust optimization techniques can be utilized; the objective is to develop a solution that is viable for all data and optimum in some way (e.g. Stochastic optimization models)

IV. Optimization Taxonomy:

Shown here are two perspectives;

"Figure 28" focused mainly on the subfields of deterministic optimization.

"Figure 29" focused on the meta-heuristic algorithms (a high-level problem-independent algorithmic framework that provides a set of guidelines or strategies to develop heuristic optimization algorithms).
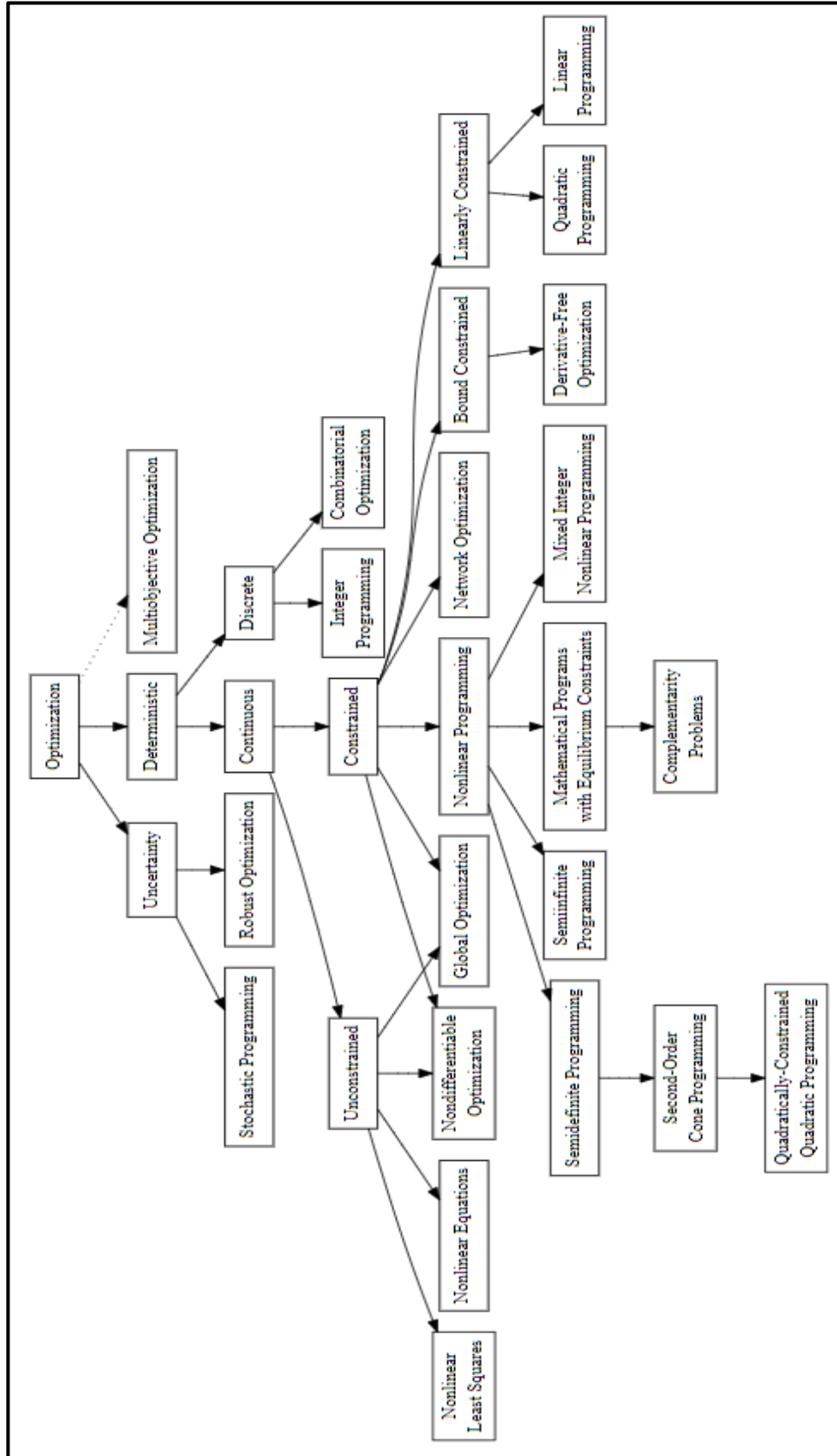
Figure 28 subfields of Deterministic Optimization
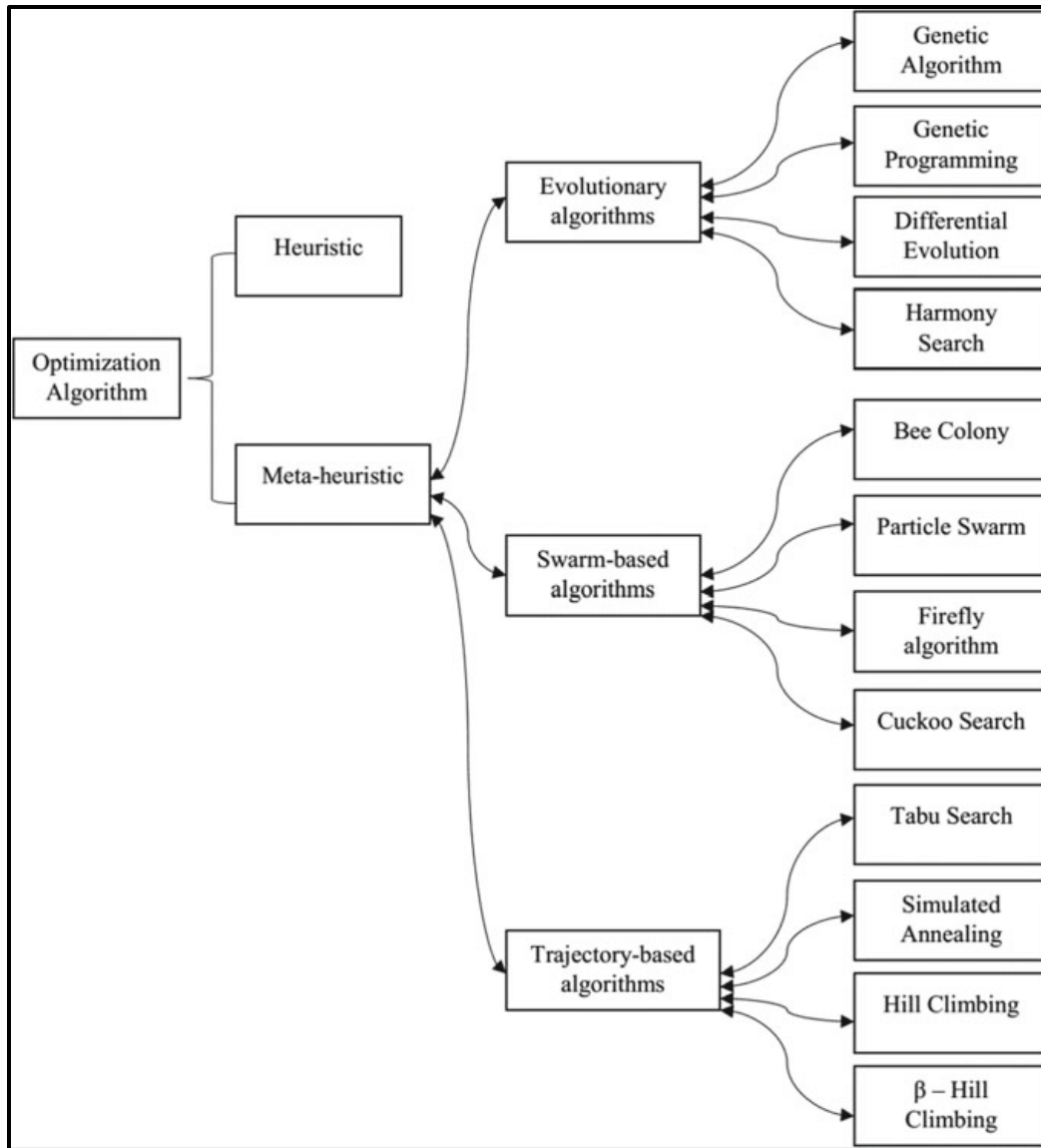
Figure 29. Meta-heuristic Optimization Algorithms Chart

IV.1.   Optimization Algorithms:

Several types of optimization algorithms may be used to solve optimization issues, as well as numerous ways to aggregate and summarize them. One method of categorizing optimization algorithms is based on the quantity of information accessible about the target function being optimized, which can then be exploited and harnessed by the optimization process. In general, the more information is known about the target function, the easier it is to optimize the function if the knowledge can be successfully employed in the search [49].

Perhaps the most significant distinction in optimization algorithms is whether or not the objective function can be distinguished at a location. That is, whether or not the function's first

derivative (gradient or slope) can be computed for a given potential solution. This divides algorithms between those that can and cannot use the derived gradient information.

And from that the following has been established:

A. Differentiable Objective Function:

A differentiable function is one whose derivative can be determined at any point in the input space. A function's derivative at a given value is the pace or quantity of change in the function at that moment. It is commonly referred to as the slope.

- ❖ **<u>First-Order Derivative:</u>** The slope or rate of change of an objective function at a particular position. The gradient is the derivative of a function having more than one input variable (e.g., multivariate inputs).
- ❖ **<u>Gradient:</u>** A multivariate continuous objective function's derivative. A derivative for a multivariate objective function is a vector, and each element in the vector is referred to as a partial derivative, or the rate of change for a specific variable at the point assuming all other variables remain constant.
- ❖ **<u>Partial Derivative:</u>** A component of a multivariate objective function's derivative. We may compute the derivative of the objective function's derivative, which is the rate of change of the rate of change in the objective function. This is known as the second derivative.
- ❖ **<u>Second-Order Derivative:</u>** The rate at which the objective function's derivative changes. This is a matrix and is known as the Hessian matrix for a function that accepts numerous input variables.
- ❖ **<u>Hessian matrix</u>**: The second derivative of a function with two or more input variables. Calculus may be used to optimize simple differentiable functions. Typically, the objective functions of interest cannot be solved analytically.

Among the algorithms that take advantage of gradient information are:

1) Bracketing Algorithms:

Bracketing optimization algorithms are designed for optimization problems with a single input variable where the optima are known to exist within a certain range; they can quickly travel the known range and discover the optima even though they presume that a single optima exists (referred to as unimodal objective functions).

Some examples of bracketing algorithms:
- Fibonacci Search
- Golden Section Search
- Bisection Method

2) Local Descent Algorithms:

Local descent optimization techniques are designed for situations with several input variables and a single global optimum. The "line search" method is the most common example of a local descent algorithm. The line search method has various versions (e.g., the Brent-Dekker algorithm), but the technique typically includes selecting a direction to travel in the search space, then doing a bracketing type search along a line or hyperplane in the chosen direction. This technique is continued until no more advancements are possible. The issue is that optimizing each directional motion in the search space is computationally costly.

3) First-Order Algorithms:

The first gradient is explicitly used in first-order optimization algorithms to pick the direction to travel in the search space. Unlike "local descent algorithms," which perform a full line search for each directional move, the procedures involve first calculating the gradient of the function, then following the gradient in the opposite direction using a step size, which is a hyperparameter that controls how far to move in the search space. A search that is too tiny will take a long time and may become stuck, whereas a search that is too large would zig-zag or bounce about the search area, missing the optima entirely.

First-order algorithms are often known as gradient descent, with more specific names relating to slight modifications to the technique, such as:
- Gradient Descent
- Momentum
- Adagrad
- RMSProp
- Adam

The gradient descent technique also serves as a foundation for the popular stochastic variant of the approach, Stochastic Gradient Descent (SGD), which is used to train artificial neural network (deep learning) models. The key distinction is that the gradient is appropriated rather than explicitly generated, utilizing prediction error on training data, such as one sample (stochastic), all samples (batch), or a limited portion of training data (mini-batch).

Extensions aimed to speed up the gradient descent algorithm (momentum, for example) may and are widely employed with SGD.

a. Gradient Descent:

Gradient descent is a first-order optimization process that is based on a loss function's first-order derivative. It determines how the weights should be changed so that the function can attain a minimum. Backpropagation transfers the loss from one layer to the next, and the model's parameters, also known as weights, are updated based on the losses to minimize the loss.

Algorithm:

$$\theta = \theta - \alpha * \Delta j(\theta)$$

Benefits:

Simple computation, to put into action and grasp.

Disadvantages:

➤ Local minima may be used to trap.
➤ After computing the gradient on the entire dataset, the weights are modified. If the dataset is too vast, it may take years to reach the minima.
➤ Calculating gradient on the entire dataset necessitates a considerable amount of memory.

b. Stochastic Gradient Descent:

Gradient Descent is a variation. It attempts to update the model's parameters more regularly. The model parameters are changed after each training example's loss computation. As a result, if the dataset comprises 1000 rows, SGD will update the model parameters 1000 times in one dataset cycle, rather than once as in Gradient Descent. [50]

Algorithm:

$$\theta = \theta - \alpha * \Delta j(\theta; x_i; y_i)$$

where $\{x_i, y_i\}$ are the training examples.

Advantages:

➤ As a result of frequent modifications to model parameters, the model converges in less time.
➤ Less memory is required since the values of loss functions are not stored.
➤ New minima's are possible.

Disadvantages:

➤ Model parameters have a high degree of variation.
➤ It is possible to shoot even after reaching global minima.
➤ To achieve the same convergence as gradient descent, the learning rate must be gradually reduced.

c. Mini-Batch Gradient Descent:

It outperforms all other gradient descent techniques. It outperforms both SGD and traditional gradient descent. After each batch, it changes the model parameters. As a result, the dataset is separated into batches, and the parameters are updated after each batch.

Algorithm:

$$\theta = \theta - \alpha * \Delta j(\theta; B_i)$$

Where {B_i} are the batches of training examples.

Benefits:

➢ Updates the model parameters often and has reduced volatility.
➢ Memory requirements are moderate.

4) Second-Order Algorithms:

The Hessian is explicitly used in second-order optimization methods to pick the direction to travel in the search space. These approaches are only applicable to objective functions that can be computed or estimated using the Hessian matrix. Newton's Method and The Secant Method are an example of second-order optimization procedures for univariate objective functions.

Quasi-Newton Approaches are second-order methods for multivariate objective functions.

- Quasi-Newton Method

There are several Quasi-Newton Methods, which are usually named after the algorithm's creators, such as:

- Davidson-Fletcher-Powell
- Broyden-Fletcher-Goldfarb-Shanno (BFGS)
- Limited-memory BFGS (L-BFGS)

B. Non-Differential Objective Function:

Optimization techniques that employ the objective function's derivative are fast and efficient. However, there are some objective functions for which the derivative cannot be determined, usually, because the function is complicated for several real-world reasons. Or the derivative can be calculated in some but not all parts of the domain, or it is not a reliable guide.

The following are some challenges with objective functions for the classical algorithms mentioned in the preceding section:

- There is no analytical description of the function (e.g., simulation).
- Several global optimums (e.g., multimodal).
- Evaluation of stochastic functions (e.g., noisy).
- Objective function with discontinuity (e.g., regions with invalid solutions). As such, there are optimization algorithms that do not expect first- or second-order derivatives to be available.

These algorithms are frequently referred to as black-box optimization algorithms since they make little or no assumptions about the objective function (in comparison to traditional approaches).

- Among these algorithms we find:

1) Stochastic Algorithms:

Stochastic optimization techniques employ randomization in the search phase for objective functions whose derivatives cannot be determined. Unlike deterministic direct search approaches, stochastic algorithms often need much more sampling of the objective function but are capable of dealing with difficulties including false local optima.

Stochastic optimization algorithms include:

- Simulated Annealing
- Evolution Strategy
- Cross-Entropy Method

2) Population Algorithms:

Population optimization algorithms are stochastic optimization algorithms that keep a pool (a population) of candidate solutions to sample, explore, and narrow in on an optima. This sort of algorithm is meant for more difficult objective problems with noisy function evaluations and several global optima (multimodal), when finding a good or good enough solution is difficult or impossible using existing approaches.

The pool of possible solutions increases the search's resilience, boosting the possibility of overcoming local optima. Algorithms of this type are intended for more challenging objective problems that may have noisy function evaluations and many global optima (multimodal), and finding a good or good enough solution is challenging or infeasible using other methods.

Examples of population optimization algorithms include:

- Genetic Algorithm

- Differential Evolution
- Particle Swarm Optimization

3) Direct Algorithms:

Direct optimization procedures are used for objective functions that do not have derivatives. The algorithms are deterministic techniques that frequently assume the goal function has a single global optimum, for example, unimodal. Direct search methods are often known as "pattern searches" since they may explore the search space using geometric forms or judgments, such as patterns. Gradient information is derived directly from the objective function's outcome of assessing the relative difference between scores for points in the search space. These direct estimations are then utilized to select a search direction and triangulate the location of the optima. Examples of direct search algorithms:

- Cyclic Coordinate Search
- Powell's Method
- Hooke-Jeeves Method
- Nelder-Mead Simplex Search
- Neural Network

In This Part we'll go through the principles of neural networks in detail. starting by artificial neural networks and how they are inspired by the biological neural networks in human bodies. Following that, we'll look at the classic Perceptron method and its place in neural network history. Finally, we'll go through the four components that every neural network need.

V.   Neural Networks:

The adjective form of "neuron" is "neural," and "network" suggests a graph-like structure; hence, an "Artificial Neural Network" is a computer system that aims to emulate (or is inspired by) the neural connections in our nervous system. "Neural networks" or "artificial neural systems" are other terms for artificial neural networks. Artificial Neural Networks are commonly abbreviated as "ANN" or simply "NN."

To be termed a NN, a system must have a labeled, directed network structure with each node doing some basic computation. A directed graph, according to graph theory, consists of a collection of nodes (i.e., vertices) and a set of connections (i.e., edges) that connect pairs of nodes. Figure 1 is an example of such a NN graph.

The network below is shown with inputs. Each link transports a signal via the network's two hidden levels. The output class label is computed by a final function.

Each node does a basic calculation. Each link then transports a signal from one node to the next, tagged with a weight indicating the degree to which the signal is amplified or lessened.
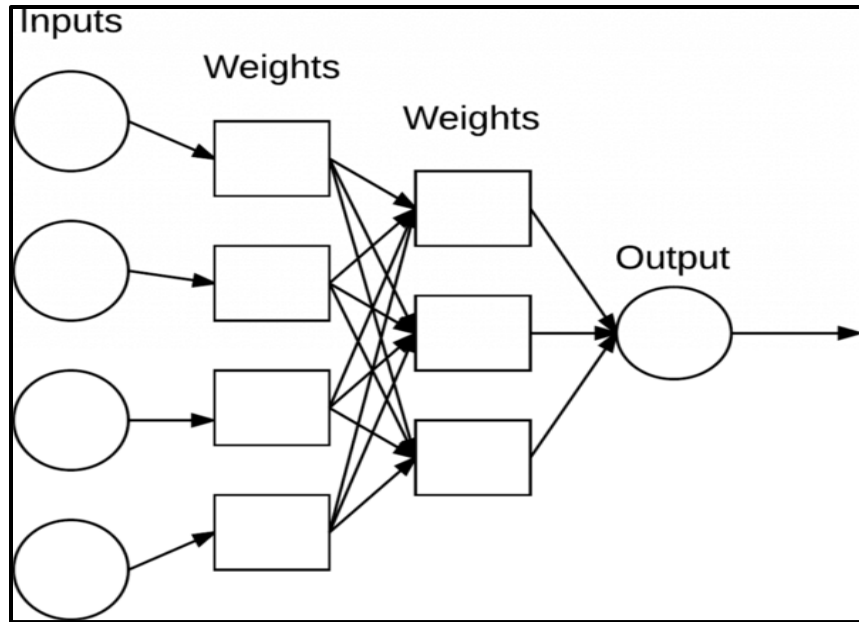
Figure 30. A simple neural network architecture

A system is called an Artificial Neural Network if it has a graph structure (as shown in Figure 30) and connection weights that can be changed using a learning algorithm.

IV.6.   Relation to Biology:

Brains are made up of around 10 billion neurons, each of which is linked to approximately 10,000 other neurons. The soma is the neuron's cell body, where inputs (dendrites) and outputs (axons) join one soma to another (Figure 31).
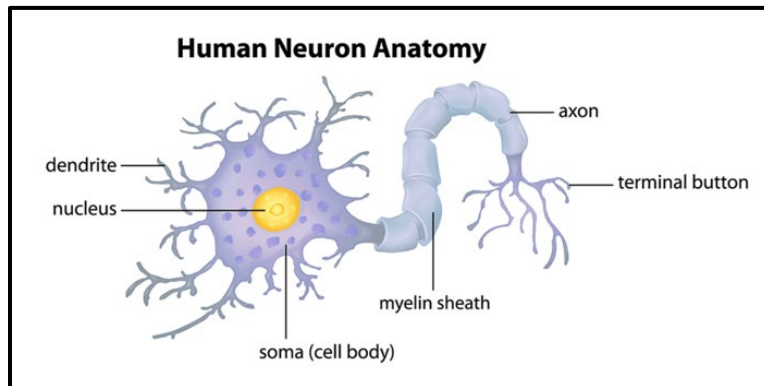
Figure 31. The structure of a biological neuron. Neurons are connected to other neurons through their dendrites and neurons.

At their dendrites, neurons receive electrochemical input from other neurons. If these electrical inputs are strong enough to activate the neuron, the stimulated neuron sends the signal via its axon to the dendrites of other neurons. These connected neurons may also fire, so continuing the message-passing process.

The main message here is that firing a neuron is a binary activity – the neuron either fires or does not fire. There are no distinct "levels" of fire. Simply expressed, a neuron will fire only if the total signal received at the soma reaches a certain threshold.

ANNs, on the other hand, are simply inspired by what we know about the brain and how it functions. The purpose of deep learning is not to duplicate how brains function, but rather to take what we know and use it to draw similarities in our own work "Seek inspiration".

IV.7.   Neural Network Components:

1. Data: The information required by the neural network.
2. Model: A neural network.
3. Objective Function: Determines how near our model's output is to the predicted one.
4. Optimization Algorithm: Improving model performance using a trial-and-error cycle

IV.8.   Artificial Models:

Starting with a simple NN in (Figure 32) that does a simple weighted sum of the inputs. The inputs to the NN are the values x_1, x_2, and x_3, which generally equate to a single row (i.e., data point) from our design matrix. The bias, represented by the constant number 1, is considered to be included in the design matrix. These inputs may be thought of as the NN's input feature vectors.

This weighted total is then processed by the activation function to determine whether or not the neuron fires.

In practice, these inputs might be vectors that are utilized to quantitatively measure the contents of a picture in a systematic, specified manner. These inputs are the raw pixel intensities of the pictures themselves in the context of deep learning [51].
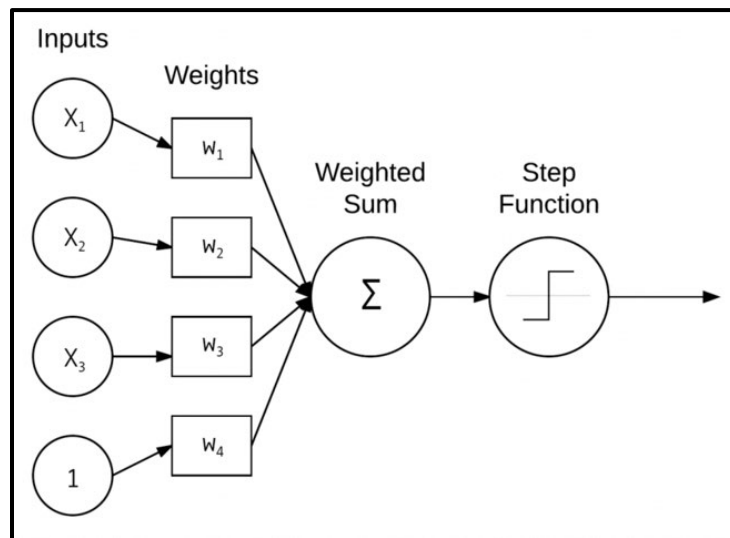
Figure 32. A simple NN that takes the weighted sum of the input x and weights w.

A weight vector connects each x to a neuron. W is made up of w_1, w_2, w_n, which means that for each input x, there is a corresponding weight w.

Finally, the output node on Figure 32's right takes the weighted sum, applies an activation function f (used to decide whether or not the neuron "fires"), and outputs a value. When the results are expressed numerically, three forms are often found:

$$f(w_1 x_1 + w_2 2 + \cdots + w_n x_n)$$

$$f\left(\sum_{i=1}^{n} w_i x_i\right)$$

•Or simply $\qquad f(net) \qquad$ where $\qquad net = (\sum_{i=1}^{n} x_i)$

Regardless of how the output value is written, a weighted sum of inputs is taken and an activation function f is applied
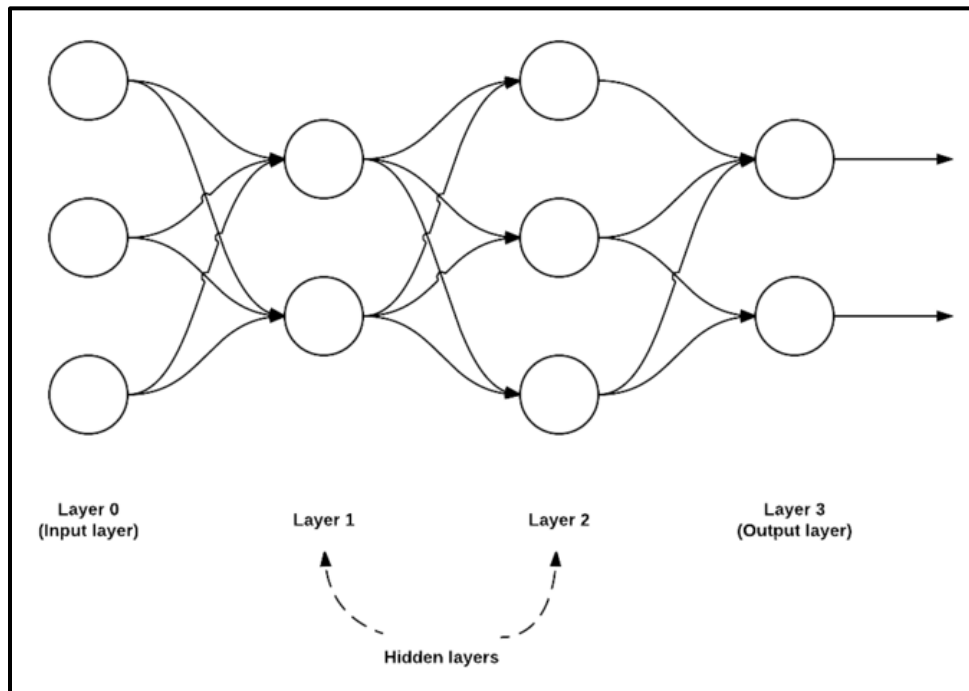
Figure 33. A feedforward neural network with three input nodes, a hidden layer of two nodes, a second hidden layer of three nodes, and a final output layer of two nodes.

IV.9.   Architectures of Feedforward Networks:

While there are other NN topologies, the feedforward network is the most prevalent, as seen in Figure 33. A connection between nodes in this design is only permitted from nodes in layer

I to nodes in layer i+1 (hence the term, feedforward). Backward or inter-layer connections are not permitted. Recurrent neural networks are formed when feedforward networks add feedback connections (output connections that feed back into the inputs).

Generally, a series of numbers is used to quickly and simply express the number of nodes in each tier when describing a feedforward network. The network in Figure 33 is a 3-2-3-2 feedforward network, for example:

- **Layer 0** has three inputs, which are our xi values. These might be an image's raw pixel intensities or a feature vector derived from the picture.
- **Layers 1 and 2** are hidden layers with two and three nodes, respectively.
- **Layer 3** is the output layer, also known as the visible layer, and it is where the network's total output categorization is acquired. The output layer normally contains the same number of nodes as class labels, one for each conceivable output [51].

IV.10.   Neural Learning:

The process of altering the weights and connections between nodes in a network is referred to as neural learning. Learning is defined biologically by Hebb's principle:

When an axon of cell A is close enough to excite cell B and regularly or consistently fires it, some development process or metabolic change occurs in one or both cells, increasing A's efficiency as one of the cells firing B.

IV.11.   Neural Networks Application:

Neural Networks may be used in both supervised and unsupervised learning tasks, as long as the suitable design is applied. To mention a few, common applications of NN include classification, regression, clustering, vector quantization, pattern association, and function approximation.

V.   Fuzzy Logic:

The term "fuzzy" refers to things that are vague or equivocal. In the actual world, we frequently meet situations in which we are unable to tell whether a condition is true or untrue; its fuzzy logic gives extremely significant flexibility for thinking. In this method, we may examine any situation's errors and uncertainties.

In the Boolean system, truth value is represented by 1.0 as the absolute truth value and 0.0 as the absolute false value. However, there is no logic in the fuzzy system for absolute truth and absolute false value. However, with fuzzy logic, there is an intermediate value that is both partially true and partially false.
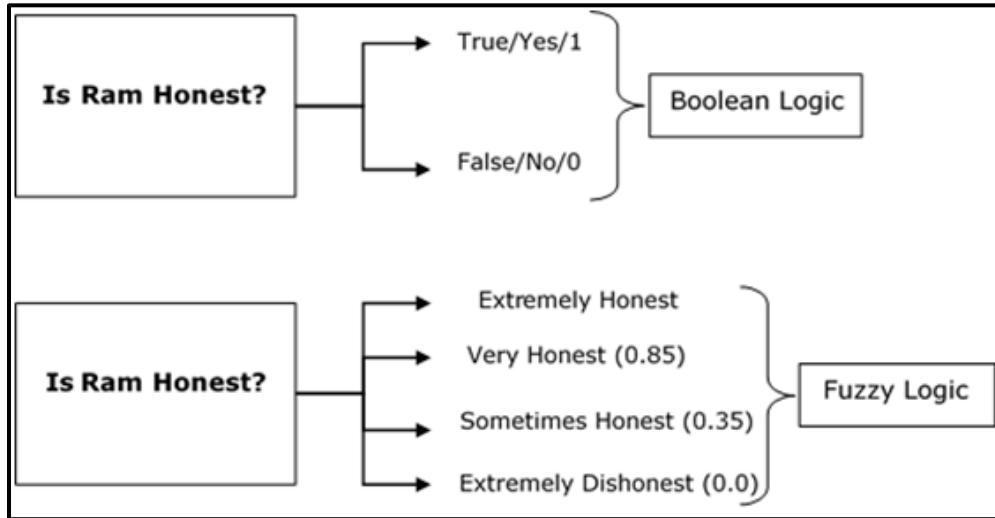
Figure 34. Graph representing "Fuzzy Logic"

V.1.   Fuzzy Logic Architecture:

Its architecture is divided into four sections:

❖ **Rule Base**: It comprises the collection of rules and IF-THEN conditions offered by experts to manage the decision-making system based on linguistic data. Recent advances in fuzzy theory provide various viable strategies for designing and adjusting fuzzy controllers. The majority of these advancements lower the number of fuzzy rules.

❖ **Fuzzification**: It is used to turn inputs, such as crisp integers, into fuzzy sets. Crisp inputs are the exact inputs measured by sensors and supplied into the control system for processing, such as temperature, pressure, rpm, and so on.

❖ **Inference Engine:** It calculates the degree of matching of the current fuzzy input with regard to each rule and picks which rules to fire based on the input field. The control actions are then formed by combining the fired rules.

❖ **Defuzzification**: It is used to turn the inference engine's fuzzy sets into a crisp value. There are numerous defuzzification strategies available, and the most appropriate one is employed in conjunction with a certain expert system to decrease error.
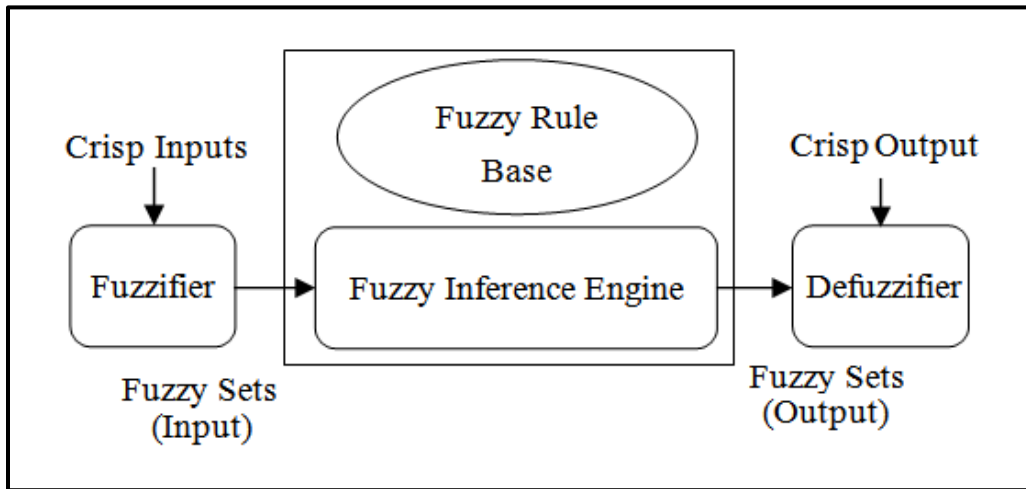
Figure 35. Architecture of Fuzzy Logic

V.2.   Definition of a membership function:

A graph that shows how each point in the input space is transformed to a membership value between 0 and 1. Input space is also known as the universe of discourse or universal set (u), and it encompasses all of the conceivable items of concern in any application.

Fuzzifiers are classified into three types:

- Fuzzifier for singletons
- Fuzzifier using Gaussian distribution
- Fuzzifiers that are trapezoidal or triangular

V.3.   Fuzzy Control:

It is a method of incorporating human-like reasoning into a control system. that intends to provide exact reasoning, rather it is intended to provide acceptable reasoning. It may mimic human deductive reasoning, which is the method by which humans draw conclusions from what they know. With the use of fuzzy logic, any uncertainties may be readily dealt with.

V.4.   The Benefits of a Fuzzy Logic System:

- Can function with any sort of input data, whether it is inaccurate, distorted, or noisy.
- Fuzzy logic is based on set theory mathematical principles, and the rationale behind it is relatively straightforward which is simple to build and comprehend.
- Because it is similar to human thinking and decision-making, it gives a very efficient solution to difficult issues in many aspects of life.
- Because the methods may be explained with minimal data, memory is not required.

V.5.   The Drawbacks of Fuzzy Logic Systems:

- Many scholars offered many approaches to solving a specific problem using fuzzy logic, resulting in uncertainty. There is no systematic strategy to using fuzzy logic to tackle a specific problem.
- In most circumstances, proving its properties is difficult or impossible since we never acquire a mathematical description of our technique.
- Because fuzzy logic operates on both exact and imprecise input, accuracy is frequently compromised.

V.6.   Applications:

- Used in the aerospace industry to regulate the altitude of spacecraft and satellites, and in automobile systems to manage speed and traffic.
- Decision-making support systems and personal evaluation in major corporations.
- Used in the chemical industry to manage the pH, drying, and chemical distillation processes.
- Natural language processing and a variety of intense AI applications.
- Fuzzy logic is utilized in conjunction with Neural Networks because it simulates how humans make judgments, only much faster. It is accomplished by data aggregation and transformation into more relevant data by producing partial truths as Fuzzy sets.

VI.   Multi Adaptive Neuro Fuzzy Inference System (MANFIS):

MANFIS is an extension of the neuro-fuzzy system ANFIS [52], to produce multiple outputs. A neuro-fuzzy system can serve as a nonparametric regression tool, which models the regression relationship without reference to any pre-specified functional form. Originally, ANFIS could only produce a single output but MANFIS aggregates many independent ANFIS to obtain multiple outputs [53]. The architecture of MANFIS is depicted in "Figure 36-a".
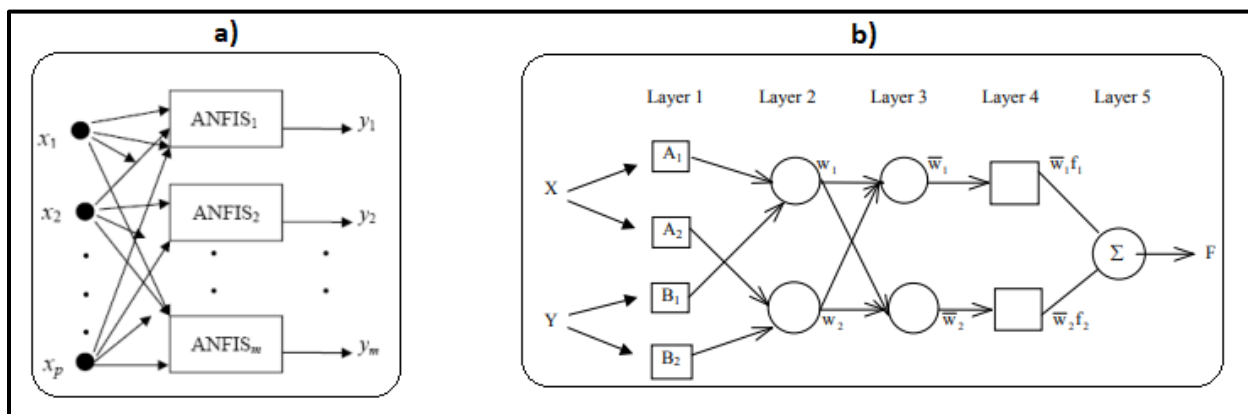
Figure 36. The artchitechteures of adaptive neuro fuzzy networks, a) MANFIS, b) ANFIS

The ANFIS is a combination of fuzzy logic and neural network algorithm, initially proposed in the early 90s by J S Jang [52]. It combines the greatest features of both because it offers fuzzy logic qualitative analysis as well as learning skills. The Hybrid Learning Rule is applied by ANFIS to optimize the final inference system through NN's Training. ANFIS is equivalent to TAKAGI SUGENO first-order system [52]. It is represented by the following two IF-THEN rules:

$$1^{st} rule: IF\ x is A_1\ and\ y is B_1\ THEN f_1 = p_1 x + q_1 y + r_1 \quad (1)$$

$$2^{nd} rule: IF\ x is A_1\ and\ y is B_1\ THEN f_2 = p_2 x + q_2 y + r_2 \quad (2)$$

Where x and y denote system inputs. A_i, B_i are fuzzy subsets coded by fuzzy membership functions (MFs), and f_i are system outputs within the fuzzy layer is based on fuzzy IF-THEN rules. p_1 and f_1 are linear adaptive parameters tuned during the training phase.

The ANFIS flowchart is shown in in "Figure 36-b". It consists of five layers where three layers are fixed nodes schematized by circles, and two adaptive layers schematized by squares.

Fuzzification layer: Subset of adaptive nodes. Expressing the fuzzy membership conditions of each input where:

$$O_i^1 = U_{A_i}(x) \quad (3)$$

Where: x denotes the input to the node i; A_i denotes the linguistic label associated with the node i; and U_{A_i} is a membership function (MF). In this study, the Gaussian membership function given by (4) is used:

$$U_{A_i}(x) = e^{-\frac{1}{2}\left(\frac{x-c}{\sigma}\right)^2} \quad (4)$$

Gaussian MF is fully defined by two nonlinear parameters c and σ where c is the MF center and c determines Gaussian MF width. These nonlinear parameters are known as premise parameters which are adjusted during the training phase.

Product layer: Subset of fixed nodes, producing the firing strengths of the rules. Acting as a simple multiplier of received signals from the previous layer as:

$$W_i = U_{A_i}(x) \times U_{B_i}(x) \quad (5)$$

Normalization layer: Subset of fixed nodes that normalize each weight W_i, by dividing it according to the total of all the weights associated with each rule as follows:

$$\overline{W} = \frac{W_i}{W_1 + W_2}, \quad i = 1, 2. \quad (6)$$

$\overline{W}$ is called normalized firing strengths[52,53].

Defuzzification layer: The output of each node given by (7) is the product of each normalized firing strength and a first-order polynomial:

$$O_i^4 = \overline{W}f_i = \overline{W_i(p_i x + q_i y + r_i)} \quad (7)$$

Where $\{p_i, q_i, r_i\}$ are the consequent parameters to be defined during the training phase [52,54].

Output layer: is a single of fixed nodes that sums all received information from the previous layer and delivers the network output, such as [52,53]:

$$O_i^5 = \sum \overline{W}f_i \quad (8)$$

In the present research, a hybrid training algorithm is used to adapt the network parameters. The least-squares approach and the backpropagation gradient descent method are combined in the hybrid algorithm and the backpropagation gradient descent method to optimize premise and consequent parameters [55, 56].

VI.1.   Performance Criterions:

In this work, both training and testing errors can be evaluated by Mean Squared Error(MSE) [55], and correlation Coefficient (R^2) [53], expressed by (9-10),for the MANFIS model validation and to determine the performance of the models predicted by the output values of the corresponding experimental dataset.

$$RMS = \frac{1}{n}\sum_{i=0}^{n}(X_i - Y_i)^2 \quad (9)$$

$$R^2 = 1 - \frac{\sum_{i=1}^{n}(X_i - Y_i)^2}{\sum_{i=1}^{n}(X_i - \overline{Y}_i)^2} \quad (10)$$

Where:

- ❖ n is the number of samples;
- ❖ X_i and Y_i are the measured and predicted values respectively.
- ❖ $\overline{Y}_i$ is the mean value of the predicted data.

ANFIS can be used for classification, approximation of highly nonlinear functions, on-line identification in discrete control system and to predict a chaotic time series. And can serve as a basis for constructing a set of fuzzy 'if–then' rules with appropriate membership function to generate the stipulated input–output pairs.

Chapter IV

Experimental and Result Discussion

I.   Introduction:

Characterizing and understanding the performance of FFF-processed PLA components is critical, and many shortcomings may be mitigated by carefully selecting processing settings.

This dissertation, aims to characterize the mechanical characteristics in terms of yield Stress, Young Modulus, and so on to evaluate the impacts of various printing settings on the properties of PLA printed components using the FFF technique in conjunction with a Central Composite Design.

Another goal of this project is to determine the ideal combination of printing settings to increase the printed part's strength. While using Desirability function prediction to do so. To prevent producing a large number of specimens, a Central Composite Design was used, which refers to how parameters are assigned to various conditions.

II.   Specimen manufacturing:

The specimen was designed with the precise shape and dimensions by the SolidWorks software according to the ASTMD638 Type IV Standard and exported to an STL file so that it could be read and interpreted by the printer parameterization software. The Repetier-Host (Cura) software was used in this project to generate G-Code so that it could be printed. The "ANYCUBIC I3 MEGA" printer was used to print all of the specimens.
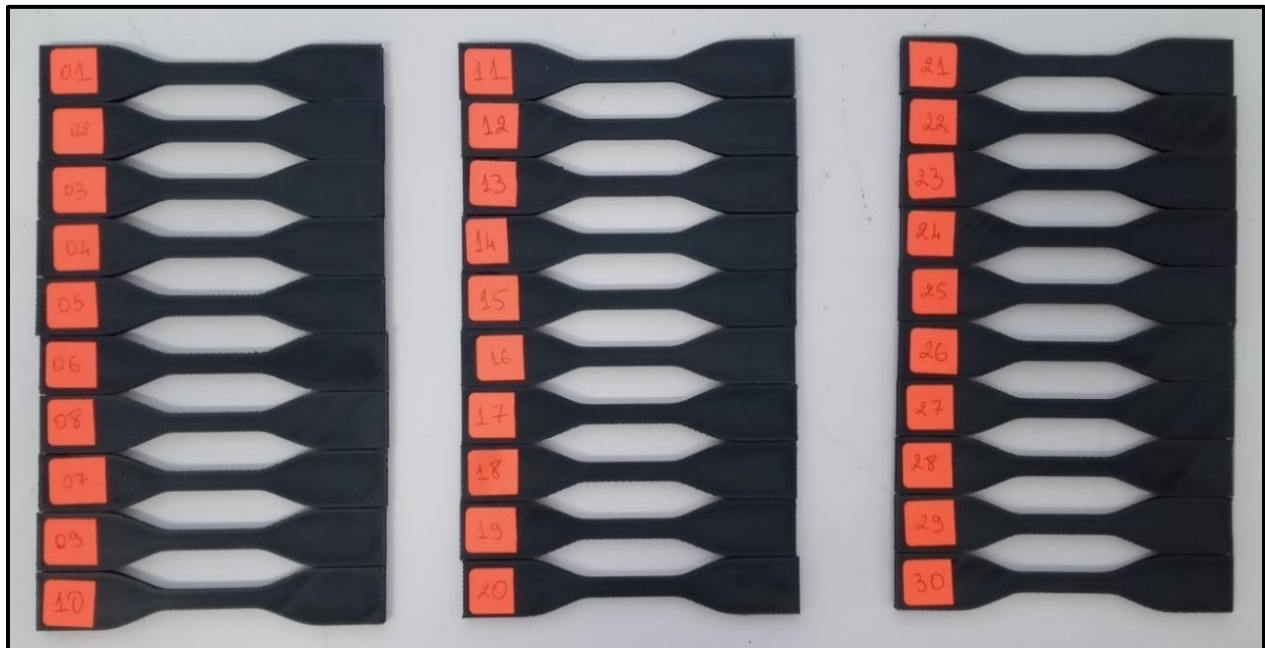
Figure 37. The 30 Printed specimens

III. Tensile testing and specimens:

The tensile specimens used in this study were printed according to ASTM D-638 "Type IV" standard test procedure for plastics and composites, and are dumbbell-shaped as shown in Figure 38.

To characterize the mechanical behavior of PLA components subjected to tensile stresses, the elastic modulus (Young's modulus), and elastic limit (Yield stress), are computed.

Table 10. ASTM D638 Type IV Specimen Dimensions

Standard	Type	L_0	L	W_0	W	B	G	D	R	R_0
ASTMD 638	IV	115	33 ± 0.5	19 ± 6.4	6 ± 0.05	3.2 ± 0.4	25 ± 0.2	64.5 ± 5	14	25
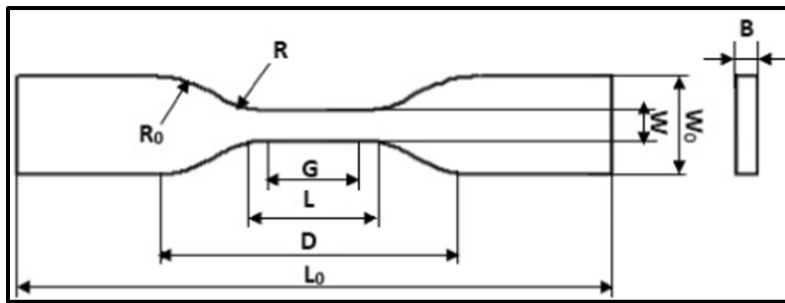
Figure 38. Geometrical drawing of specimens for tensile test.

IV. Materials and methods:

The specimens for this investigation were made from PLA (Graphite Gray) Filament [BGRL7043425C], a commercial material developed and manufactured by the American company Paramount 3D in accordance with ISO9001 standards (Fig. 39 A) and printed with "ANYCUBIC I3 MEGA" printer. (Fig. 39 B)

Material discerption

- ❖ Material: 100% virgin PLA
- ❖ Color: Graphite Gray
- ❖ Thickness: 1.75 mm
- ❖ Spool Weight: 1.0 kg (2.2 lb.)
- ❖ Spool Size: 2.25" ID / 7.75" OD / 2.25" Depth
- ❖ Printing temperature: 190 - 220 C

Technical Specification For the "ANYCUBIC I3 MEGA" printer

- ❖ Technology: FDM Fused Deposition Modeling
- ❖ Build Size: 210×210×205 (mm3)
- ❖ Nozzle/Filament Diameter: 0.4 mm/1.75mm
- ❖ Positioning Accuracy: X/Y 0.0125mm，Z 0.002mm

- ❖ Print Speed: 20~100mm/s (suggested 60mm/s)
- ❖ Operational Extruder Temperature: 260°C max
- ❖ Slicer Software: Cura
- ❖ Software Input / Output Formats: STL, OBJ, DAE, AMF / GCode
- ❖ Printer Dimensions: 405mm×410mm×453mm
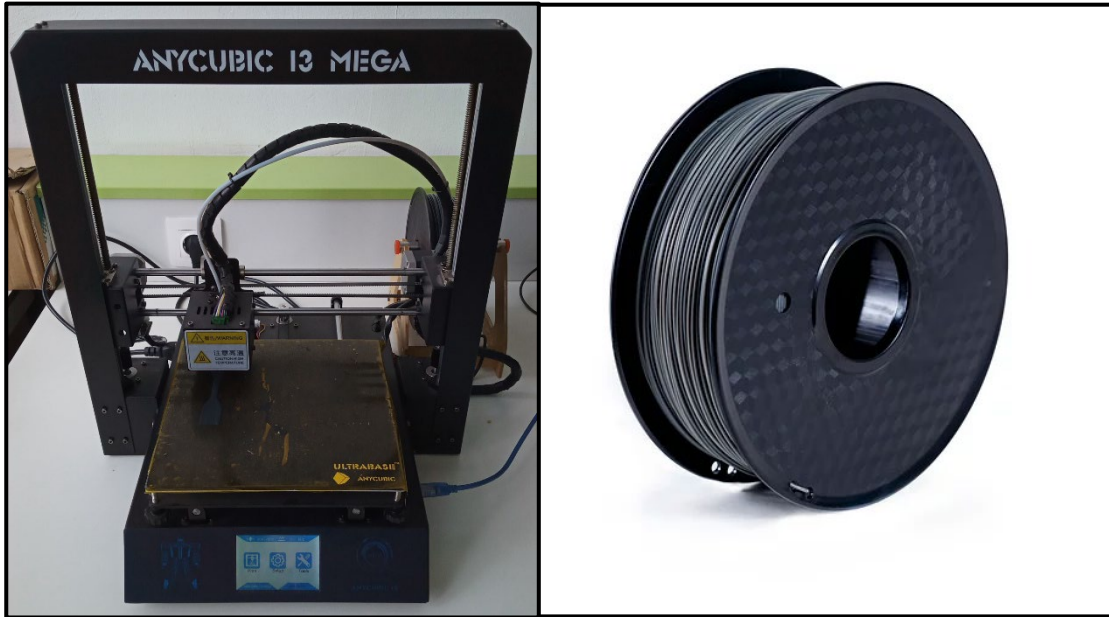
Figure 39. Left "A" "ANYCUBIC I3 MEGA" printer, Right "B" PLA Filament used

V.   Experimental setup:

The universal MTS Criterion Model43 machine, equipped with a 50 kN load cell and a 1 mm/min displacement rate, was employed for these tensile tests once all the samples were printed. The tests are carried out for all 30 specimens after the setup is equipped and adjusted.

Specifications of the MTS MODEL 43
- ❖ Maximum Rated: 30 kN
- ❖ Force Capacity: 6600 ibf
- ❖ Maximum/Minimum Test Speed: 1020 / 40.16 mm/min
- ❖ Position Resolution / Accuracy: 0.00006 mm / within ± 0.5%
- ❖ Vertical Test Space: 1500 mm
- ❖ Crosshead Travel: 1300 mm
- ❖ Frame Height / Width / Depth: 2050/ 826 / 768 mm
- ❖ Frame Weight: 305 kg
- ❖ Speed Accuracy / Set speed < 0.01mm/min
- ❖ Data Acquisition Rate: 1000 Hz
- ❖ Motor & Drive System: AC Servo Motor
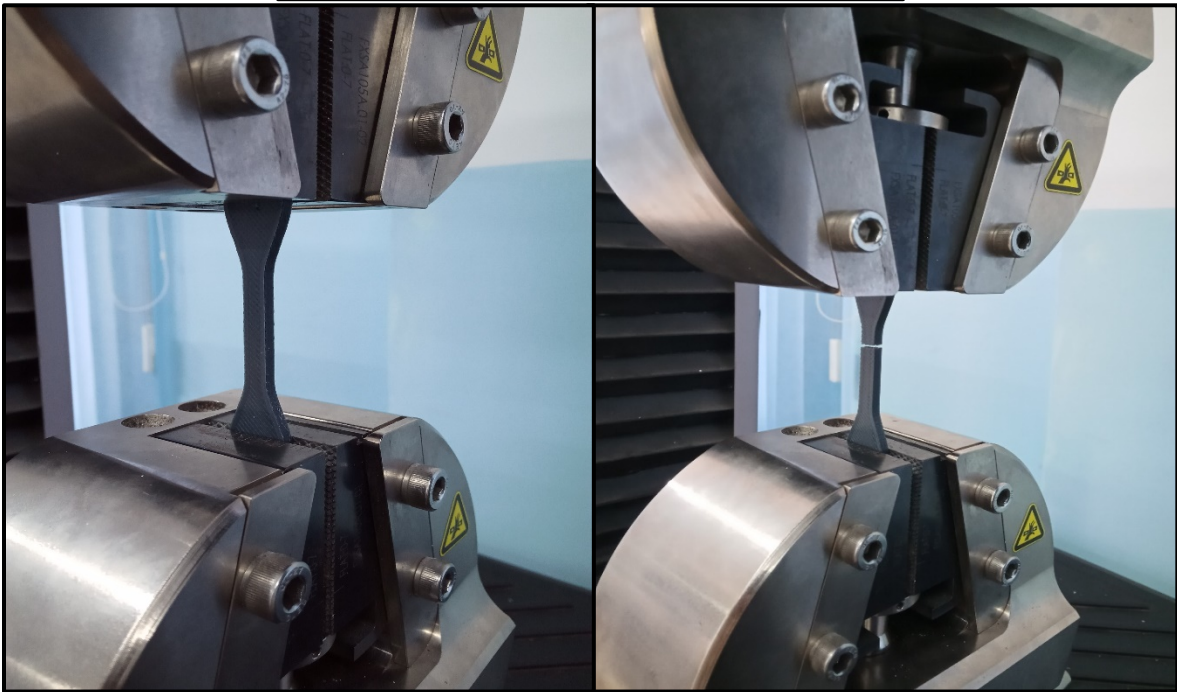
Figure 40 Top "the MTS Criterion Model43", Bottom "tensile test before and after the specimen rupture"

Figure 41. All the printed specimens after the tensile test

VI.   Central Composite Design:

To carry out the research, a design of experiment (DOE) based on the Central Composite approach was used, which is a robust optimization strategy for creating experiments to anticipate responses and optimize the FFF process parameters in terms of accuracy. Based on past research, printer setups, and material manufacturer recommendations, the parameters and levels given in "Table 11" were chosen for their high efficacy on mechanical qualities. Finally, layer height, fill density, printing velocity, and Nozzle temperature were chosen.

Table 11. Factors and levels used for the DOE

Parameters	Lowest Level	Highest Level	Alpha -	Alpha +
Layer height (mm)	0.14	0.22	0.1	0.26
Fill density (%)	30	50	20	60
Velocity (mm/s)	48	58	43	63
Nozzle temperature (C°)	199	213	192	220

A Central Composite Design was used to assess the effect of the selected factors and levels using Design-Expert software for statistical analyses "Table 12".

Table 12. Central Composite Design array of DOE.

Runs	Infill Density	Temperature	Printing Velocity	Layer Height
1	40	206	53	0.18
2	50	199	58	0.14
3	30	199	58	0.14
4	30	199	48	0.14
5	50	213	58	0.14
6	40	206	53	0.18
7	40	220	53	0.18
8	40	192	53	0.18
9	40	206	53	0.18
10	30	213	58	0.22
11	40	206	53	0.1
12	30	199	48	0.22
13	50	213	58	0.22
14	30	199	58	0.22
15	30	213	48	0.22
16	40	206	53	0.26
17	50	213	48	0.22
18	40	206	53	0.18
19	40	206	53	0.18
20	60	206	53	0.18
21	20	206	53	0.18
22	30	213	48	0.14
23	50	199	48	0.22
24	40	206	53	0.18
25	50	213	48	0.14
26	40	206	63	0.18
27	50	199	58	0.22
28	40	206	43	0.18
29	50	199	48	0.14
30	30	213	58	0.14

Table 13. Main constant printing parameters used in the experiments

NOZZLE Diameter	INFILL PATERN	SKIRT LAYER	ORIANTAION
1.75	Gyroid	2 Layers	X-axis

VII.   Infill Type:

Personalized bone scaffolds with unparalleled structural and functional features are now possible thanks to additive manufacturing (AM). The main problem is to realize such structures via melt-extrusion 3D printing and which infill to use, that's why Specific biological and mechanical functionality, such as increased regeneration via enhanced cell migration and higher structural integrity, can be produced for scaffolds designed as temporary guiding structures for endogenous tissue regeneration using such a methodology.

And that is how the gyroid structure was chosen in this work to be used as an infill, because according to [57] where the gyroid infill was used as an infill to print out scaffolds where they were tested mechanically and in conclusion the results reveal that gyroid scaffolds have high reliable mechanical properties. Dudescu et al. [58] determined that an increase in relative infill density had a beneficial effect on elastic modulus while the printing orientations did not. And that Gyroid infill doesn't need more support structure

The architecture of an open cell foam is represented by the gyroid Figure 42 "Middle". Alan Schoen discovered it in 1970 [58,59] and it belongs to the class of triply periodic minimal surfaces (TPMS) [60]. The gyroid has a mean curvature of zero and is periodic in its three primary directions. Eq. (1) shows the implicit function, where "a" is a parameter for the size of the gyroid unit cell and "t" is the level parameter of the isosurface that may efficiently manage the relative density of the gyroid surface [61]:

$$\text{SIN}(\frac{2\pi}{a}x)\,\text{COS}\left(\frac{2\pi}{a}y\right) + \text{SIN}\left(\frac{2\pi}{a}y\right)\text{COS}\left(\frac{2\pi}{a}z\right) + \text{SIN}\left(\frac{2\pi}{a}z\right)\text{COS}\left(\frac{2\pi}{a}x\right) = t \quad (1)$$
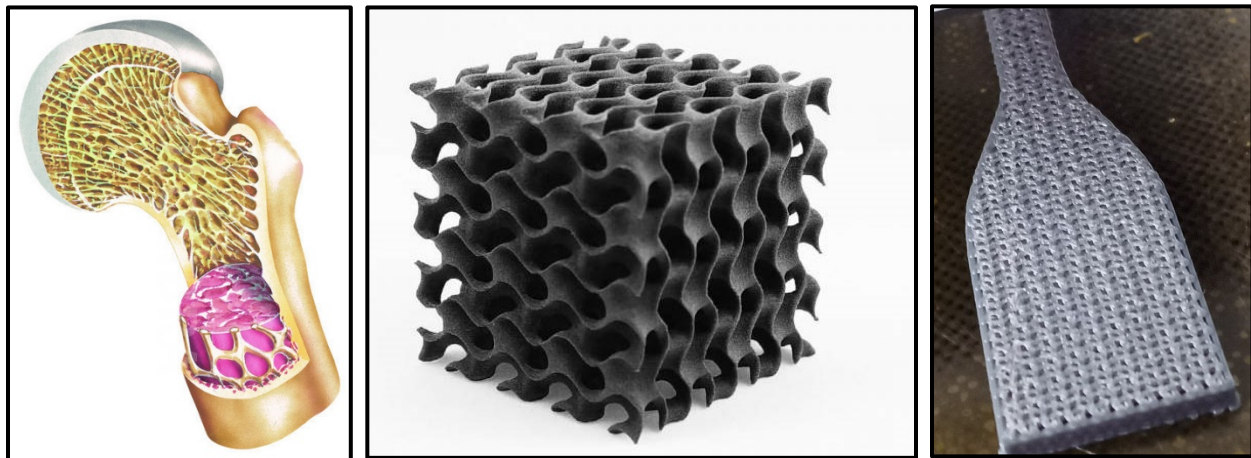
Figure 42. Left "Bone scaffolds", Middle "Representation of Gyroid Infill IRL", Right "Infill of one of the printed Specimens"

Figure 43 depicts the cut portion of the samples, which illustrates the varied density percent of Gyroid infill pattern that was applied in the slicer software to print the samples to clarify the specified parameters.

Figure 43. Cut sections with Different % density in gyroid infill pattern.

VIII.   Process of analysis:

A file is obtained from the data logger when each test is completed. First, a file containing the force measured by the load cell and the displacement measured by the Crosshead.

To obtain the defined mechanical properties such as young's modulus (E), yield strength (σ), maximum strength (σ_{max}), Design Expert v13. Software is used to analyze the data. The results obtained from the experiments are presented in "Table 14". Central Composite approach to experimental design is described below. The first step of the Central Composite method is to measure the quality characteristic that needs to be optimized.

The output variable or response that is an important index on the quality of the part is called quality indicator. In this study, yield stress, and Young Modulus are the quality indicators. In the second step, the control of the test parameters that have significant effects on the quality are identified with the required number of tests and their levels. Then, an appropriate orthogonal table for the control parameters is selected after calculating the minimum number of experiments to be conducted considering the interactive effects. The experimental test conditions and the observed data are presented in "Table 14". In order to obtain a certain young modulus, it is necessary to use optimization techniques to find the optimal process parameters. Desirability function can be conveniently used for these purposes, and therefore, the above methodologies are chosen to optimize the machining parameters in this work.

The output response (y) can be predicted from the quadratic model described by the following equation:

$$\hat{Y} = a_0 + a_1 x_1 + a_2 x_2 + a_3 x_3 + a_4 x_4 + a_{11} x_1^2 + a_{22} x_2^2 + a_{33} x_3^2 + a_{44} x_4^2 + a_{12} x_{12}$$

$$+ a_{13} x_{13} + a_{14} x_{14} + a_{23} x_{23} + a_{24} x_{24} + a_{34} x_{34} + e$$

Table 14. The experimental test conditions and the observed data

Run	Space Type	Infill Density %	Temperature C°	Printing Speed mm/s	Layer Height mm	Young Modulus GPa	Yield Stress MPa
1	Center	40	206	53	0.18	1.94635	13.211
2	Factorial	50	199	58	0.14	2.20791	13.954
3	Factorial	30	199	58	0.14	1.53071	10.118
4	Factorial	30	199	48	0.14	1.53167	8.899
5	Factorial	50	213	58	0.14	2.2375	11.814
6	Center	40	206	53	0.18	1.94635	13.211
7	Axial	40	220	53	0.18	1.96077	12.294
8	Axial	40	192	53	0.18	1.93645	11.36
9	Center	40	206	53	0.18	1.94635	13.211
10	Factorial	30	213	58	0.22	1.74318	13.283
11	Axial	40	206	53	0.1	2.01484	12.658
12	Factorial	30	199	48	0.22	1.84257	13.625
13	Factorial	50	213	58	0.22	2.00436	12.263
14	Factorial	30	199	58	0.22	1.81758	12.578
15	Factorial	30	213	48	0.22	1.76788	14.532
16	Axial	40	206	53	0.26	2.15707	17.688
17	Factorial	50	213	48	0.22	2.29542	16.527
18	Center	40	206	53	0.18	1.94635	13.211
19	Center	40	206	53	0.18	1.94635	13.211
20	Axial	60	206	53	0.18	2.38375	13.492
21	Axial	20	206	53	0.18	1.39515	9.501
22	Factorial	30	213	48	0.14	1.59238	8.153
23	Factorial	50	199	48	0.22	2.29424	14.729
24	Center	40	206	53	0.18	1.94635	13.211
25	Factorial	50	213	48	0.14	2.26241	14.588
26	Axial	40	206	63	0.18	1.87821	10.687
27	Factorial	50	199	58	0.22	2.29609	12.501
28	Axial	40	206	43	0.18	1.95464	13.272
29	Factorial	50	199	48	0.14	2.16411	15.798
30	Factorial	30	213	58	0.14	1.54716	9.809

A. Effect of the printer parameters on young modulus:

Figure 44 depicts the influence of infill density, Nozzle Temperature, Printing Speed, and Layer Height on Young Modulus. As seen in the image, Infill density has the greatest influence on Young Modulus, with the higher the density, the greater the increase in Young Modulus. While the remainder of the factors have minimal impact on young modulus,
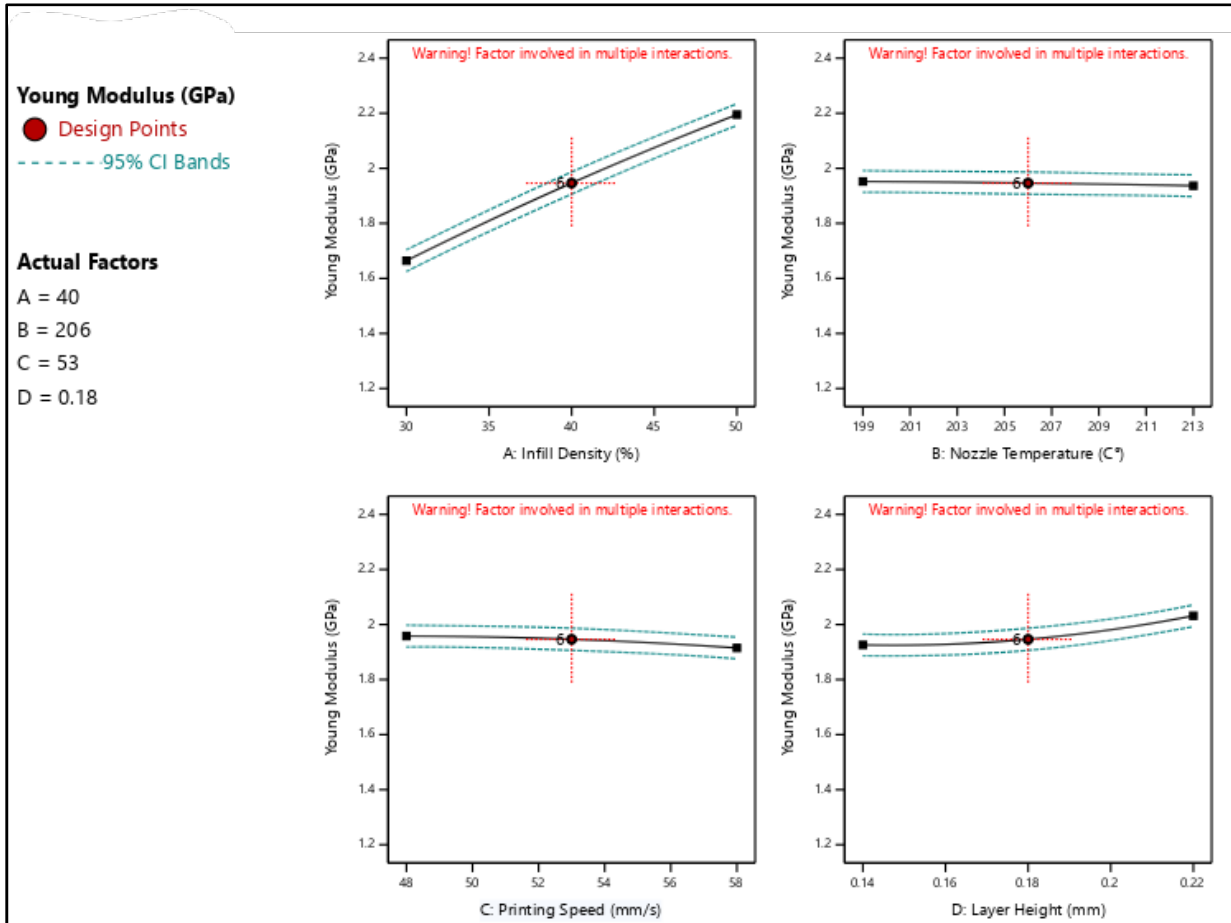
Figure 44. The influence of infill density, Nozzle Temperature, Printing Speed, and Layer Height on Young Modulus

i) Model of young modulus Response:

Design Expert v13. software was used to perform the quadrature model for the prediction of the output responses (young's module), which allows the analysis of variance (ANOVA) to extract the important factors that influence the response and to determine and evaluate the importance of the model coefficients and thus the contribution of each of the parameters on the output responses.

The most important model coefficients are those whose value surpasses that of the standard Student's coefficient computed with a 5% error (p-value). If the probability (p-value) is less than 0.05, the model is considered statistically significant (95 percent confidence). A low p-value suggests that the related response source is statistically significant. Another crucial variable is the

coefficient of determination R^2, which quantifies the ratio of variance between the model and experiment outcomes. When this coefficient approaches unity, the model precisely fits the measurement findings of the expected output responses.

The model coefficients, coefficient of determination, and ANOVA of the response for the Young's modulus are shown in Tables 15 and 16. According to the connection, Young Modulus is directly related to the four factors but mainly impacted by two "density and layer height".

ii) Final Equation in Terms of Coded Factors:

Young Modulus = -17.536 + 0.0947 A -0.0815 B - 0.213 C + 34.753 D - 0.000081 AB - 0.000218 AC - 0.149 AD - 0.0000724 BC - 0.144 BD - 0.0974 CD - 0.000166 A²- 0.000037 B² 0.00039 C² + 20.338 D²

A-Infill Density B-Printing Temperature C-Printing Speed D-Layer Height

The equation in terms of actual factors can be used to make predictions about the response for given levels of each factor.

Table 15. Young Modulus Coefficients in Terms of Coded Factors

Factor	Coefficient Estimate	Df	Standard Error	95% CI Low	95% CI High	VIF
Intercept	1.95	1	0.0188	1.91	1.99	
A-Infill Density	0.2653	1	0.0094	0.2452	0.2853	1.0000
B-Nozzle Temperature	-0.0077	1	0.0094	-0.0278	0.0123	1.0000
C-Printing Speed	-0.0216	1	0.0094	-0.0417	-0.0015	1.0000
D-Layer Height	0.0530	1	0.0094	0.0329	0.0731	1.0000
AB	-0.0057	1	0.0115	-0.0303	0.0189	1.0000
AC	-0.0109	1	0.0115	-0.0355	0.0137	1.0000
AD	-0.0594	1	0.0115	-0.0840	-0.0348	1.0000
BC	-0.0254	1	0.0115	-0.0499	-0.0008	1.0000
BD	-0.0403	1	0.0115	-0.0649	-0.0157	1.0000
CD	-0.0195	1	0.0115	-0.0441	0.0051	1.0000
A²	-0.0166	1	0.0088	-0.0354	0.0022	1.05
B²	-0.0018	1	0.0088	-0.0206	0.0170	1.05
C²	-0.0098	1	0.0088	-0.0286	0.0089	1.05
D²	0.0325	1	0.0088	0.0138	0.0513	1.05

The coefficient estimate represents the expected change in response per unit change in factor value when all remaining factors are held constant. The intercept in an orthogonal design is the overall average response of all the runs. The coefficients are adjustments around that average based on the factor settings. When the factors are orthogonal the VIFs are 1; VIFs greater than 1 indicate multi-collinearity.

iii) Fit Summary:

Source	Sequential p-value	Lack of Fit p-value	Adjusted R²	Predicted R²	
Linear	< 0.0001		0.8933	0.8564	
2FI	0.0081		0.9390	0.8876	
Quadratic	**0.0069**		**0.9683**	**0.9055**	**Suggested**
Cubic	0.0387		0.9881	0.5872	**Aliased**

iv) Fit Statistics:

Std. Dev.	0.0462		R²	0.9836
Mean	1.95		**Adjusted R²**	0.9683
C.V. %	2.37		**Predicted R²**	0.9055
			Adeq Precision	32.5038

The **Predicted R²** of 0.9055 is in reasonable agreement with the **Adjusted R²** of 0.9683; i.e., the difference is less than 0.2.

Adeq Precision measures the signal to noise ratio. A ratio greater than 4 is desirable. The ratio of 32.504 indicates an adequate signal. This model can be used to navigate the design space.

Table 16. ANOVA for Young Modulus Quadratic model

Source	Sum of Squares	DF	Mean Square	F-value	p-value	
Model	1.92	14	0.1368	64.21	< 0.0001	Significant
A-Infill Density	1.69	1	1.69	792.37	< 0.0001	Significant
B-Nozzle Temperature	0.0014	1	0.0014	0.6761	0.4238	
C-Printing Speed	0.0112	1	0.0112	5.27	0.0366	Significant
D-Layer Height	0.0674	1	0.0674	31.63	< 0.0001	Significant
AB	0.0005	1	0.0005	0.2414	0.6303	
AC	0.0019	1	0.0019	0.8924	0.3598	
AD	0.0565	1	0.0565	26.53	0.0001	Significant
BC	0.0103	1	0.0103	4.82	0.0442	Significant
BD	0.0260	1	0.0260	12.19	0.0033	Significant
CD	0.0061	1	0.0061	2.85	0.1122	
A²	0.0075	1	0.0075	3.54	0.0794	
B²	0.0001	1	0.0001	0.0415	0.8413	
C²	0.0027	1	0.0027	1.25	0.2818	
D²	0.0290	1	0.0290	13.63	0.0022	Significant

Residual	0.0320	15	0.0021			
Lack of Fit	0.0320	10	0.0032			
Pure Error	0.0000	5	0.0000			
Cor Total	1.95	29				

Factor coding is **Coded**.
Sum of squares is **Type III - Partial**

The **Model F-value** of 64.21 implies the model is significant. There is only a 0.01% chance that an F-value this large could occur due to noise.

P-values less than 0.0500 indicate model terms are significant. In this case A, C, D, AD, BC, BD, D² are significant model terms. Values greater than 0.1000 indicate the model terms are not significant.
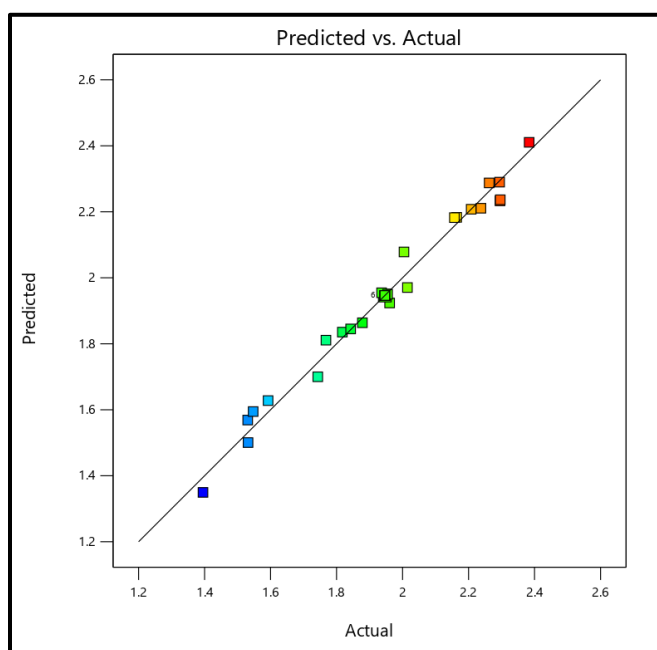

Figure 45. Alignment of experimental points and predicted responses

From the graph above, we notice that the Tendency of the experimental points aligns with the Model of young modulus response.
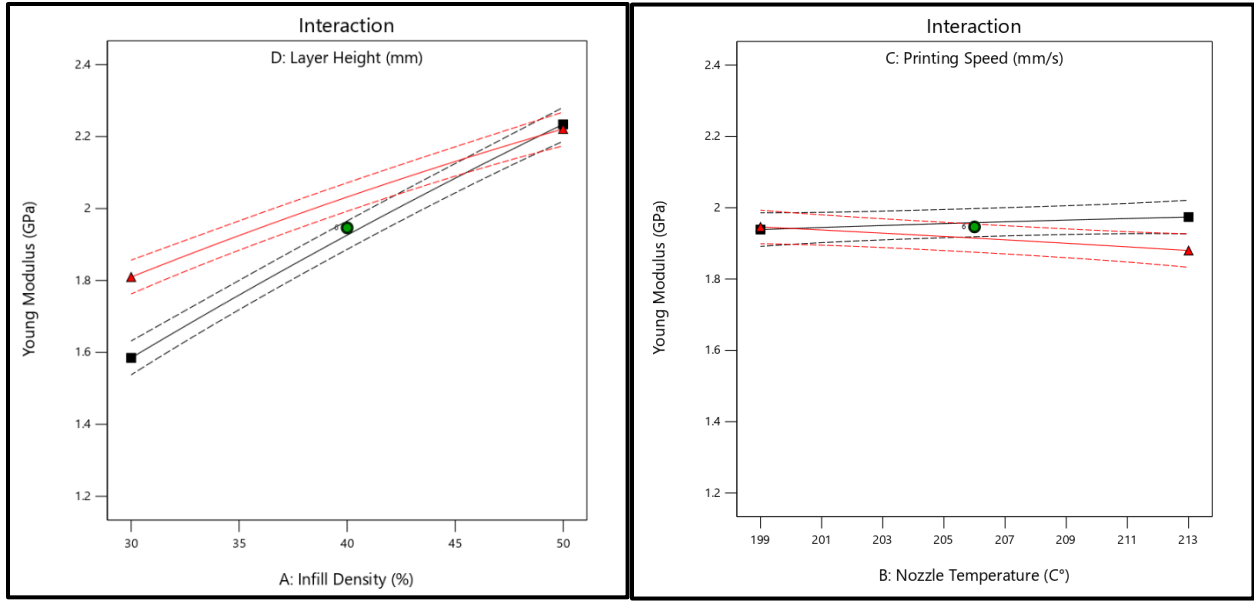
Figure 46. Interaction graphs of Factors "Left "A,D"" "Right "B,C"
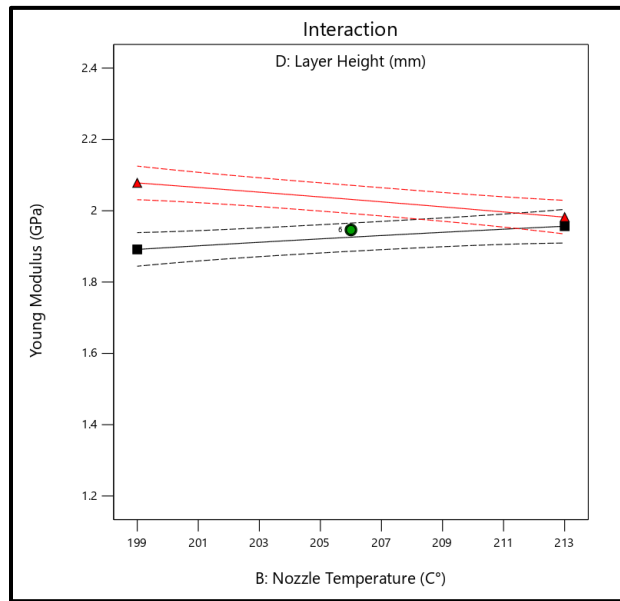
Figure 47. InteractionGraphs of Factors "B,D"

In these interaction plots, the slopes are not parallel. This interaction effect indicates that the relationship between "Fig 46 left" Infill density and Layer height strengthens young modulus the higher their value gets. "Fig 47" Young modulus is associated with the highest Nozzle temperature and layer height. However, in "Fig 46 Right" the two factors don't have any impact on young modulus because the slope is slightly parallel.
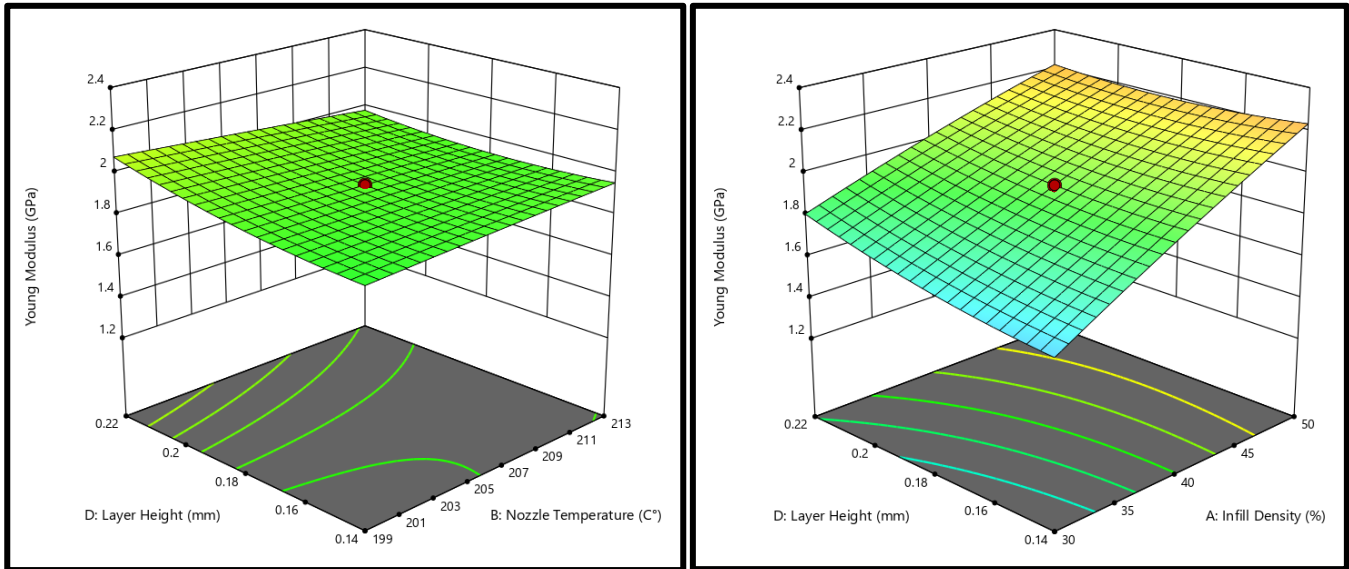
Figure 48. 3D Graph of the simultaneous influence of "Left 'Layer height and nozzle temperature'" and "Right 'layer height and infill density'" Both on young modulus

Figure 48 shows the influence of two parameters on the response simultaneously in the form of 3D graphs, while keeping the third parameter at the maximum value.

It can be concluded that infill density had the most significant impact on young modulus, since a significant increase in YM can be seen upon increasing infill density in interaction with layer height.

The interaction of layer height and nozzle temperature had a slight influence on young modulus; thus, the plotted surface area appeared almost flat.

B. Effect of the printer parameters on Yield Stress:

Figure 49 shows the influence of before mentioned printer's parameters on Yield Stress. As seen in the graphs, Stress rises the more Infill density and layer height are higher. While nozzle

temperature has little impact on it, finally printing speed got the opposite effect on stress than infill density and layer height, since the faster the printing is the lower the stress gets
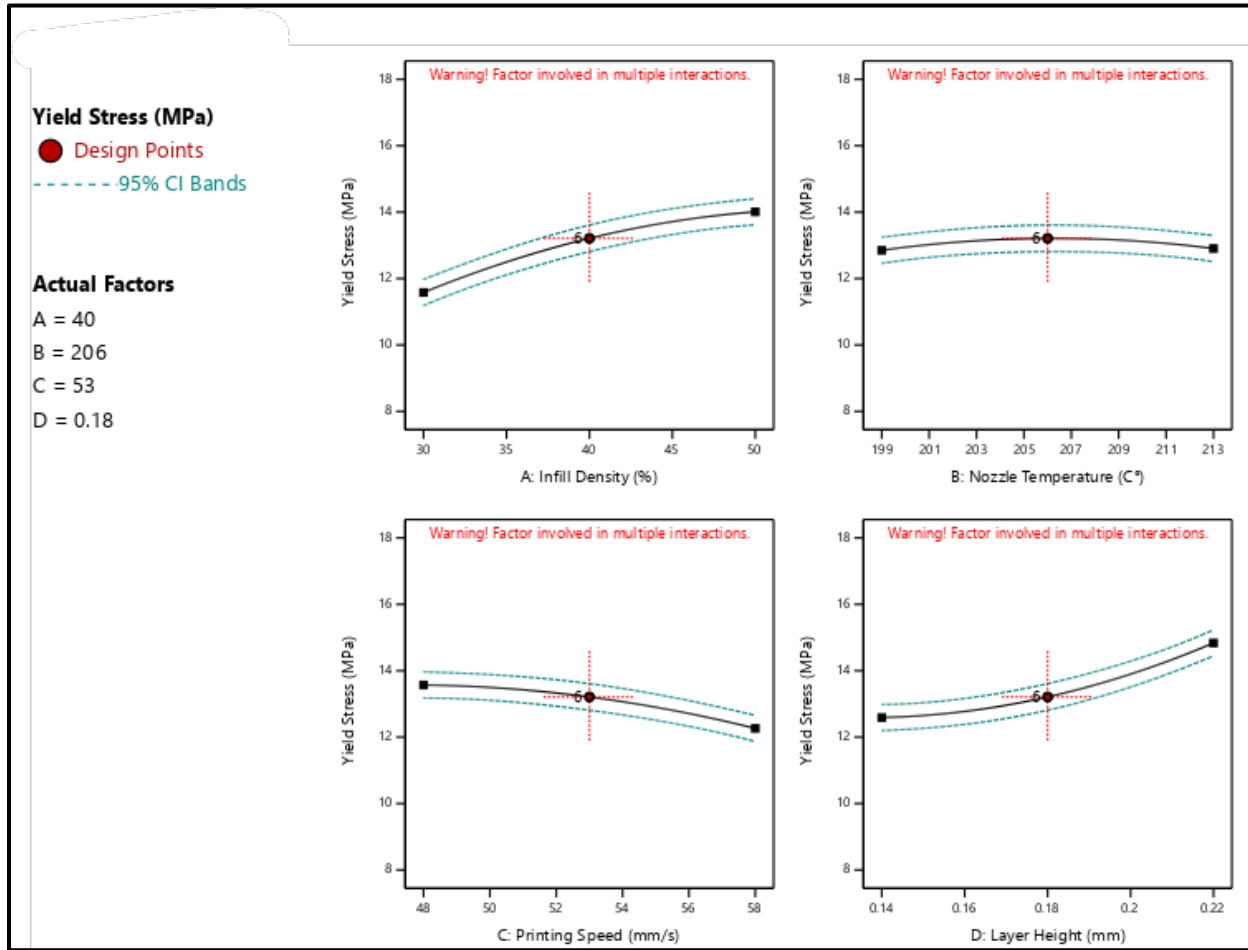
Figure 49. The influence of infill density, Nozzle Temperature, Printing Speed, and Layer Height on Yield Stress

i) Model of Yield Stress Response:

The model coefficients, coefficient of determination, and ANOVA of the response for the Yield Stress are shown in Tables 17 and 18. According to the connection, Yield Stress is directly related to the four factors except "Nozzle Temperature"

ii) Final Equation in Terms of Coded Factors:

Yield Stress = -387.423 + 2.143 A + 2.839 B + 3.104 C – 209.64 D - 0.00209 AB - 0.0146   AC - 2.683AD – 0.00488 BC + 1.691 BD – 2.206 CD - 0.00415 A² - 0.00679 B² - 0.0117   C² + 314.81 D²

A-Infill Density B-Printing Temperature C-Printing Speed D-Layer Height

Table 17. Young Modulus Coefficients in Terms of Coded Factors

Factor	Coefficient Estimate	DF	Standard Error	95% CI Low	95% CI High	VIF
Intercept	13.21	1	0.1876	12.81	13.61	
A-Density	1.21	1	0.0938	1.02	1.41	1.0000
B-Temperature	0.0265	1	0.0938	-0.1735	0.2264	1.0000
C-Printing Speed	-0.6542	1	0.0938	-0.8542	-0.4543	1.0000
D-Layer Height	1.12	1	0.0938	0.9236	1.32	1.0000
AB	-0.1467	1	0.1149	-0.3916	0.0982	1.0000
AC	-0.7306	1	0.1149	-0.9755	-0.4857	1.0000
AD	-1.07	1	0.1149	-1.32	-0.8284	1.0000
BC	-0.1707	1	0.1149	-0.4156	0.0742	1.0000
BD	0.4736	1	0.1149	0.2287	0.7185	1.0000
CD	-0.4403	1	0.1149	-0.6852	-0.1954	1.0000
A²	-0.4154	1	0.0878	-0.6025	-0.2284	1.05
B²	-0.3328	1	0.0878	-0.5198	-0.1458	1.05
C²	-0.2947	1	0.0878	-0.4817	-0.1076	1.05
D²	0.5037	1	0.0878	0.3167	0.6907	1.05

The intercept in an orthogonal design is the overall average response of all the runs. The coefficients are adjustments around that average based on the factor settings. When the factors are orthogonal the VIFs are 1; VIFs greater than 1 indicate multi-collinearity, the higher the VIF the more severe the correlation of factors. As a rough rule, VIFs less than 10 are tolerable.

iii) Fit Summary:

Source	Sequential p-value	Lack of Fit p-value	Adjusted R²	Predicted R²	
Linear	0.0002		0.5045	0.3368	
2FI	0.0034		0.7446	0.6715	
Quadratic	**< 0.0001**		**0.9538**	**0.8625**	**Suggested**
Cubic	< 0.0001		0.9985	0.9489	**Aliased**

iv) Fit Statistics:

Std. Dev.	0.4596		R²	0.9761
Mean	12.78		Adjusted R²	0.9538
C.V. %	3.60		Predicted R²	0.8625
			Adeq Precision	27.2615

The **Predicted R²** of 0.8625 is in reasonable agreement with the **Adjusted R²** of 0.9538; i.e., the difference is less than 0.2.

Adeq Precision measures the signal to noise ratio. A ratio greater than 4 is desirable. Your ratio of 27.261 indicates an adequate signal. This model can be used to navigate the design space.

Table 18. ANOVA for Yield Stress Quadratic model

Source	Sum of Squares	Df	Mean Square	F-value	p-value	
Model	129.52	14	9.25	43.80	< 0.0001	Significant
A-Infill Density	35.43	1	35.43	167.73	< 0.0001	Significant
B-Nozzle Temperature	0.0168	1	0.0168	0.0795	0.7818	
C-Printing Speed	10.27	1	10.27	48.63	< 0.0001	Significant
D-Layer Height	30.30	1	30.30	143.44	< 0.0001	Significant
AB	0.3443	1	0.3443	1.63	0.2211	
AC	8.54	1	8.54	40.43	< 0.0001	Significant
AD	18.43	1	18.43	87.27	< 0.0001	Significant
BC	0.4661	1	0.4661	2.21	0.1581	
BD	3.59	1	3.59	16.99	0.0009	Significant
CD	3.10	1	3.10	14.69	0.0016	Significant
A²	4.73	1	4.73	22.41	0.0003	Significant
B²	3.04	1	3.04	14.38	0.0018	Significant
C²	2.38	1	2.38	11.28	0.0043	Significant
D²	6.96	1	6.96	32.95	< 0.0001	Significant
Residual	3.17	15	0.2112			
Lack of Fit	3.17	10	0.3168			
Pure Error	0.0000	5	0.0000			
Cor Total	132.69	29				

The **Model F-value** of 43.80 implies the model is significant. There is only a 0.01% chance that an F-value this large could occur due to noise.

P-values less than 0.0500 indicate model terms are significant. In this case A, C, D, AC, AD, BD, CD, A², B², C², D² are significant model terms. Values greater than 0.1000 indicate the model terms are not significant.
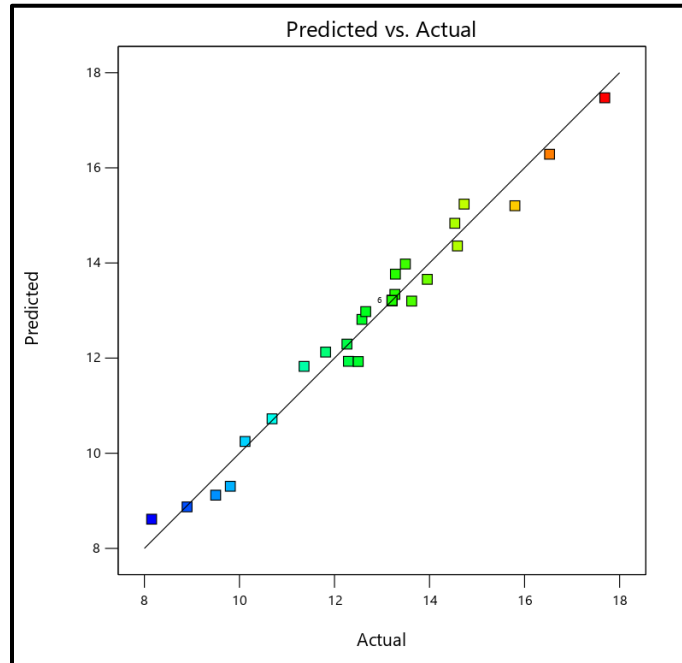
Figure 50. Alignment of experimental points and predicted responses

From the graph above we notice that the Tendency of the experimental points aligns with the Predicted Model of Young Modulus response
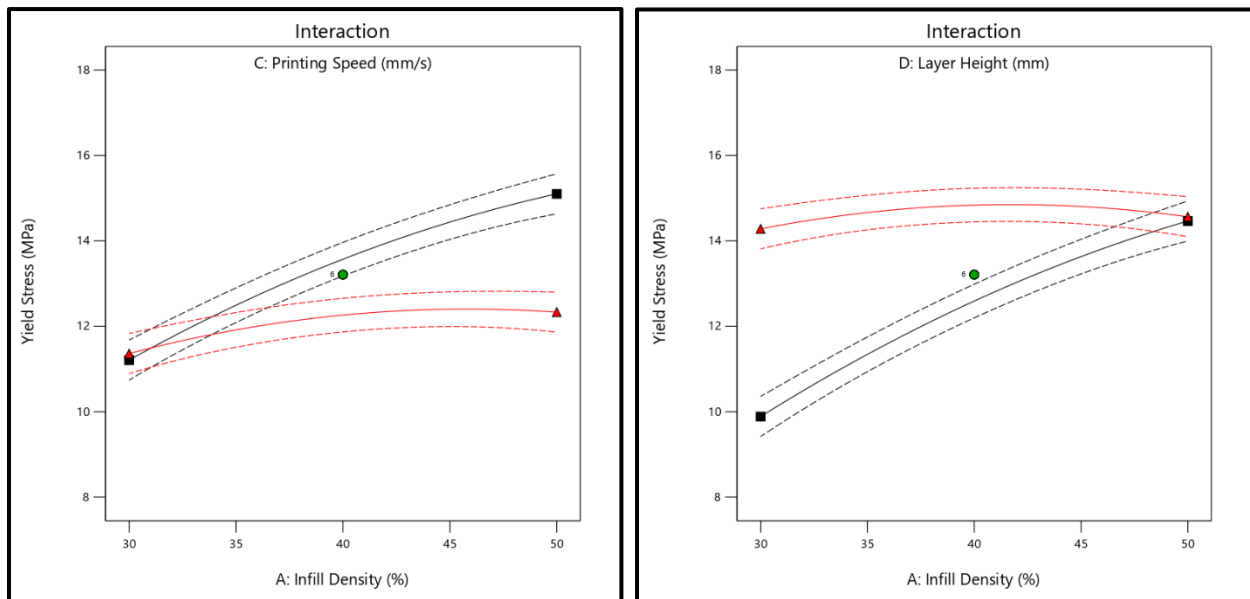

Figure 51. Interaction graphs of Factors "Left "A,C"" "Right "A,D"

These graphs indicates that the interaction between Infill density and printing speed weakens yield stress the lower their value gets "Fig 51 left" but the less the interaction between them the higher the stress gets. However, in "Fig 51 Right" Yield stress is correlated with the highest infill density and layer height.
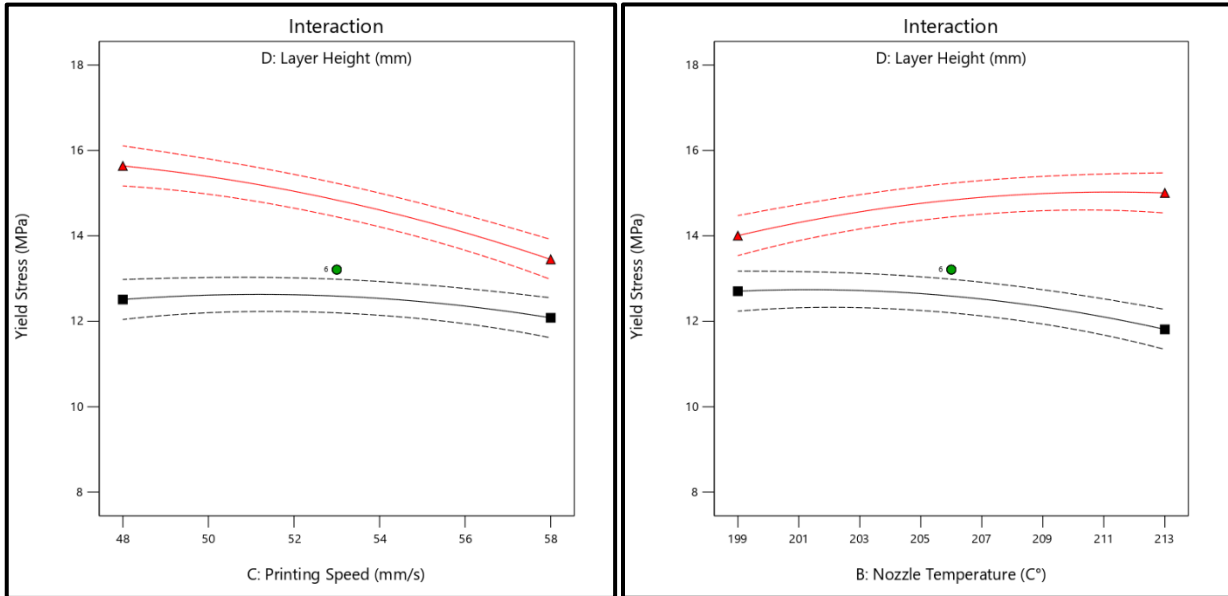

Figure 52. Interaction graphs of Factors "Left "D,C"" "Right "B,D"

In Figure 52 we can see there is no statistical interaction between all three factors "Layer height, printing speed, nozzle temperature" which mean they have a minimal impact on yield stress or that one explanatory variable's effect is constant across all levels of the others.
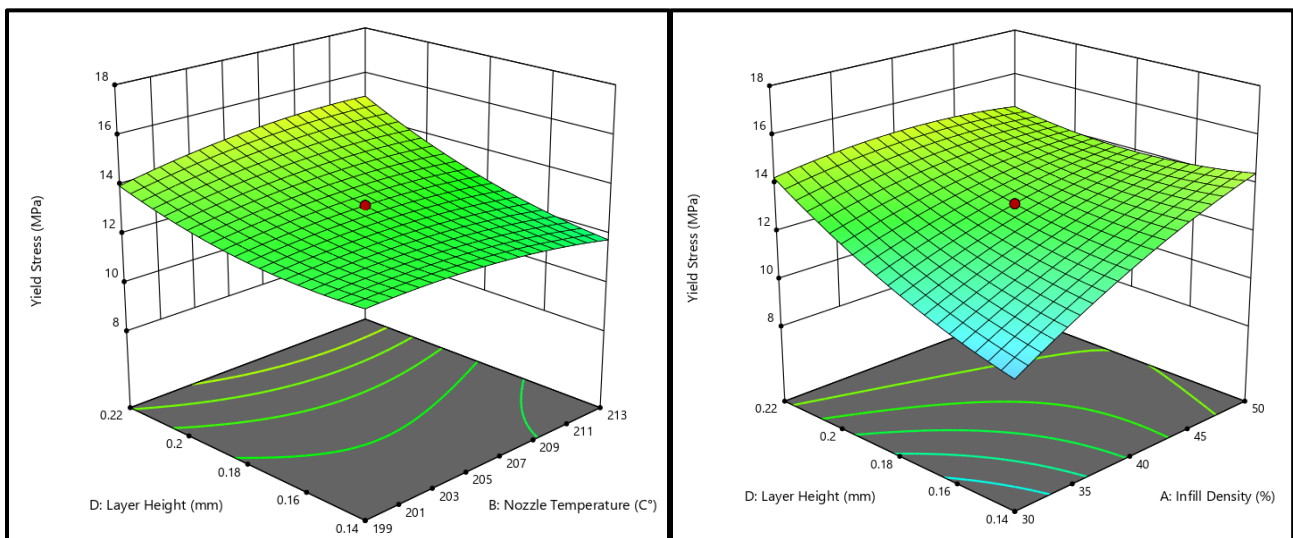

Figure 53. 3D Graph of the simultaneous influence of "Left 'Layer height and printing speed" and "Right 'printing speed and infill density'" on Yield stress

Graph above shows that there is significant increase in Yield stress upon increasing infill density in interaction with layer height.

The interaction of layer height and nozzle temperature only influence yield stress when layer height is increased.
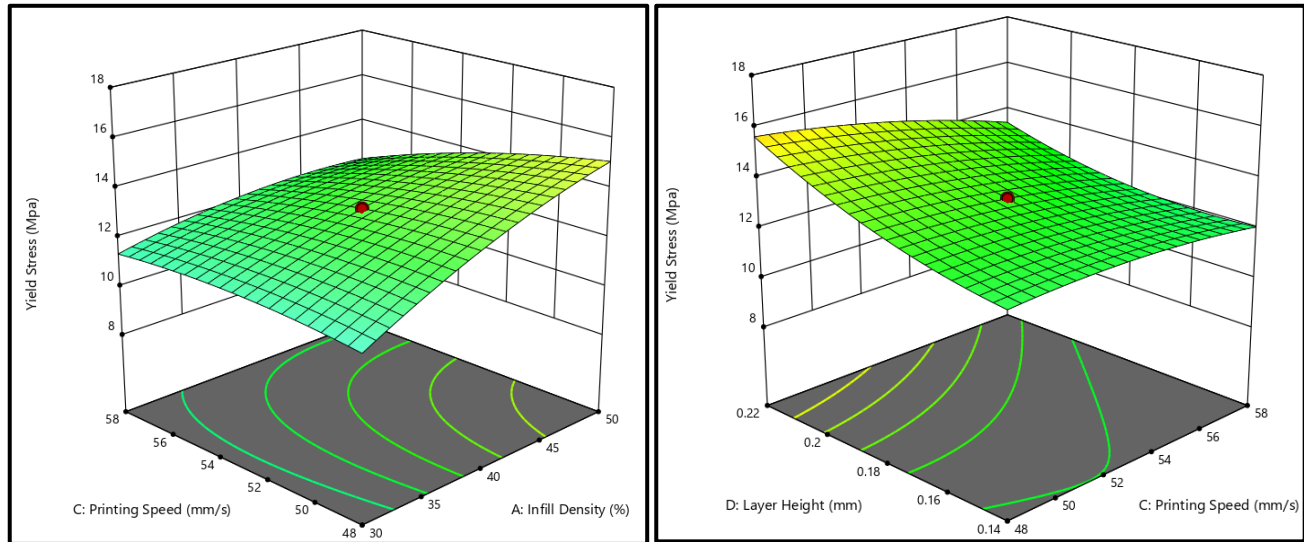

Figure 54. 3D Graph of the simultaneous influence of "Left 'Infill density and printing speed" and "Right 'printing speed and layer height '" on Yield stress

From figure 54 it can be concluded that infill density and layer height have the most significant impact on Yield Stress, since a significant increase in YS can be seen upon increasing those parameters. While printing speed in both graphs has minimal impact.

C. Young modulus and Yield Stress modeling based MANFIS:

a) MANFIS Construction:

To enhance the MANFIS model for Young Modulus and Yield Stress of the printed specimens, 30 data samples were used for structuring the model, using MATLAB v.16

As shown in Figure 55, the MANFIS architecture of the model consisted of:

- ❖ Four input parameters: Infill Density (%), Printing Temperature (°C), Printing speed (mm/min) and Layer Heigh (mm)
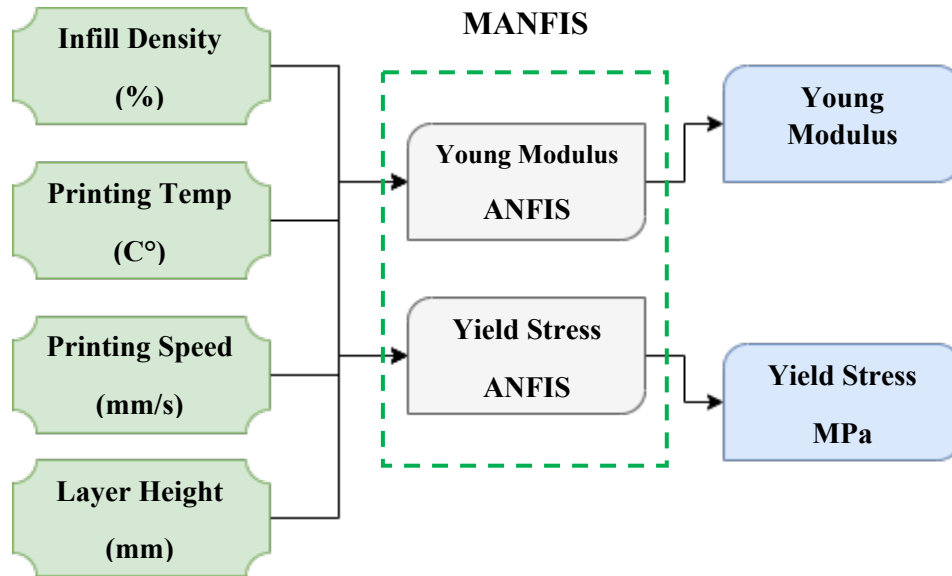- ❖ Two output parameters: Young Modulus (GPa) and Yield Stress (MPa).

.

Figure 55. Structure of the proposed MANFIS

The development of MANFIS begins with the construction of an initial fuzzy inference system, which subsequently allows for training. Since the number of inputs is relatively small, the method of identification grid partitioning is used. This method consists of dividing the universe of discourse into a grid of equal units according to the number of inputs and membership functions (MFs). In the present study, 4 bell-type MFs are used to model the universe of discourse of each - input (Figure 56-57). As for the output, a linear fuzzy output is chosen.

The training phase is an extremely important part of the adaptive fuzzy neuro network, as it allows the tuning of the fuzzy rules that govern the model. For this purpose, a series of experiment have been done using 20 iteration based on the hybrid training algorithm. as it has been proven to be the most effective training algorithm in several works such as [55,62,63]
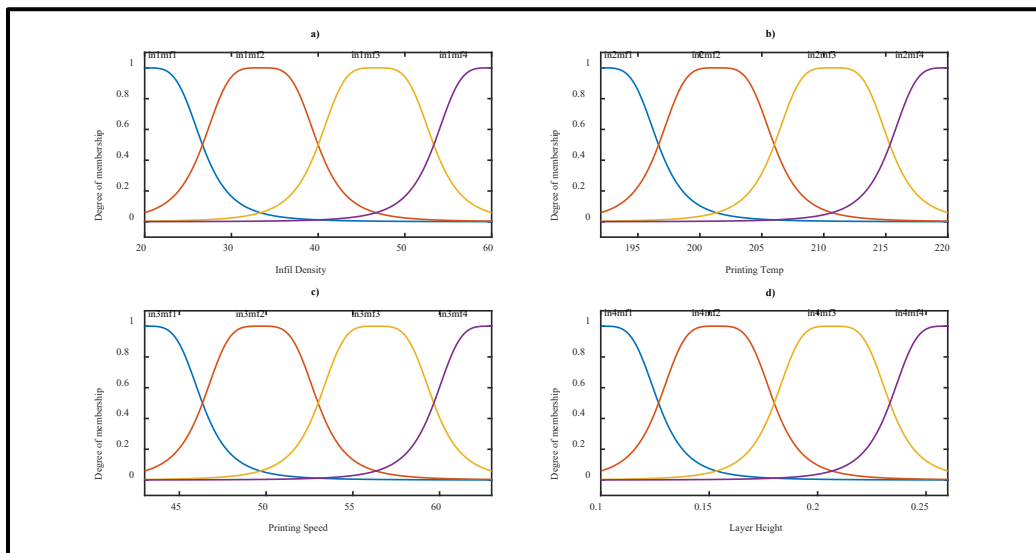
Figure 56. Inputs MFs for Young Modulus prediction
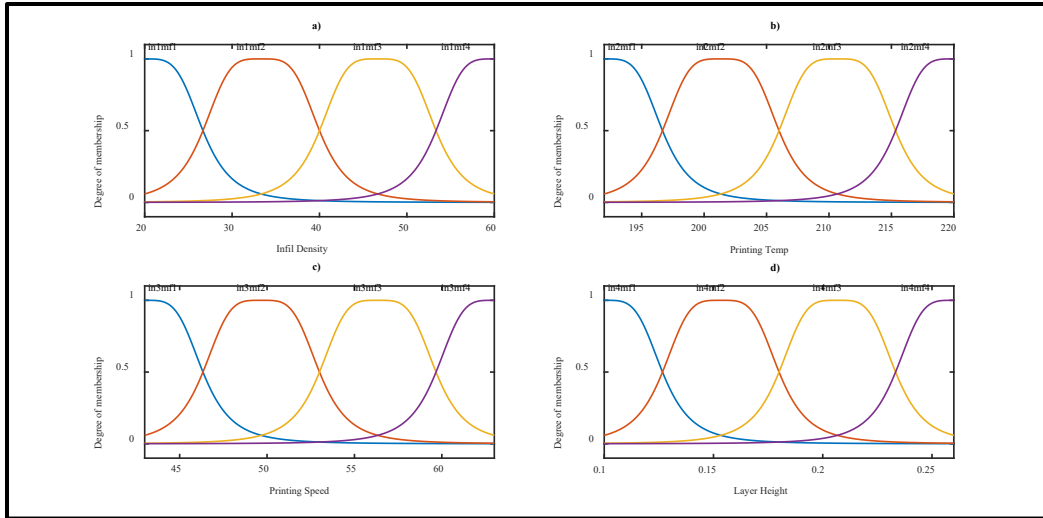
Figure 57. Inputs MFs for Yield Stress prediction

After the training process the 30 rules that govern the prediction of the young modulus are shown in (Figure 58-a), and those of the Yield stress are represented in (Figure 58-b). It can be seen from the same figures that the estimation of the desired variables is fairly accurate, due to MANFIS' ability to find the nonlinear relationship between the output and the input through machine learning.

Figure 58. Inputs MFs for Yield Stress prediction, Young Modulus, b) Yield Stress

b) Performance Comparison:

In order to verify the performance of the proposed method, a comparison between the multi-factor regression model presented in the section above and MANFIS is carried out.

"Figures 59-60" show a comparison between the experimental and predicted values. It is observed that the values estimated by MANFIS are in perfect superposition with the experimental data, far e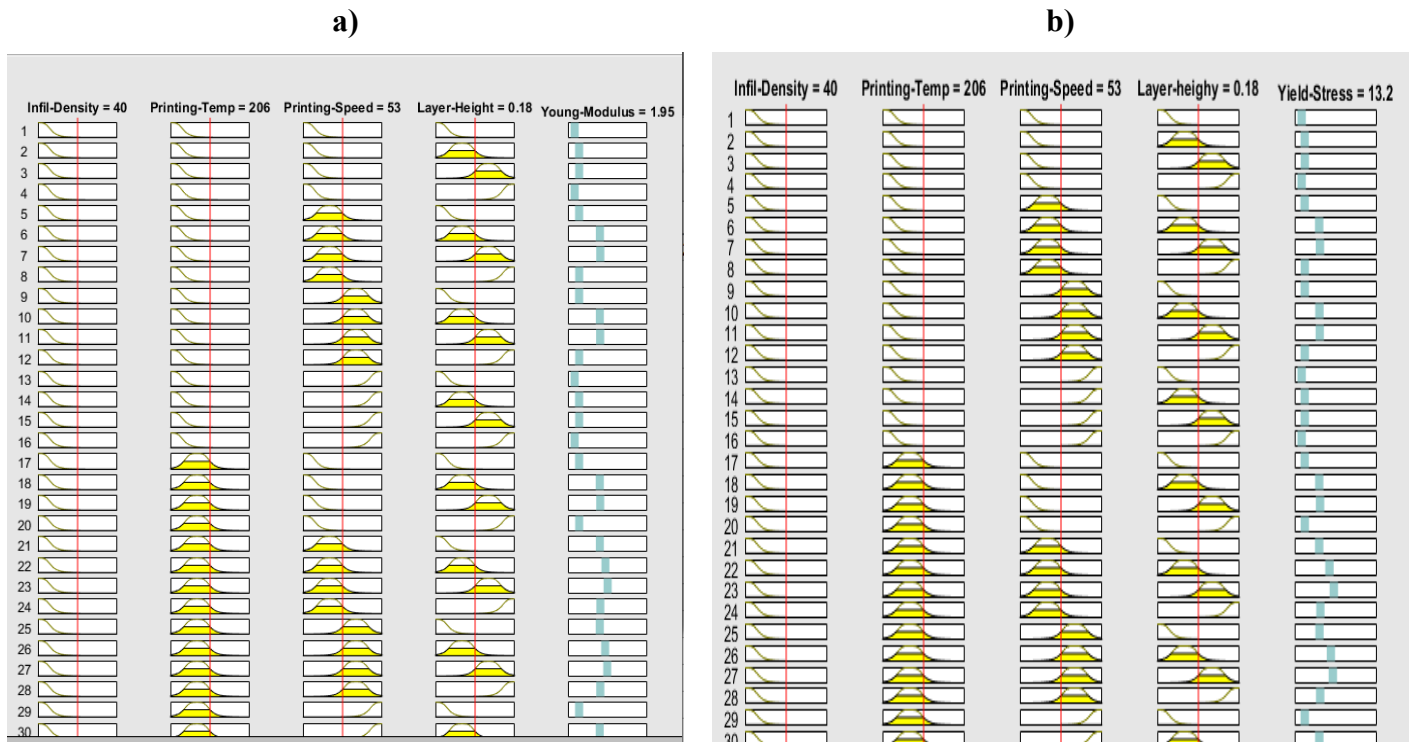xceeding the regression model in accuracy. This is due to the robustness of the proposed modeling method, which has already proven its effectiveness in several engineering applications.
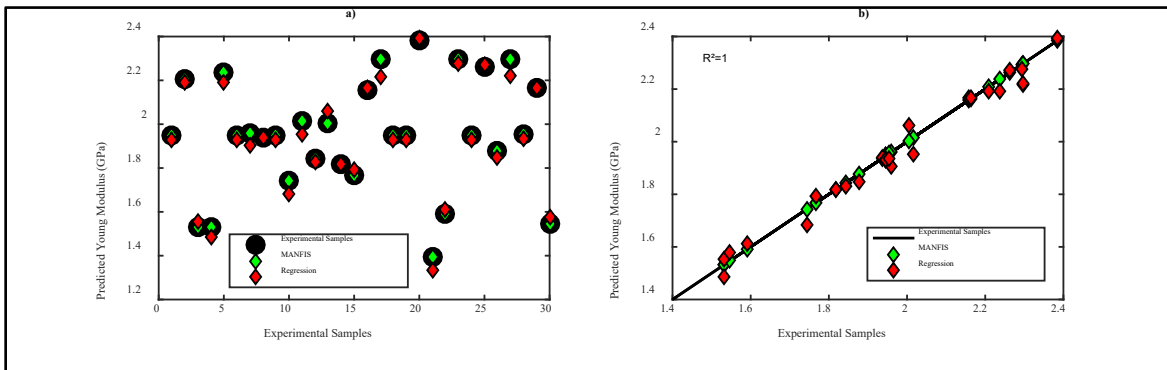
Figure 59. Young Modulus, a) predicted values, b) data correlation
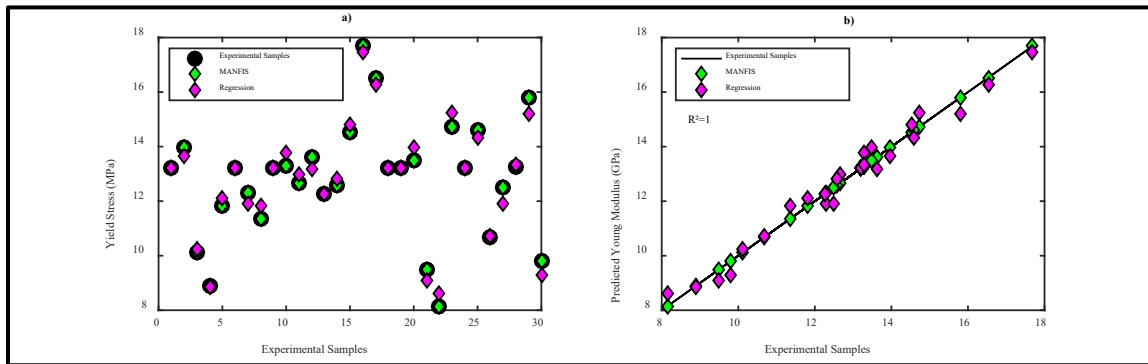
Figure 60. Yield Stress, a) predicted values, b) data correlation

This is confirmed by the evolution of the error shown in Figure 61, where, one can easily see that MANFIS faithfully reproduces the desired outputs with MSEs of 1.3536e-10 and 7.2669e-09 respectively for the young Modulus and the yield stress estimation with a correlation coefficient of 1. While for the regression model, the MSEs are much larger with values of 0.0013 and 0.1057 respectively and a correlation of 0.99. The statistical analysis is summarized in Table 19.

Table 19. Statistical Comparison

Criterion	Young Modulus		Yield Stress	
	Regression	MANFIS	Regression	MANFIS
MSE	0,0013	**1.3536e-10**	0.1057	**7.2669e-09**
R²	0,99	**1**	0,99	**1**
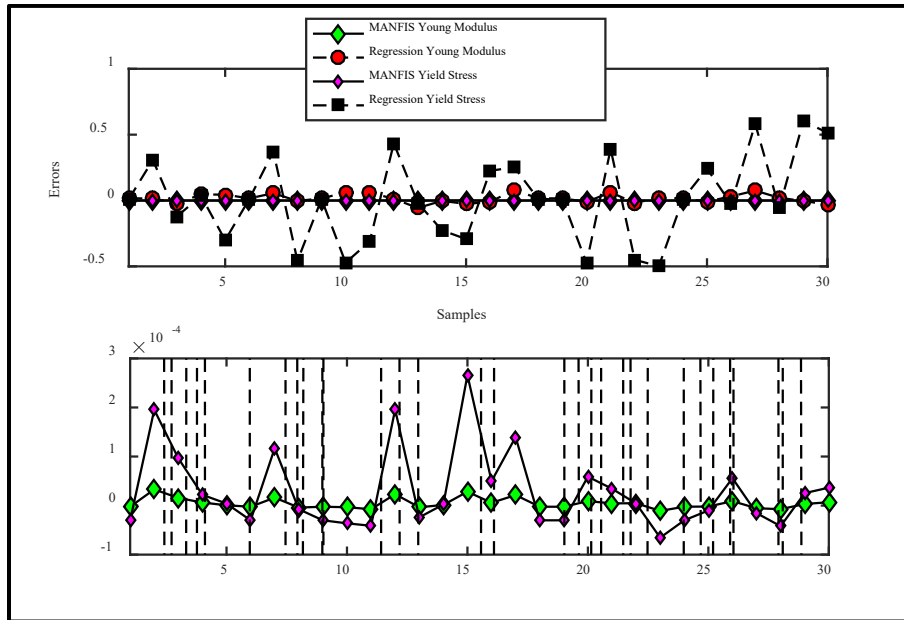
Figure 61. Global Comparison between all the data

So, we can say there was a considerable agreement between the two methodologies.

IX. Optimization of the Printers parameters:

To determine the optimal printing parameters, we first used the desirability function method using Design Expert software, which allows us to find the optimal Parameters by satisfying both responses at the same time, i.e., we look for optimal values that satisfy the objective function of both Young Modulus and Yield Stress.

To validate the approach that has been used in this work, we assume 3 cases where the target of Young Modulus and yield stress is defined by the client, numerical optimization in Design Expert Software was used, in order to get the 3D printer parameters.

We tried 3 examples:

Case 1:

Name	Goal	Lower Limit	Upper Limit
A: Infill Density	is in range	30	50
B: Nozzle Temperature	is in range	199	213

C: Printing Speed	is in range	48	58
D: Layer Height	is in range	0.14	0.22
Young Modulus	is target = 2	1.39515	2.38375
Yield Stress	is target = 15	8.153	17.688

Solutions:

After 100 runs and Solutions found the one with the best criteria was selected "1"

Number	Infill Density	Printing Temperature	Printing Speed	Layer Height	Young Modulus	Yield Stress	Desirability	Selection
1	40.457	211.640	53.087	0.220	2.000	15.000	1.000	Selected
2	39.705	210.180	51.169	0.214	2.000	15.000	1.000	
3	38.833	207.670	48.383	0.210	2.000	15.000	1.000	
4	39.909	210.540	51.950	0.216	2.000	15.000	1.000	

Case 2:

Name	Goal	Lower Limit	Upper Limit
Young Modulus	is target = 1.7	1.39515	2.38375
Yield Stress	is target = 17.5	8.153	17.688

Solutions:

Number	Infill Density	Printing Temperature	Printing Speed	Layer Height	Young Modulus	Yield Stress	Desirability	Selection
1	30.000	213.000	53.439	0.220	1.760	14.546	0.790	Selected
2	30.000	213.000	53.310	0.220	1.762	14.561	0.790	
3	30.000	213.000	53.062	0.220	1.765	14.588	0.790	
4	30.000	212.984	53.692	0.220	1.758	14.516	0.790	

Case 3:

Name	Goal	Lower Limit	Upper Limit
Young Modulus	is target = 1.4	1.39515	2.38375
Yield Stress	is target = 10	8.153	17.688

Solutions:

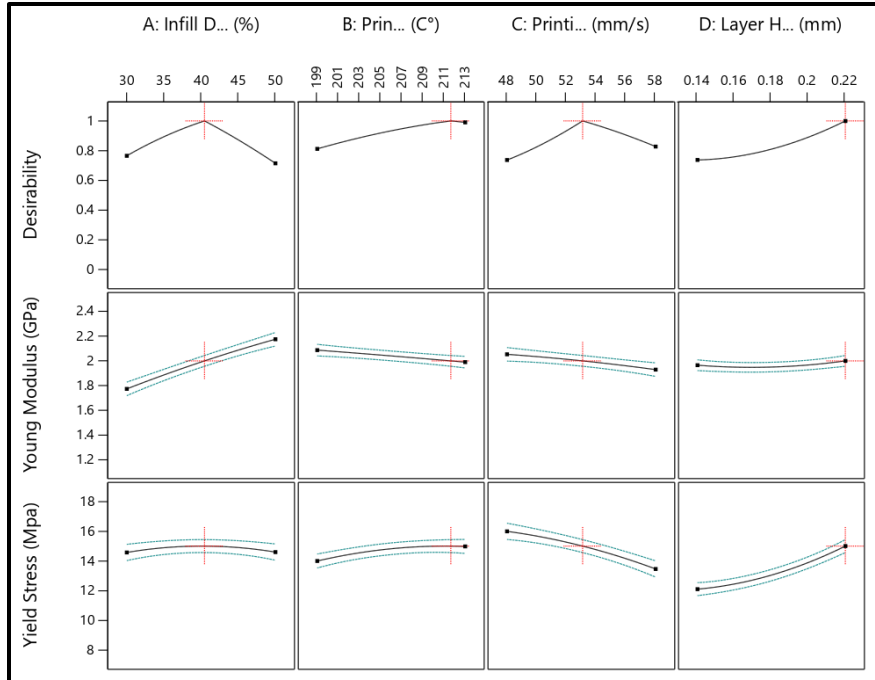| Number	Infill Density	Printing Temperature	Printing Speed	Layer Height	Young Modulus	Yield Stress	Desirability	Selection
1	30.000	199.000	54.168	0.140	1.552	10.000	0.919	Selected
2	30.000	199.000	54.113	0.140	1.553	10.000	0.919	
3	30.032	199.000	54.072	0.140	1.553	10.000	0.919	
4	30.001	199.080	53.984	0.141	1.554	10.000	0.919	

Figure 62. Graph Showing the predicted printer parameters with the desired mechanical properties for the third example

Conclusion

The influence of 3D Printing parameters on the mechanical properties of commercial PLA material according to ASTM D-638 standard tensile test has been investigated.

DoE method has been applied in the experimental task Using Central Composite Design in this study and the results are analyzed through analysis of variance (ANOVA) to determine the influence of Main Factors on Young Modulus and Yield Strength.

From ANOVA it was concluded that of all selected parameters Infill Density is the most influential parameter on both properties Young Modulus and Yield Stress followed by layer height, printing speed, and Nozzle temperature in the mentioned order.

As for the prediction model of regression the model gave an accuracy of 90% for young modulus and 86% for yield stress which is a satisfactory values for experimental data prediction.

Using MANFIS method gave a more accurate result and prediction regarding regression model. Where the correlation between the experimental data and the predicted model of MANFIS had a mean square error equal to 1.3536e-10 for young modulus and a 7.2669e-09 for yield stress compared to the regression model 0.0013 for young modulus and 0.1057 for yield strength

The desirability function is a powerful tool when combined with central composite design they can be used by designers in order to solve a multi objective optimization problem

By using the desirability function and central composite design, the designers can obtain the 3d printing parameters directly based on the needed mechanical properties implied by the client, which reduce the time and cost of the experiment.

REFERENCES:

[1] B.M. Tymrak, M. Kreiger, L.M. Pearce, Mechanical properties of components fabricated with open-source 3-D printers under realistic environmental conditions, Mater. Des. 58 (2014) 242–246.

[2] E. Ebel, T. Zinnemann, Fabrication of FDM 3D objects with ABS and PLA and determination of their mechanical properties, RTejournal (2014) (accessed Sept 12, 2017), https://www.rtejournal.de/ausgabe11/3872.

[3] B. Wittbrodt, J.M. Pearce, The effects of PLA color on material properties of 3-D printed components, Addit. Manuf. 8 (2015) 110–116.

[4] A. Lanzotti, M. Grasso, G. Staiano, M. Martorelli, The impact of process parameters on mechanical properties of parts fabricated in PLA with an open-source 3-D printer, Rapid Prototyp. J. 21 (2015) 604–617.

[5] J. Torres, J. Cotelo, J. Karl, A.P. Gordon, Mechanical property optimization of FDM PLA in shear with multiple objectives, JOM 67 (5) (2015) 1183–1193.

[6] H. Li, T. Wang, J. Sun, Z. Yu, The effect of process parameters in fused deposition modeling on bonding degree and mechanical properties, Rapid Prototyp. J. 24 (1) (2018) 80–92 https://doi.org/10.1108/RPJ-06-2016-0090.

[7] J. Torres, M. Cole, A. Owji, Z. DeMastry, A.P. Gordon, An approach for mechanical property optimization of fused deposition modeling with polylactic acid via the design of experiments, Rapid Prototyp. J. 22 (2) (2016) 387–404.

[8] X. Liu, M. Zhang, S. Li, J. Peng, Y. Hu, Mechanical property parametric appraisal of fused deposition modeling parts based on the gray Taguchi method, Int. J. Adv. Manuf. Technol. 89 (5–8) (2017) 2387–2397.

[9] J.M. Chacon, M.A. Caminero, E. Garcıa-Plaza, P.J. Nunez, Additive manufacturing of PLA structures using fused deposition modeling: effect of process parameters on mechanical properties and their optimal selection, Mater. Des. 124 (2017) 143–157.

[10] H. Gonabadi, A. Yadav, S. J. Bull, the effect of processing parameters on the mechanical characteristics of PLA produced by a 3D FFF printer, The International Journal of Advanced Manufacturing Technology (2020) 111:695–709 https://doi.org/10.1007/s00170-020-06138-4.

[11] Eustaquio García Plaza, Pedro José Núñez López, Miguel Ángel Caminero Torija, Jesús Miguel Chacón Muñoz, Analysis of PLA Geometric Properties Processed by FFF Additive Manufacturing: Efects of Process Parameters and Plate-Extruder Precision Motion, Polymers 2019, 11, 1581; doi:10.3390/polym11101581

[12] Khaled Benfriha, Mohammad Ahmadifar, Mohammadali Shirinbayan, Abbas Tcharkhtchi, Effect of process parameters on thermal and mechanical properties of polymer-based composites using fused filament fabrication, Polym. Compos. 2021, 1. https://doi.org/10.1002/pc.26282

[13] Vladimir E. Kuznetsov, Alexey N. Solonin, Oleg D. Urzhumtsev, Richard Schilling,

Azamat G. Tavitov, Strength of PLA Components Fabricated with Fused Deposition Technology Using a Desktop 3D Printer as a Function of Geometrical Parameters of the Process, Polymers 2018, 10, 313; doi:10.3390/polym10030313

[14] Bakrani Balani, Shahriar and Chabert, France and Nassiet, Valérie and Cantarel, Arthur Influence of the printing parameters on the stability of the deposited beads in Fused Filament Fabrication of poly(lactic) acid. (In Press: 2018) Additive Manufacturing.

[15] Ferretti, P.; Leon-Cardenas, C.; Santi, G.M.; Sali, M.; Ciotti, E.; Frizziero, L.; Donnici, G.; Liverani, A. Relationship between FDM 3D Printing Parameters Study: A parameter Optimization for Lower Defects. Polymers 2021, 13, 2190. https://doi.org/10.3390/polym13132190

[16] Adi Pandžić, Damir Hodžić, Edin Kadrić Experimental Investigation on Influence of Infill Density on Tensile Mechanical Properties of Different FDM 3D Printed Materials DOI: 10.18421/TEM103-25 https://doi.org/10.18421/TEM103-25

[17] Narges Dialami, Michele Chiumenti, Miguel Cervera, Riccardo Rossi, Uxue Chasco, Miquel Domingo, Numerical and experimental analysis of the structural performance of AM components built by fused filament fabrication https://doi.org/10.1007/s10999-020-09524-8

[18] Vinicius Cabreira 1, Ruth Marlene Campomanes Santana, Effect of infill pattern in Fused Filament Fabrication (FFF) 3D Printing on materials performance, ISBN 1517-7076 artigos e-12826, 2020

[19] Pandzic, A[di]; Hodzic, D[amir] & Milovanovic, A[leksa] (2019). Effect of Infill Type and Density on Tensile Properties of PLA Material for FDM Process, Proceedings of the 30th DAAAM International Symposium, pp.0545-0554, B. Katalinic (Ed.), Published by DAAAM International, ISBN 978-3-902734- 22-8, ISSN 1726-9679, Vienna, Austria DOI: 10.2507/30th.daaam.proceedings.074

[20] Aleksa Milovanovića*, Aleksandar Sedmakb, Aleksandar Grbovićb, Zorana Golubovića, Goran Mladenovićb, Katarina Čolića, Miloš Miloševića, Comparative analysis of printing parameters effect on mechanical properties of natural PLA and advanced PLA-X material, Aleksa Milovanović et al. / Procedia Structural Integrity 28 (2020) 1963–1968 (https://creativecommons.org/licenses/by-nc-nd/4.0)

[21] Can Tang, Junwei Liu, Yang, Ye Liu, Shiping Jiang, Wenfeng Hao∗, Effect of process parameters on mechanical properties of 3D printed PLA lattice structures, ∗ Corresponding authors at Faculty of Civil Engineering and Mechanics, Jiangsu University, Zhenjiang, Jiangsu 212013, China. Open Access 3 (2020) 100076, https://doi.org/10.1016/j.jcomc.2020.100076

[22] Diana Popescua, Aurelian Zapciua, Catalin Amzab, Florin Baciuc, Rodica Marinescud, FDM process parameters influence over the mechanical properties of polymer specimens: A review, Polymer Testing 69 (2018) 157–166, https://doi.org/10.1016/j.polymertesting.2018.05.020

[23] Deloitte Challenges of Additive Manufacturing "why companies don't use additive manufacturing in serial production

[24] The ISO/ASTM 52900 Standard

[25] Ben Redwood, Filemon Schoffer, Brian Garret,3D HUBS (2017), The 3D printing handbook, technologies, design, and applications

[26] M. Cotteleer and J. Joyce. 3d opportunity: Additive manufacturing paths to performance, innovation, and growth. Deloitte Review, 14:5_19, 2014

[27] R. Fisher, Statistical Methods for Research Workers, Oliver, and Boyd, 1925.

[28] R. Fisher, The design of experiments, Oliver and Boyd, 1935.

[29] G. Taguchi et Y. Wu, Introduction to off-line quality control, Central Japan Quality Control Association, 1985.

[30] F. Louvet et L. Delplanque, Les Plans d'Expériences par la méthode Taguchi, Expérimentique, 2005.

[31] M. Pillet, Les Plans d'Expériences : une approche pragmatique et illustrée, Editions d'Organisation, 1997.

[32] J. Goupy, La méthode des plans d'expériences, Editions Dunod, 1998

[33] A. Dey et R. Mukerjee, Fractional Factorial Plans, Wiley, 1999.

[34] A. Atkinson et A. Donev, Optimum Experimental Designs, Oxford Science Publications, 1992.

[35] J. Droesbeke et J. Fine, Plans d'Expériences, application à l'entreprise, Gilbert Saporta, 1992.

[36] A. Fries et W. Hunter, « minimum aberration 2k−p designs », Technometrics, vol. 22, pp. 601–608, 1980.

[37] M. franklin, « Constructing tables of minimum aberration on−m designs », Technometrics, vol. 26, pp. 225–232, 1984.

[38] M. Abramowitz et I. Stegun, Handbook of Mathematical Functions, M. Abramowitz and I.A. Stegun, 1970.

[39] A. Khuri et J. Cornell, Response Surface, Designs and Analyses, Marcel Dekker, second edition, 1996.

[40] R. Myers et D. Montgomery, Response Surface Methodology, Process and product Optimization Using Designed Experiments, Wiley, 1995.

[41] Y. Dodge et V. Rousson, Analyse de régression appliquée, Dunod, 2004.

[42] N. Draper et H. Smith, Applied regression analysis, Wiley, Ed. New-York,1981.

[43] N. Draper, «ridge analysis" of responses surfaces », Technometrics, vol. 5, pp. 469–479, 1963.

[44] E. Harrington, « The desirability function », Industrial Quality Control, pp. 494–498, 1965

[45] G. Derringer et R. Suich, « Simultaneous optimization of several response variables », Journal of Quality Technology, vol. 12, pp. 214–219, 1980.

[46] G. Derringer, « A balancing act: Optimizing a product's properties », Quality Progress, pp. 51–58, 1994.

[47] Wright, Stephen J. "optimization". Encyclopedia Britannica, 29 Jul. 2021, https://www.britannica.com/science/optimization. Accessed 25 May 2022.

[48] Gropp, W. and Moré, J. J. 1997. Optimization Environments and the NEOS Server. Approximation Theory and Optimization, M. D. Buhmann and A. Iserles, eds., Cambridge University Press, pages 167-182.

[49] Jason Brownlee, 2020 Optimization for Machine Learning "Finding Function Optima with Python"

[50] Sanket Doshi Various Optimization Algorithms for Training Neural Network The right optimization algorithm can reduce training time exponentially. Jan 13, 2019

[51] Adrian Rosebrock on May 6, 2021 Introduction to Neural Network https://pyimagesearch.com/4

[52] J.-S. Jang, "ANFIS: adaptive-network-based fuzzy inference system," IEEE transactions on systems, man, and cybernetics, vol. 23, pp. 665-685, 1993.

[53] S. G. Krishna, M. Shanmugapriya, and P. S. Kumar, "Prediction of bio-heat and mass transportation in radiative MHD Walter-B nanofluid using MANFIS model," Mathematics and Computers in Simulation, 2022.

[54] A. Parey and A. Singh, "Gearbox fault diagnosis using acoustic signals, continuous wavelet transforms and adaptive neuro-fuzzy inference system," Applied Acoustics, vol. 147, pp. 133-140, 2019.

[55] S. E. Chehaidia, A. Abderezzak, H. Kherfane, B. Boukhezzar, and H. Cherif, "An improved machine learning techniques fusion algorithm for controls advanced research turbine (Cart) power coefficient estimation," UPB Scientific Bulletin, Series C: Electrical Engineering and Computer Science, vol. 82, pp. 279-292, 2020.

[56] F. Cheng, L. Qu, and W. Qiao, "Fault Prognosis and Remaining Useful Life Prediction of Wind Turbine Gearboxes Using Current Signal Analysis," IEEE Transactions on Sustainable Energy, vol. 9, pp. 157-167, 2018.

[57] Hongyu Jin1, Yue Zhuo1, Yang Sun2, Hongya Fu1 and Zhenyu Han1(2019) Microstructure design and degradation performance in vitro of three-dimensional printed bio scaffold for bone tissue engineering DOI: 10.1177/1687814019883784

[58] Dudescu C, Racz L (2018) Effects of raster orientation, infill rate and infill pattern on the mechanical properties of 3D printed materials. ACTA Univ Cibiniensis 69(1):23–30. https:// Doi. org/10. 1515/ aucts- 2017- 0004

[59]. Khaderi S, Deshpande V, Fleck N (2014) The stiffness and strength of the gyroid lattice. Int J Solids Struct 51(23–24):3866–3877. https:// doi. org/ 10. 1016/j. ijsol str. 2014. 06. 024

[60]. Schoen AH (1970) Infinite periodic minimal surfaces without self-intersections. National Aeronautics and Space Administration, Washington

[61] Gibson LJ, Ashby MF (1999) Cellular solids: structure and properties. Cambridge University Press, Cambridge

[62]. Li D, Dai N, Jiang X, Chen X (2016) Interior structural optimization based on the density-variable shape modelling of 3D printed objects. Int J Adv Manuf Technol 83(9–12):1627–1635.

 https://doi. org/ 10. 1007/ s00170- 015- 7704-z